FULL-SCALE WIND LOADING ON GREEN ROOF SYSTEMS

By

TUAN D. VO

A THESIS PRESENTED TO THE GRADUATE SCHOOL
OF THE UNIVERSITY OF FLORIDA IN PARTIAL FULFILLMENT
OF THE REQUIREMENTS FOR THE DEGREE OF
MASTER OF ENGINEERING

UNIVERSITY OF FLORIDA

2013

To my parents, Duc and Chin, for always believing in me

ACKNOWLEDGMENTS

I would like to thank the Florida Building Commission's (FBC) Hurricane Research Advisory Committee (HRAC), the Florida Department of Emergency Management (FDEM), Kurt Fischer of Weston Solutions, and Nathan Griswold of American Hydrotech for providing the necessary funding and materials required for the completion of this project. I would also like to thank my advisor David O. Prevatt, Ph. D., and my committee members, Forrest Masters, Ph. D., and Glenn A. Acomb, FASLA, for their support and guidance throughout this project. Finally, I want to thank my mentors, colleagues, and co-workers: Scott Bolton, Nick Schild, Alon Krauthammer, Jeandona Doreste, David Roueche, Alex Esposito, Abraham Alende, Walter Lindon, Duzgun Agdas, Ph. D., Mark Clark, Ph. D., Aaron Weiner, Craig Dixon, Scott-Foss Kilburn, Ashlie Kerr, Barrett Mooney, and James Austin for their unprecedented aid and assistance throughout the progression of this project.

TABLE OF CONTENTS

page

LIST OF TABLES

LIST OF FIGURES

LIST OF ABBREVIATIONS

ANSI	American National Standards Institute
AP	*Aptenia cordifolia*
ASTM	American Society for Testing and Materials
ATC	Applied Technology Council
ASCE	American Society for Civil Engineers
BIP	Built-in-Place
C.R.	Coverage ratio
DE	*Delosperma nubigenum*
DI	*Dianthus gratianopolitan*us
FBC	Florida Building Commission
FEMA	Federal Emergency Management Agency
FIU	Florida International University
FLL	*Forshungsgesellschaft Landschaftsentwicklung Landschaftsbau*
FM	Factory Mutual
GA	*Gaillardia aristata*
HAPLA	High airflow pressure loading actuator
IBHS	Institute for Business and Home Safety
IQR	Interquartile range
LA	*Lantana montevidensis*
MC	Moisture content
PLA	Pressure loading actuator
SIUE	Southern Illinois University Edwardsville

UCF	University of Central Florida
UF	University of Florida
USDA	United States Department of Agriculture
UTM	Universal testing machine

Abstract of Thesis Presented to the Graduate School
of the University of Florida in Partial Fulfillment of the
Requirements for the Degree of Master of Engineering

FULL-SCALE WIND LOADING ON GREEN ROOF SYSTEMS

By

Tuan Vo

December 2013

Chair: David O. Prevatt
Major: Civil Engineering

The lack of understanding of how green roof systems perform under extreme wind loading conditions has led to an apparent disparity within the current North American green roof industry. The concentrated growth of this industry has left hurricane-prone states like Florida behind. This further exacerbates the issue that high winds have the capability to cause significant damage to green roof systems, but until sufficient research is conducted, their wind performance will only be speculated through design guidelines and anecdotal evidence. The primary focus of this study is to investigate how full-scale wind loading affects green roof systems. The goal of this research is to identify and offer recommendations to potential wind-induced risks and unify the current green roof industry via growth in hurricane-prone regions. This research was conducted in four divisions: an extensive literature review, full-scale wind testing, in-field plant uproot testing, and development of design wind load worksheets.

The literature review highlighted the existing risk of green roof wind damage, as scour and displacement failures were documented in non-hurricane-prone states like Wisconsin and Illinois. Further, the existing design guidelines offer some guidance towards the wind design of green roofs, but primarily derive from existing design

methodologies. Existing research does not adequately address the potential risk of uplift.

Wind testing was conducted on both modular tray and built-in-place green roof systems. Parapets were found to play a vital role in containing loose growth media from exiting the roof. The wind tests showed that the use of low-lying, resilient plants was required to not only maintain high vegetation coverage during storm events, but also to reduce plant stresses – both of which are necessary to reduce wind damage of a green roof. Two instances of catastrophic blow-off failures were documented for modular tray green roof systems, further reinforcing the fragility of a green roof to wind.

Plant uproot testing was conducted to assess the root anchorage of five plant species. The combined effect of higher plant establishment and density showed a strong indication towards higher uproot capacities. Further, the tall, *Lantana montevidensis* species showed the most consistent and resistive uproot behavior. It is recommended that a dense mixture of both low-lying extensive spread plants and taller, more-resilient plants with strong roots be used to fully bind the growth media from wind damage.

Two design worksheets were developed according to ASCE 7 wind load provisions. The primary worksheet calculated the design wind loads while the supplementary worksheet determined failure wind speeds. With rigid connections, the worksheets were deemed to provide conservative results. Further, an efficient envelope design procedure was developed in which the user only needs to compare the failure wind speeds with the building's design wind speed to select suitable green roof systems.

CHAPTER 1
INTRODUCTION

Current Industry Issues with Green Roof Wind Loads

For over 40 years, Germany has led as the leader in green roof installations worldwide. However, since their introduction in Chicago, Illinois atop the Chicago City Hall in 2001, green roofs have become increasingly popular roofing options in the United States, with annual installations growing steadily each year (Green Roofs for Healthy Cities, 2012). Green roofs are ballasted roofing systems that consist of growth media and live vegetation, which can effectively reduce the carbon footprint within a city by replacing otherwise impervious, traditional roofing systems. Numerous research studies have since explored and concluded that green roofs have the capability of providing a wide range of environmental benefits when properly installed, such as: reduced stormwater runoff, mitigation of urban heat island effects, increased runoff water quality, cleaner air, and even attenuation of outdoor sound (Prevatt, Masters, & Vo, 2011). Despite their potential for positively impacting the surrounding environment, closer inspection of most newly installed green roofs in the U.S. shows that the current growth of the green roof industry has been predominantly concentrated in non-hurricane-prone regions (Greenroofs.com, 2012). Further, this concentration of growth in the U.S. has led to an industry which utilizes plant species which may not necessarily be appropriate for subtropical and tropical climates like Florida. Therefore, this continuing trend of avoiding green roofs in hurricane-prone states will perpetuate until sufficient research on the green roof wind performance has been conducted to address potential wind-induced hazards.

Given the limited published research on green roof wind performance, the issue has not been completely overlooked prior to their installation in the U.S. There are several green roof design guidelines available in the United States, but only three green roof design guidelines/standards which specifically address and offer guidance towards the wind design of green roofs: Germany's *Forshungsgesellschaft Landschaftsentwicklung Landschaftsbau e.V.* (FLL), Factory Mutual's 1-35 Data Sheets (FM 1-35), and American National Standards Institute/Single Ply Roofing Industry's (ANSI/SPRI) RP-14 Wind Design Standard for Vegetative Roofing Systems (FLL, 2008; ANSI/SPRI, 2010; FM Global, 2011). However, these design guidelines and standards formulated much of their wind design approaches primarily from extending information from existing wind performance research on ballast roof systems (ANSI/SPRI RP-14) or requiring green roof systems to resist uplift pressures calculated from external design wind loads (e.g. ASCE 7 or DIN 1055-4). The former approach relies on green roof systems to behave like more-traditional ballasted roof systems (e.g. roof gravel and pavers), and although similarities exist, the direct translation between how green roofs perform in relation to how roof gravel and paver systems perform in high winds has only been speculated, not proven. A question arises following a review of these design guidelines: are these approaches valid and/or appropriate for green roof systems when dealing with hurricane-force winds? The answer to that question is still unknown, since none of these existing guidelines have been adopted as an accepted wind design standard for green roofs.

As earlier mentioned, green roofs are loosely-laid, roofing assemblies consisting underlayment layers (e.g. intermediate layers which promote drainage, prevent root

intrusion, filter runoff etc.) which combine to support the two primary surface layers of growth media and vegetation. These roofing assemblies are most commonly installed atop commercial flat or low-sloped roof decks, and can be constructed as either continuous built-in-place plots (Figure 1-1), or arrays of compact modular trays (Figure 1-2). Further, green roofs can be designed to two primary types: extensive or intensive. Growth media depths in the shallower extensive systems typically range between 80 to 100 mm (3 to 4 in.), while the intensive systems are typically greater than 150 mm (6 in.) in depth (FLL, 2008; FM Global, 2011). Consequently, the choice between extensive or intensive systems will dictate the type of suitable vegetation, and the degree of maintenance and irrigation required after installation of the green roof system is complete.

Figure 1-1. Built-in-place green roof atop the Perry Construction Yard at the University of Florida. Photo courtesy of Clark, Acomb, & Lang, 2008.

The current limited state of knowledge of the green roof wind performance stems from the relatively low importance placed on the wind design of green roofs – which paradoxically, is due to the existing avoidance of green roof installations in hurricane-prone regions of the United States. In other words, the *potential* for wind-induced

failures has directly influenced the limited number of green roofs installed in those high-wind regions of the United States. However, that is not to say that green roofs are immune to wind damage.

Figure 1-2. Modular green roof system installed at Grand Valley State University, Michigan. Photo courtesy of Fischer, 2013.

Currently, anecdotal evidence of field-installed green roofs following various high wind events has suggested that green roofs can be prone to wind-induced damages if the right conditions exist. Fischer (2013) conducted field inspections on three green roof installations in Chicago, Milwaukee, and Central Wisconsin, and found that the problematic regions of the green roofs were primarily located in the corners and edges of the building's roof deck. This reinforces the need to address the wind issue for green roofs, as wind-induced roof pressures are more a function of the building geometry rather than the type of installed roof system.

The purpose of this research is to advance the knowledge of how realistic, full-scale wind loads affect built-in-place and modular tray green roof systems. By better understanding the wind behavior of green roofs, the end goals of both increasing risk

mitigation as well as shifting from the concentrated installation trends in the United States can be better achieved.

Scope of Research

The two-year study was funded by the Florida Building Commission's (FBC) Hurricane Advisory Committee (HRAC) in an effort to determine the feasibility of green roofs in Florida. The author was a part of an interdisciplinary research team consisting of members from UF's Civil and Coastal Engineering and Landscape Architecture Departments, assembled to complete three primary tasks: 1) collect and present the most recent public research and installation and design criteria for green roofs, 2) conduct wind uplift tests on green roofs to develop preliminary understanding of the wind performance of green roofs, and 3) perform parametric studies of factors affecting uproot resistances and breakage strengths of plants used in green roofs and develop a standardized test procedure for wind testing green roofs. It should be clearly noted that the plant selection utilized in this study was based primarily on availability and should not be assumed to represent the recommended plant selection for Florida.

The initial literature review conducted in Fall 2010 encapsulated all existing green roof research available in the public domain (e.g. studies focused on energy savings, stormwater runoff, etc.) and resulted in a short pilot wind study on an extensive, sloped green roof system (Prevatt et al., 2011). The literature review has since evolved into a constantly-growing body of knowledge, primarily aimed at collecting, reviewing, and disseminating wind-related research, design guidelines/standards, and case studies for green roof systems.

Experimental, full-scale wind testing was conducted in two phases on both built-in-place and modular tray green roof specimens. The roof systems were placed atop a

mock-up building measuring 2.44 m long, 2.44 m wide, and 2.44 m high (8 ft. by 8 ft. by 8 ft.) utilizing UF's hurricane simulator. The goal of this testing was to provide benchmark results which describe the biomass loss behavior, scouring characteristics, and plant performance when subject to varying degrees of simulated wind and other factors.

Plant uproot tests were performed concurrently with Phase 2 of the wind testing on various plants from both wind-tested and untested green roof modules utilizing a Plant Uproot Device. The ultimate goal from the plant uproot tests was to determine relation between the root anchorage of field-planted vegetation and a green roof's wind resistance. The plant uproot tests were performed to identify the uproot capacities for different plant species while considering the effect from various parameters.

Two wind load design worksheets were developed for modular-tray green roof systems. The design worksheets followed the procedures set forth by ASCE 7 Components and Cladding loads for box-shaped buildings measuring up to 152 m (500 ft.) high. These two worksheets were created to provide green roof designers an efficient tool for: 1) determining ASCE 7 Components and Cladding wind loads for a specific-sized modular green roof array efficiently, and 2) designing a modular green roof system solely based off of the building's design wind speed.

Organization of this Document

Chapter 2 will review documented post-storm green roof case studies, explore existing green roof wind studies and wind design guidelines/standards. It will then compare the green roof-specific research and guidelines with existing literature focused on the wind loading mechanics for both ballasted roof systems and ground-level vegetation to develop a new wind design approach. Chapter 3 describes the

development, construction, and full-scale wind testing of the built-in-place and modular tray green roof systems utilizing the hurricane simulator. Chapter 4 discusses the development of the Plant Uproot Device, the conducted uproot testing, and the general results and findings. Chapter 5 describes the wind load design worksheets that were developed for modular green roof systems, using ASCE 7-10. Key findings and recommendations for future research are discussed in Chapter 6.

CHAPTER 2
LITERATURE REVIEW FOR WIND EFFECTS ON GREEN ROOF SYSTEMS

This chapter presents a literature review primarily-focused on the wind performance of green roof systems. It first reviews case studies which documented the post-storm wind performances of several existing green roofs. Then, existing wind-related research studies and design guidelines for green roof systems are discussed. Finally, this compiled green roof information is compared with well-established failure mechanics and wind interaction research studies conducted on ground-level vegetation and ballasted roof systems. Utilizing the reviewed literature, an alternative approach to design green roofs for high winds, thus formulating the motivation towards full-scale wind testing.

Post-Storm Wind Performance Case Studies on Green Roof Systems

Only a handful of post-storm wind performance case studies have been documented for green roof systems. A summary of reported post-storm green roof damage and successful performances can be found in Tables 2-1 and 2-2, respectively.

Successful Post-Storm Performance of Green Roof Systems

2004 – Bonita Bay green roof in Ft. Myers, Florida

On August 13, 2004, Hurricane Charley made landfall over Port Charlotte, FL as a Category 4 hurricane (58 – 70 m/s) with the eye of the storm measuring approximately 8 km (5 mi.) in diameter. It caused significant damage to many asphalt shingle, clay tile, and even metal roofing systems located in the area (FEMA, 2005). A 223 m^2 (2400 ft^2) extensive green roof located approximately 50 miles southeast of Port Charlotte in Ft. Myers, FL was evaluated following Hurricane Charley. The green roof was installed atop

a storage facility at the Shadow Wood Preserve Country Club, with its surrounding terrain best-fitting an open terrain, Exposure C category (Figure 2-1).

Its successful performance during the hurricane can best be attributed to both the storm's small size and the considerable distance (about 40 km) between the green roof and the storm's center. Further, the vegetation was comprised of mostly low-lying plants (i.e. various species of sedums and delospermas) and the roof had a surrounding border made of a reinforced steel mesh which extended 2 m (6.5 ft.) inwards from the roof edge which may have added protection against any wind-induced damage (Livingston, Fikoski, Miller, Lohr, & Denison, 2009; Miller, 2007).

Figure 2-1. Aerial photo of the Bonita Bay green roof and its surroundings at the Shadow Wood Preserve Country Club. Photo courtesy of Bing Maps, 2013.

2008 – Three intensive garden roofs in Downtown Houston, Texas

Hurricane Ike made landfall in Galveston, TX as a Category 2 hurricane (43 – 49 m/s) in September 13, 2008, extending hurricane force winds about 193 km (120 mi) away from its center. It caused extensive rooftop covering damage to several high-rise buildings in Downtown Houston, but three intensive green roof gardens in the same area experienced few, if any, tree limb losses based on the ground-level observations made by the damage assessment team (example of a green roof garden shown in

Table 2-1. Reported wind-induced damage/failures on green roofs

Ref	Year	Storm Event	Location	Wind Speed (m/s)	System Type	Size (m^2)	Height	Parapet? (Y/N)	Erosion Control Method	Observations
(Breuning, 2008)	1999	Cyclone Lothar	Germany	63	Extensive BIP	52,000	18 m	Y	Non-vegetation border	Designed via FLL but 0.8% of green roof failed; all green roof components remained on roof
(Fischer, 2013)	2004	Non-specific	Milwaukee, WI	n/a	Extensive modular	n/a	9.1 m	Y; ~90 cm	n/a	Low vegetation coverage; severe scour, then displacement in corner
(Fischer, 2013)	n/a	Non-specific	Stevens Point, WI	n/a	Extensive modular	n/a	7.6 m	Y	n/a	Low vegetation coverage observed; localized, severe scour
(Fischer, 2013)	n/a	Non-specific	Chicago, IL	n/a	Extensive BIP	n/a	~30 m	Y; ~30 cm	Wind control netting at time of planting	Plant distress in corners and edges; growth media displacement in these regions

Table 2-2. Reported green roofs with successful performances following storms

Ref(s)	Year	Storm Event	Location	Wind Speed (m/s)	System Type	Size (m^2)	Height	Parapet? (Y/N)	Erosion Control Method	Observations
(Livingston et al., 2009; Miller, 2007)	2004	Hurricane Charley	Lee County, FL	~58[a]	Extensive BIP	223	4.6 m	Y; very low edging	High-strength reinforcing mesh border	No visible damage but roof was sufficiently far away from the storm center
(FEMA, 2013)	2008	Hurricane Ike	Houston, TX[b]	42	Intensive BIP	n/a	n/a	n/a	n/a	Minimal tree limb losses reported, however observations were made at ground-level, not roof-level
(Webb, 2009)	2008	Hurricane Ike	Webster, TX	49	Intensive BIP (3.6 cm deep)	1356	~9 m	Y; 61 cm	n/a	No green roof damage or roof gravel scour, but picnic table in central roof location was overturned.

[a] Estimated based off of the lower rated wind speed for Hurricane Charley which was small in size and approximately 40 km from the green roof
[b] FEMA made the observations from three separate green roofs in the Downtown Houston area

Figure 2-2). It should be noted that besides the ground-level observations of the green roofs, the damage assessment team did not further explore the green roofs at roof level. The minimal amount of tree damage was attributed with the sheltering effect provided by neighboring buildings (FEMA, 2013).

Figure 2-2. Ground-level view of one of the green roof gardens in Downtown Houston following Hurricane Ike. Photo courtesy of FEMA, 2013.

2008 – Intensive built-in-place green roof in Webster, Texas

For the same storm (Hurricane Ike), about 40 km (25 mi.) southeast of Houston, an isolated intensive green roof located in Webster, TX was exposed to wind speeds up to 49 m/s (110 mph), measured at the Lyndon B. Johnson Space Center. The green roof measured 3.6 cm (9 in.) in depth, 1,356 m^2 (14,566 ft^2) in plan area, and was installed atop a three-story medical office building with a building footprint of 1,474 m^2 (15,863 ft^2). The green roof was exposed to approximately nine hours of high wind speeds and 25 cm (10 in.) of rain. Further, the incoming wind direction and exposure category changed from east-west, Exposure B to west-east, Exposure C as the eye of the storm moved north (Webb, 2009).

A post-storm review of the rooftop showed that no losses or visible signs of damage were incurred on the green roof, similarly attributed to the vegetation's ability to

form a roughness layer, and force higher wind speeds above the roof surface (Colbond, 2008a; 2008b; Webb, 2012). Figure 2-3 shows the green roof's undamaged condition on September 19, shortly following the storm. Although observed damaged occurred to the green roof itself, it was reported that the picnic table shown in Figure 2-3 was overturned. Webb (2009) further attributes the successful performance of the green roof with the inclusion of a 61 cm (24 in.) parapet, as reflected by the absence of scour damage to the rooftop gravel used for the roof's walkways.

Figure 2-3. Photograph of undamaged green roof following Hurricane Ike, taken on September 19, 2008. Photo courtesy of Webb, 2009.

Reported Green Roof Damage due to Wind

1999 – Catastrophic failure of an extensive green roof, Germany

One of the first documented cases of wind-induced failures with green roofs occurred in Germany when Cyclone Lothar struck in 1999. The storm damaged large portions of the nearby Black Forest as it moved across Western Europe. Although the 52,000 m^2 (560,000 ft^2) green roof was designed according to the existing FLL design standard at the time, the wind design provisions were insufficient to prevent the high sustained 63 m/s (140 mph) winds and 80 m/s (180 mph) gusts from damaging 0.8% of the green roof (372 m^2) (Figure 2-4). However, the damage was likely a result from

exceedance of the design wind load, as the green roof was also located atop an 18 m (60 ft.) high building, situated on a hill with a surrounding open field terrain condition. It was noted that the waterproofing and steel deck remained undamaged in the failed regions of the roof (Breuning, 2008).

Figure 2-4. Documented damage on the extensive green roof following Storm Lothar in Germany. Photo courtesy of Breuning, 2008.

2012 – Green roof wind damage in the Midwest United States

Fischer (2013) describes three separate site investigations on two modular tray green roof systems in Milwaukee, WI and Stevens Point, WI, and a built-in-place green roof located in Chicago, IL. These investigations were performed following reported evidence of wind-induced damage occurring on the green roof systems.

While investigating the modular tray green roof systems in Milwaukee and Stevens Point, Fischer (2013) found that the level of vegetation coverage on the green roof modules affected the amount of scour damage observed. Green roof modules, where damaged, were determined to have severe scouring of growth media occur before wind-borne displacement of the module, and was observed in corner regions of the roof for the modular tray green roof system in Stevens Point, WI (Figure 2-5B). For the green roof modules located in the field region of the roof located in Milwaukee, WI,

where vegetation coverage was limited, growth media scour occurred without displacement (Figure 2-5A).

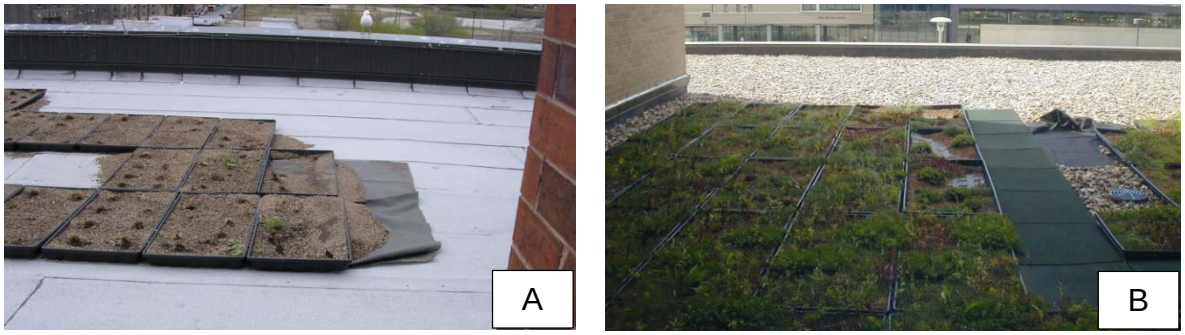

Figure 2-5. Modular tray green roof failures documented in two locations. Shown for A) Milwaukee, WI and B) Stevens Point, WI. Photos courtesy of Fischer, 2013.

The extensive built-in-place green roof investigated in Chicago, IL was installed atop a 30-story building with a relatively low parapet. To account for the edge regions of the roof, perimeter of concrete blocking was installed in place of the green roof system. However, a combination of periodic drought conditions and non-irrigation of the green roof resulted in the roof never achieving full vegetation coverage. With regular exposure to high winds, the green roof showed higher signs of plant distress in the corner and edge regions of the roof. In these areas, growth media displacement was observed, leading to plant die-off and exposed wind control netting, as shown in Figure 2-6 (Fischer, 2013).

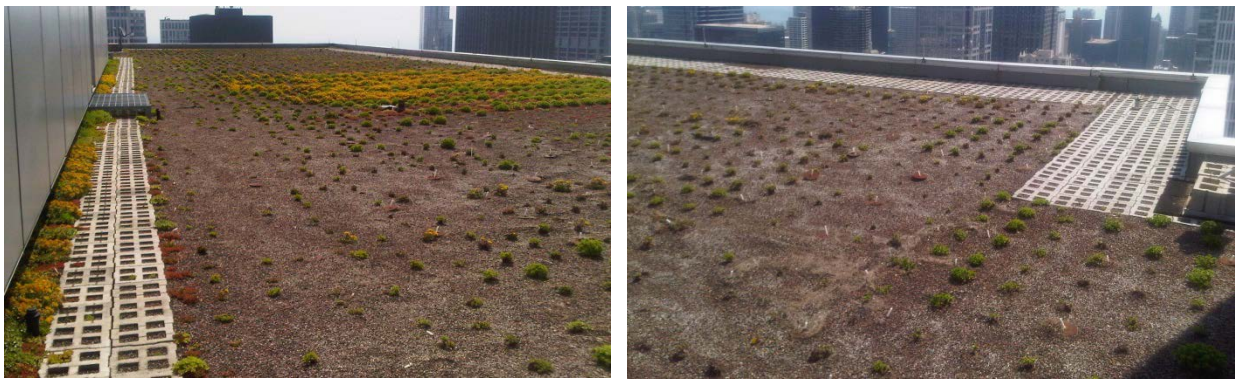

Figure 2-6. Extensive built-in-place green roof located atop a 30-story building in Chicago, IL with limited vegetation coverage shown. Photos courtesy of Fischer, 2013.

Discussion

From the reviewed case studies, it is clear that the risk of wind-induced damage is present for green roofs. Although green roof wind performance will vary from building to building, from the case studies presented in this section, two general findings can be made. First, it can be seen that taller building heights expose green roofs to higher winds, and therefore cause more damage. It is troubling to find that tall building heights alone can create sufficient wind gusts that can cause significant damage to green roofs in the Midwest United States. This finding highlights both the importance in proper installation procedures as well as the need to understand how green roofs perform under high wind loads on a per-component-basis. Second, it appears that modular tray green roof systems are more susceptible to wind damage than built-in-roof systems. However, given that only two modular tray green roofs were investigated, this finding may only be anecdotal. As such, the findings presented in this section should be taken with caution, as the small sample size of case studies considered are not representative for all existing green roofs.

Wind-Related Studies on Green Roof Systems

To address the potential risk of wind-induced damage identified (shown in the previous section), several research studies focusing on the wind loading of green roofs have been conducted since 1999. This section reviews and discusses the research previously conducted by Kramer and Gerhardt (1999), Retzlaff et al. (2009), Prevatt et al. (2011), and Wanielista et al. (2011). It also reviews a chamber pressure test reported by the LiveRoof green roof manufacturer (2012).

1999 – WSP Engineering, Aachen, Germany

One of the first documented studies focusing on the wind uplift effects on green roof systems was completed by Kramer and Gerhardt (1999) for XeroFlor America, LLC. First, Kramer and Gerhardt (1999) performed pressure chamber testing on a 5 m by 1 m XF301 system (which consisted of the root barrier, drainage mat, retention fleece, pre-cultivated vegetation mat, and growth media) while systematically varying the gap height between the XF301's underside and the impermeable roof slab's base. Dynamic uplift (i.e. negative, upward acting) pressures were applied into the chamber and the resulting differential pressure between the chamber and green roof mat (XF301) were measured (i.e. ΔP = Applied pressure – mat pressure) at each gap height.

They determined that the differential pressure between the chamber and mat increased with increasing gap height, in which uplift would occur if the differential pressure exceeded the system dead weight. The investigators stated that in a porous systems like green roofs, pressure equalization between the upper surface and underside of the system would typically occur, allowing the system to only experience a small percentage of the rooftop uplift pressure (also suggested by Miller (2007)). A moderating factor, as shown in Eqn. 2-1 below, was utilized to simplify the procedure of quantifying this equalization effect, and then correlated with the ratio of the gap spacing area and specimen plan area. The researchers determined that at a gap spacing of 0 m^2, the moderating factor for the XF301 system was 0.01. The researchers conservatively chose a moderating factor to be 0.04 for their analysis of the XF301 system, which corresponded to relatively large gap spacing area to specimen plan area ratio.

$$R = \frac{Cp_{res}}{Cp_{ex}} \tag{2-1}$$

Where:

R = moderating factor accounting for pressure equalization

Cp_{res} = resulting wind load coefficient (measured on specimen)

Cp_{ex} = external wind load's coefficient in chamber (applied to specimen)

The moderating factor chosen by the investigators was important, as the rest of their study consisted of a comparative analysis of the prospective design wind load via the DIN 1055-4 with the green roof's resistive load. For the design wind load, they determined the design dynamic pressure at varying building heights up to 100 m (330 ft.), and then applied the corresponding design external pressure coefficient for the desired roof location (i.e. edge, corner, or field) and the moderating factor, as shown in Eqn. 2-2 below.

$$W_{res} = R \cdot Cp_{ex} \cdot q_b \tag{2-2}$$

Where:

W_{res} = design wind load

R = moderating factor taken as 0.04

Cp_{ex} = design pressure coefficient for corresponding roof location (according to DIN 1055-4)

q_b = dynamic pressure for corresponding roof height

This design wind load was multiplied by an additional safety factor of 1.44 to obtain the factored design load that would be compared with the resistive dry weight of the XF301 green roof system. Kramer and Gerhardt (1999) determined that even for the worst-case scenario of a corner position on a building measuring between 20 to 100 m

high, the highest factored design load was predicted to be only 0.190 kN/m^2 (3.97 psf), suggesting that the XF301 green roof system, which weighed 0.267 kN/m^2 (5.58 psf), would be able to resist the “worst-case” uplift pressure solely from its dead load.

2009 – Southern Illinois University Edwardsville, Illinois

Retzlaff et al. (2009) conducted a wind scour performance study on individual green roof modules at Southern Illinois University Edwardsville (SIUE). The researchers used an aerodynamic recirculating wind tunnel to test green roof modules at varying degrees of vegetation coverage and wind speeds. The researchers sought to test three hypotheses:

1. Four inches of fully vegetated growth media can sustain two minute wind gusts greater than 90 mph
2. There is a minimum level of vegetation required to bind the growth media in order to resist scour during two minute wind gusts greater than 90 mph. Identify that level.
3. There are surface treatments that are effective in minimizing scour at various wind speeds. Identify the treatment and the wind speed at which it is no longer effective.

For the wind tests, the researchers utilized a recirculating wind tunnel with a longitudinal turbulence (Iu) of 0.22%. The wind tunnel had a test section that measured 1.8 m long, 0.76 m wide and 0.6 m high (72 in. by 30 in. by 24 in.) and utilized a 224 kW (300 HP) electric motor to generate wind speeds up to 62.6 m/s (140 mph). The aluminum green roof modules initially measured 600 mm by 600 mm by 100 mm (24 in. by 24 in. by 4 in.) tall, and were first tested with the windward face of the module normal to the incoming wind. However, after module displacement occurred (via sliding), the investigators reduced the plan area dimensions of the green roof modules to 450 mm wide by 450 mm long (18 in. by 18 in.) and tethered the specimens to prevent

displacement from occurring (Figure 2-7). They rotated the green roof modules 45 degrees to the incoming wind direction to simulate the worst localized wind conditions for each module tested.

Testing of the 21 modular tray specimens was conducted over a course of two test dates, June 13 and August 19, 2009. Wind speeds were incrementally increased until failure occurred, which was defined as when either the modular tray, green roof growth media, or vegetation experienced excessive displacement. The wind speeds and durations considered for each test trial were: 26.8 m/s (60 mph) at 1 min., 33.5 m/s (75 mph) at 1 min., 40.2 m/s (90 mph) at 2 min., 46.9 m/s (105 mph) at 3 min., 53.6 m/s (120 mph) at 5 min. and 62.6 m/s (140 mph) at 5 min.

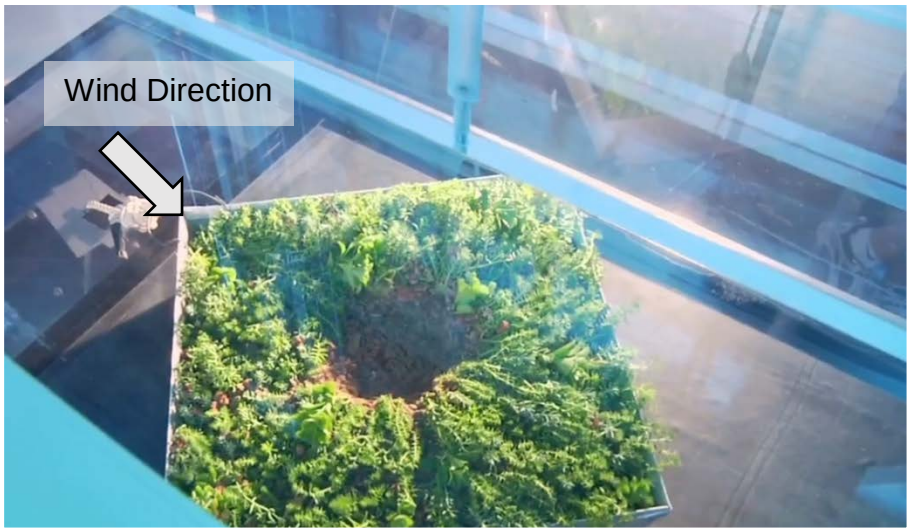

Figure 2-7. Tethered green roof module with a 127 mm (5 in.) diameter exposed area tested inside SIUE's aerodynamic wind tunnel. Photo courtesy of Retzlaff et al., 2009.

From their testing, it was determined that partially vegetated green roof modules were far less effective at resisting growth media scour than fully vegetated modules (i.e. 100% vegetation coverage), experiencing growth media scour at wind speeds as low as 34 m/s (75 mph). At 100% vegetation coverage, modules could withstand 63 m/s (140

mph) wind speeds for over 5 minutes without growth media scour (or module displacement if air flow was prevented from reaching the underside of the tested specimen). Also, the researchers showed that in the extreme case where no vegetation coverage or moisture was provided, growth media scour could occur at wind speeds as low as 13 m/s (30 mph). The research team also tested and confirmed that several methods of erosion control were effective at preventing growth media scour at 40 m/s (90 mph).

For incorporation into ANSI/SPRI's RP-14 Wind Design Standard for Vegetative Roofing Systems, Retzlaff et al. (2009) specified that nonvegetated (unprotected) regions of a green roof should be limited to no more than 127 mm (5 in.) diameter opening. Their research provided experimental evidence of vegetation coverage effects on green roof growth media scour prevention, but did not address the potential wind uplift issue (Retzlaff et al., 2009).

2010 – University of Florida, Gainesville, Florida

As part of their first task in determining the state of knowledge and feasibility of green roofs in Florida, Prevatt et al. (2011) performed a pilot wind study on a sloped, extensive, residential green roof with UF's hurricane simulator (further details provided in Chapter 3) in October 2010. The green roof was an existing system that was donated from UF's Department of Agricultural and Biological Engineering, and had been growing with no artificial irrigation for over 17 months before it was tested. Due to the drought conditions and transport-induced stresses, the green roof's plant health was poor at the time of testing (Figure 2-8).

The system's design was based out of Jacksonville, FL as a retrofit option for residential homes to be directly applied over a shingled roof. The vegetation would grow

within a layer of growth media and weave into a fibrous root mat, which were all placed over the root barrier membrane that was adhered to the shingles. The 1.2 m by 3.7 m (4 ft. by 12 ft.) green roof was raised 2.4 m (8 ft.) off of the ground so that the roof section would sit in the central test section of the hurricane simulator. The green roof was then set to a 3:12 slope, and placed 45 degrees to the wind flow to simulate the worst wind direction. Walls which extended from the exterior, windward edges of the green roof to the ground were placed to introduce a more-representative bluff body condition. The purpose of this study was to determine whether full-scale wind testing of green roof systems was a viable option with the existing equipment at UF.

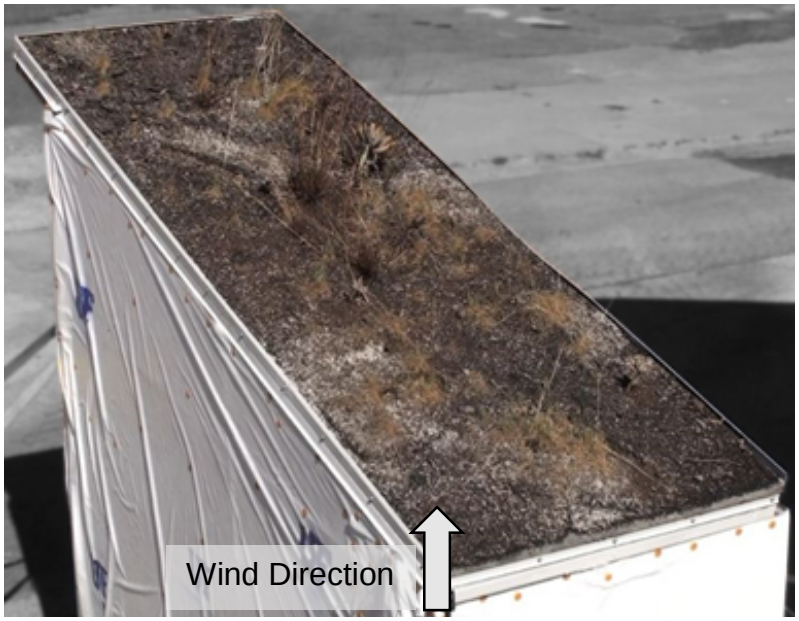

Figure 2-8. Sloped, extensive green roof tested with UF's Hurricane simulator in 2010. Photo courtesy of author.

A single wind test trial was conducted on the green roof at the end of October, 2010. A total of six wind speeds were considered: 8.9 m/s (20 mph),13.4 m/s (30 mph), 22.4 m/s (50 mph), 31.3 m/s (70 mph), 40.2 m/s (90 mph), and 53.6 m/s (120 mph). Because the nature of how the system would respond to high winds was unknown, the green roof was tested at each wind speed for a one minute duration before the

hurricane simulator was allowed to cool down (the final wind speed of 53.6 m/s was maintained for an additional three minutes).

From the testing, the investigators witnessed some evidence of losses: two Echevaria plants blew off of the roof when wind speeds exceeded 40.2 m/s (90 mph), and clumps of unattached soil were observed to blow off at each wind speed. However, the pre- and post-test weights of the structure showed that losses were negligible within a 0.5 kg (1 lb.) accuracy.

2011 – University of Central Florida, Orlando, Florida

In 2011, Wanielista et al. completed a year-long study on green roof wind loading in the state of Florida for the Florida Department of Environmental Protection (FDEP). Their study consisted of a 9 month field monitoring study on two green roofs on opposite coasts of Florida, as well as a single full-scale wind test conducted on an unplanted built-in-place green roof at Florida International University's Hurricane Research Center.

Wind testing was conducted by constructing an unplanted built-in-place green roof atop an existing 3 m by 3 m by 3 m high (10 ft. by 10 ft. by 10 ft.) structure, and subjecting it to the six-fan Wall of Wind – a hurricane simulator capable of producing up to 44.7 m/s (100 mph) wind speeds. The green roof was constructed, from the deck up, with: thermoplastic membrane, drainage layer, 25 mm (1 in.) of pollution control media, a separation fabric, and 76 mm (3 in.) of growth media. An edge restraint was then installed on the perimeter of the roof. It should be noted that none of the components were anchored. The structure was oriented at 45 degrees to the incoming wind and no vegetation coverage (i.e. utilizing only bare growth media) was implemented to represent the worst-case scenario. After 90 seconds of testing, the Wall of Wind

reached 35 m/s (78 mph) and caused the green roof to fail catastrophically in the windward corner (Figure 2-9).

Figure 2-9. Windward corner failure of unprotected built-in-place green roof tested at FIU's Wall of Wind. Photo courtesy of Wanielista et al., 2011.

For the field monitoring study, the research team designed and constructed two full-scale, built-in-place green roof systems in both the East (area of 4.65 m^2) and West (area of 149 m^2) coasts of Florida, located in Indiatlantic, FL and Port Charlotte, FL, respectively. Each green roof was outfitted with a grid of SETRA differential pressure transducers and an RM Young wind anemometer. Both sites collected pressure, wind speed, and wind direction data from July 2009 to February 2010, with the collection periods dependent upon a minimum threshold wind speed.

In analyzing their data, they found that the Indiatlantic green roof yielded uniform roof pressures due to its small size, whereas the Port Charlotte green roof displayed more random pressures, attributed to rooftop obstructions. Despite the low wind speeds observed by the two green roofs (approximately 8.9 m/s), evidence of growth media displacement was observed on the Indiatlantic green roof where little vegetation coverage was present. This vast size difference between the two test sites prevented

meaningful comparisons to be made, and the lack of high-speed winds limited the sample size of pressure measurements collected in their field study. However, they extrapolated the available pressure data for the green roofs to compare with design wind loads utilizing ASCE 7-05 for a design wind speed of 58.1 m/s (130 mph). The authors found that while the Indiatlantic green roof pressures agreed with the ASCE 7-05 predicted values, the Port Charlotte green roof pressures exceeded them by a factor of two (Wanielista et al., 2011).

Although the field monitoring portion of their study provided limited evidence of wind uplift issues for green roofs, the investigators documented evidence of growth media displacement on the Indiatlantic green roof due to its lack of vegetation coverage. Combined with the catastrophic failure of the built-in-place green roof during experimental testing, the study successfully highlights the vulnerability of green roofs to high winds when critical conditions are met.

2012 – LiveRoof WindDisc™ chamber uplift testing

Successful scour testing in 2008 of the LiveRoof hybrid modules (Figure 2-10), showed that the green roof plants could survive tests surpassing 49.2 m/s (110 mph) for test durations surpassing one hour. In 2012, LiveRoof LLC, along with U.S. and Canadian code officials and engineers, performed dynamic uplift testing on LiveRoof green roof modules with and without their patent-pending WindDisc™ connectors. Although public information is limited, the manufacturers claimed that the WindDisc™ connectors were able to withstand upwards of 9.58 kPa (200 psf) uplift pressures (LiveRoof, 2012).

Review of their informational video shows that the WindDisc™ connectors consist of small metal discs which slide between and attach the thermoplastic hybrid

modules made at their corners (Figure 2-11). Little detail is provided for their uplift tests, but a video clip from their testing is shown, in which a green roof plot is uplifted slightly, until a release valve is opened (circled in red in Figure 2-12). This appears to be a pressure chamber test which applies an overall negative suction load on the system.

Figure 2-10. Scour wind testing of LiveRoof vegetation with blower. Photo courtesy of LiveRoof, 2012.

Figure 2-11. Depiction of a WindDisc™ connector attaching either two modules or four modules together. Photos courtesy of LiveRoof, 2012.

Figure 2-12. Chamber pressure testing of LiveRoof modules connected with WindDisc connectors, passing a 9.58 kPa (200 psf) uplift test. Photo courtesy of LiveRoof, 2012.

Pressure chamber testing has regularly been employed as an economical alternative to wind tunnel testing to investigate load paths and connection influence functions due to uplift (Prevatt & Dixon, 2010; Prevatt, Schiff, Stamm, & Kulkarni, 2008). Chamber testing allows for full-scale components that are not dependent upon surrounding wind flow conditions (e.g. asphalt shingles, clay tiles) to be subjected to uniformly distributed pressures, applied in a static. Such approaches for uplift testing of roofing components have been detailed in several industry-standard test methods (ASTM, 2001; Laboratories, 1996). Further, recent advances have allowed researchers to reproduce spatially and temporally varying pressure traces on full-scale panel systems, as developed by Cook et al. (1988) and Kopp et al. (2010). A summary of how pressure chamber testing of roof systems is performed is shown by the following:

1. A rigid pressure box is placed and tightly sealed around the desired building component. Applicable components can range from roofing panels, siding, doors, and windows (Kopp et al., 2010)
2. A pressure loading actuator's (PLA) exhaust valve (operates in suction and positive pressures) is attached to an open port in the pressure box
3. A blower provides a constant air supply into the PLA, which is regulated to either supply a negative or positive air flow into the pressure chamber. All of this is controlled by a computer which commands a target pressure time history (obtained via wind tunnel testing).

In the case with the LiveRoof testing, it appears that the pressure chamber used is an inversed system, in which the pressure box is lowered onto a test deck as seen at the National Research Council (NRC) in Canada. Thus, with the NRC's system, the green roof system is installed on the deck of the chamber, the pressure box is lowered, and a net negative uplift pressure is applied into the space above the green roof (Figure 2-13). Thus, one can utilize ASCE 7's wind provisions for components and cladding (C&C) loads to estimate the equivalent wind speed at roof height required to generate

an applied suction of 9.58 kPa (200 psf) (ASCE, 2010). Using Eqns. 5-6 and 5-9 in junction with Figure 5-7A, assuming that K_z = 1.0, K_{zt} = 1.0, Zone 3 G_{cp} = 1.1 (for a sufficient effective area), and $U_{tot}(V)/A$ = 9.58 kN/m^2, a wind speed of 125 m/s (280 mph) is required to generate that pressure.

Figure 2-13. Inversed pressure chamber used for dynamic uplift tests, located at the National Research Council. Photo courtesy of Molleti, Ko, & Baskaran, 2010.

Summary

- Following chamber testing of the green roof mat system, Kramer and Gerhardt (1999) conservatively assumed that the green roof mat will only experience 4% of the design uplift pressure, the green roof mat system only consisted of permeable components. This resulted in a drastic reduction of the design uplift load, allowing for the green roof mat's dead load sufficient to resist uplift.

- While Retzlaff et al. (2009) found that fully-protected (i.e. 100% vegetation coverage) green roof modules are resistant to scour from wind speeds measuring up to 62.6 m/s (140 mph), they also inadvertently discovered that individual green roof modules are susceptible to sliding failures (hence the need to tether their specimens prior to testing). They also found that erosion control techniques in the form of coverings and spray tackifiers were effective in preventing scour.

- Prevatt et al. (2011) found that with with minimal vegetation coverage and a fibrous underlayment for plants grow into, minimal losses occurred on an established, sloped green roof exposed to wind speeds up to 53.6 m/s.

- Contrastingly, Wanielista et al. (2011) performed testing on an unprotected BIP green roof, and found that catastrophic failure occurred at 35 m/s. The BIP green roof components were held down by the ballast weight of 76 mm (3 in.) of growth media and 25 mm (1 in.) of filter media alone. Their field monitoring study of wind pressures for two field-planted green roofs in Florida provided little evidence of

uplift issues, but showed the presence of growth media displacement at relatively low wind speeds.

- A LiveRoof pressure chamber uplift test determined that their LiveDisc™ connectors were able to attach and prevent uplift of hybrid green roof modules subjected to 9.58 kPa (200 psf). Using ASCE 7 wind provisions for C&C loads, a 125 m/s (280 mph) wind speed was required to produce the uplift pressure if the system was installed in a corner region of the roof.

Discussion

The five green roof wind studies reviewed provided several considerations subject for further inspection, as summarized by the following list:

- Can a pressure equalization effect be applied to larger BIP systems and modular tray systems which have an additional tray layer?
- How will green roof modules (and BIP systems) perform in more-realistic wind conditions, where the turbulence intensity is much higher? Will vegetation resist these turbulent winds?
- Is the anchorage of green roof components critical to a green roof's successful wind uplift resistance?
- If uplift of over 9.58 kPa is able to be resisted by green roofs, is the predominant failure mode a result to uplift or overturning? If uplift is considered the predominant failure mode, can the surrounding wind flow be ignored?

Green Roof Wind Design Guidelines and Standards

Only three green roof design guidelines exist which specifically address the wind issue: the FLL, FM 1-35, and ANSI/SPRI RP-14. Two distinct approaches to designing green roofs to withstand high winds can be identified: 1) ensure that the green roof dead load exceeds the design wind loads determined from an external minimum building design load guideline (e.g. DIN 1055 or ASCE 7), and 2) from the project site's building geometry and basic design wind speed, enter design tables which dictate the type of green roof system permitted. A summary of the restrictions and approaches for the wind design of green roofs specified by these three guidelines/standards can be found in

Table 2-4. For conciseness, the wind design approaches presented in each design guideline/standard will be the main focus of this section.

FLL

The FLL - Guideline for the Planning, Execution, and Upkeep of Green Roof Sites utilizes a holistic approach to ensure proper installation, upkeep and maintenance of green roofs. The FLL considers three main factors to determine a specific project site's conditions: climate and weather-dependent factors, the structure-dependent factors, and the plant-specific factors (summarized in Table 2-3).

In regards to wind loads, the FLL considers its effects in each of the three main factors listed above (e.g. wind effects on the structure *and* vegetation). The bulk of the wind uplift design approach presented by the FLL primarily consists of first calculating the building's design wind loads in accordance to the European standard, the DIN 1055-4 (Structural Design Loads – Part 4: Wind Loads), and then applying a coefficient of wind action found in the DIN 1055-100 (Structural Design Loads – Part 100: Fundamentals for Planning – Safety Concepts and Measuring Standards). Further, the FLL states that the overall design uplift load obtained from the DIN 1055-4 should naturally decrease with the usage of green roof systems, due to the effect from a combination of various factors associated with green roofs. These factors include: the coarseness of the vegetation, additional dead load found from residual substrate moisture and vegetation, root systems' ability to bind growth media, and the wind permeability of vegetation.

Aside from resisting the design uplift pressures, the FLL also provides several other recommendations to resist wind-induced failures. In recognition of the higher susceptibility to wind damage in corner and edge regions of the roof, it recommends

that roof gravel or pavers be placed in those regions, as opposed to green roof vegetation and growth media. Further, because green roofs introduce living material whose wind resistance is a factor of its overall coverage ratio and establishment age, the FLL recommends various methods of erosion control during the vegetation's establishment including: utilizing fast-growing, stable vegetation, keeping growth media permanently moist during the vegetation's growth, and implementing erosion control mats (FLL, 2008).

Table 2-3. Project site condition factors (FLL, 2008)

Climate and weather-dependent	Structure-dependent	Plant-specific
Regional climate	Sunny, shaded and half shade areas	Hardiness (robustness) of selected plant species
Local microclimate	Deflection of precipitation by structure	Wind stability in exposed positions (especially for shrubs and perennials)
Pattern and volume of annual precipitation	Effect of flue gas emissions	Sensitivity to reflected light and thermal build-up
Average exposure to sunshine	Wind flow conditions	Sensitivity to airborne chemical and exhaust contaminations, as well as warm and cold air emissions
Any periods of drought	Exposure of the roof surfaces	Plant runners (stems which run horizontally within the ground)
Any periods of frost, with or without snow cover	Stress due to reflecting facades	Aggressiveness of rhizome-growth (portion of the plant stem under the ground surface where root-growth occurs)
Prevailing wind direction	Additional water load from adjoining structural elements	Growth pressure of plant rhizome and roots on building elements
	Gradient or pitch of the roof surfaces and lengths	Competitiveness of plant species in shallow substrate thicknesses
	Design loads and the resulting depth of the layered structure	Effect of wind and intensity of solar radiation on water storage
	Additional technical installations	Demands of aeration in the substrate made by plants in dry locations
	Roof ponding effects	

Table 2-4. Summary of wind-specific design guidelines/standards for green roofs (FLL, 2008; ANSI/SPRI, 2010; FM Global, 2011)

	FLL	FM 1-35	ANSI/SPRI RP-14
Latest edition	2008	2011	2010
Guideline type	Comprehensive design	Comprehensive design	Wind design standard
Plant selection guide	Yes (Figure A-1)	No	No
Wind design reference(s)	DIN 1055-4, DIN 1055-100	FM 1-28, FM 1-29, FLL	RP-4, ASCE 7-05, FLL, DIN 1055-4, Ballast roof studies, Retzlaff et al.
Wind speed restriction	None – determine wind loads	< 45 m/s (100 mph) (3-sec gust) restriction	If > 63 m/s (140 mph) (3-sec gust), defaults to engineer
Roof edge and corner restriction	Roof gravel or pavers to be used	Roof gravel or pavers; width > 0.9 m (3 ft.); see building height restriction	#4 or #2 ballast, as per design specifications
Growth media depth restriction	> 30 mm (1.1 in)	> 80 mm (3 in.)	None – dead load > 0.86 kPa (18 psf)
Building height (h) restriction	None – determine wind loads	If h > 46 m (150 ft.), use concrete pavers rather than stone ballast in non-vegetated borders	If > 46 m (150 ft.), defaults to engineer
Deck material restriction	All; Roofs with coverings require further permit	Only use metal or structural concrete	All; Determine impervious or pervious deck
Parapet wall requirement	No	Yes; If h > 46 m provide > 760 mm (30 in.), otherwise provide > 150 mm	Yes
Roof slope	1.1 - 45°	1.1 - 40°	1.1 - 7°

FM 1-35

The FM 1-35 Property Loss Prevention Data Sheets for Green Roof Systems provides a somewhat comprehensive design guideline for green roof systems and their support structure, utilizing a similar approach as the FLL. It provides design load considerations similar to the ASCE 7, such as: wind, hail, dead and live loads, future load allowances, surface loads from vegetation, and seismic loads. Unlike the FLL, the FM 1-35 leaves the plant selection and design to the green roof supplier or installer, but incorporates several of the FLL's recommendations for plant selection such as: 1) a minimum of 60% of the plant species must be sedums, 2) no mosses or grasses can be used, 3) prohibit plants whose mature height is greater than 0.9 m (3 ft.), and 4) use mesh "wind blankets" during the establishment period of plants.

The wind design approach presented by the FM 1-35 is very similar to the FLL, in that users must ensure that the green roof systems must be designed to withstand the design wind loads obtained from a separate design load document (FM 1-28). However, the wind speed restrictions require that green roofs be installed in regions where the design 3-second gust is no more than 45 m/s (100 mph). To address the increased wind speeds for taller buildings, the FM 1-35 makes alterations to the requirements once the building height exceeds 46 m (150 ft.). The usage of stone ballast in the non-vegetated borders is prohibited after 46 m, and must be replaced with concrete pavers. Also, if the building height surpasses 46 m, the parapet height must be increased from a minimum of 150 mm to 760 mm, measured from the top surface of the green roof (e.g. vegetation layer) to the top edge of the parapet.

A distinction between the FM 1-35 and the FLL is that the former provides further restrictions to aid in the prevention of wind-borne debris generation. For instance,

woody vegetation is limited to only rooftops where the design uplift pressure is less than that calculated for a basic 3-second gust wind speed of 49.2 m/s (110 mph), 4.5 m (15 ft.) roof elevation, and a ground roughness B category. The specified building's non-vegetated border zones (i.e. edge and corner regions) can be defined from the FM 1-28, and must provide stone ballast or concrete paver blocks in place of vegetation and growth media to limit wind-borne debris in those regions. The green roof areas must be partitioned into sections with areas not exceeding 1,450 m^2 (15,625 ft^2) and section lengths not exceeding 39 m (125 ft.). This requirement discretizes the green roof area and should be expected to cause some localized changes in the wind-flow behavior at those regions. The FM 1-35 also employs different safety factors (e.g. final design load = safety factor x design pressure) based on the usage of green roof growth media: 1.7 if growth media is used as ballast with a minimum depth of 200 mm (8 in.), 0.85 if growth media is used as secondary ballast, and 1.0 if pre-cultivated mats are used in lieu of planting of plugs or cuttings (FM Global, 2011).

ANSI/SPRI RP-14

The ANSI/SPRI RP-14 was developed following the scour performance study on modular tray green roofs conducted by Retzlaff et al. (2009). A distinction that sets the RP-14 apart from the FLL and FM 1-35 is that it is a wind design standard, and not a comprehensive green roof design guideline. The RP-14 derived primarily from the RP-4 – Wind Design Standard for Ballasted Single-ply Roofing Systems, as reflected by the identical design tables and similar sections found in both design standards (ANSI/SPRI, 2010; 2008). The design approach taken by the RP-14 to address the wind issue for green roofs is as follows:

1. Based on the building location and risk category, determine the basic wind speed and Exposure category,
2. Determine the building height, green roof depth, and the parapet height which extends above the top surface of the green roof,
3. Enter the design tables with the information from Step 2 and compare the allowable green roof system types (i.e. the selected system's design table wind speed must exceed the basic wind speed found in Step 1),
4. Determine the ballast requirements from the green roof system type selected

Because the design procedure requires users to enter design tables that were originally developed for ballasted roof systems in the RP-4, the RP-14 makes an implicit requirement that green roofs behave like gravel and/or roof paver systems at its most critical condition – where no vegetation exists. To control and prevent scour from creating this critical condition, the RP-14 design standard implements Retzlaff et al.'s (2009) findings, and require that the maximum diameter of exposed green roof media be limited to 127 mm (5 in.), otherwise denoted as "nominal coverage." If this condition is not met, the standard requires that the growth media be protected with appropriate erosion control methods (ANSI/SPRI, 2010). Unfortunately, this is the extent of guidance for the plant selection when utilizing the RP-14. The only additional provision in regards to vegetation is given in the commentary, which requires the limited usage of woody vegetation in wind-borne debris regions (i.e. hurricane-prone regions).

The RP-14 accounts for different roof regions by expanding upon the ballast definitions and requirements already set by the RP-4 in their system selection by also including modular tray green roof systems, but still requiring minimum dead loads of 1.05 kN/m^2 (22 psf) in the corners and edges, and 0.862 kN/m^2 (18 psf) in the field of the roof. Further, an additional clause in the standard advises users to increase the basic wind speed found in Step 1 by 8.9 m/s (20 mph) to account for Importance

Factors of III or IV, although this prescription would be invalid with the implementation of unique wind speed maps for each Importance Factor in ASCE 7-10 (ANSI/SPRI, 2010).

Summary

The reviewed green roof design guidelines show several reoccurring themes when determining a suitable wind design for green roofs, summarized as follows:

- Roof gravel and concrete pavers should be used in edge and corner regions of a building, where the highest wind loads are expected.
- Parapets are required to limit wind loads on green roofs.
- Design uplift loads can be mitigated by ballast weight of green roofs. The full uplift load should not be expected to act on the green roof system due to the additional roughness provided by vegetation, as delineated by the FLL (2008).
- Erosion control is required during establishment of the green roof.
- Woody plants should be limited to control wind-borne debris hazards.

Discussion

From these three reviewed guidelines, restrictions prohibit green roofs installed in edge and corner regions of a roof, as high wind loads and conical vortices typically occur there and can result in significant damage. However, if green roofs are installed strictly in the field (Zone 1) of a roof, could flow reattachment on a roof still cause damage to a green roof in an otherwise “safe” region? The FLL and FM 1-35 address the wind issue by only requiring the green roof dead load to resist the design uplift, but is that sufficient for design? Further, the FM 1-35 has a strict limitation on the maximum allowable wind speed as well as the requirement that the plant selection consists of at least 60% sedums, both of which are not suitable for hurricane-prone, subtropical/tropical states like Florida. The ANSI/SPRI RP-14 indirectly assumes that green roofs should be designed as ballast roof systems through its design tables, which

are identical to the ANSI/SPRI RP-4. Thus, a better understanding of how green roof components perform in response to high winds would prove beneficial in addressing the green roof's total resistance/capacity to wind loads.

Review of Indirect Wind Studies Related to Green Roofs

This section reviews the indirect studies that have been considered in the wind loading of green roofs. The purpose is to identify the similarities and differences between green roof systems, ballast roof systems, and ground-level wind studies on vegetation. In green roofs, the order in which catastrophic wind failure occurs typically initiates with plant losses. This then induces growth media exposure and eventual scour and blow-off, and potentially, the complete failure of the green roof.

Wind effects on vegetation at ground level

Miller (2007) identified that green roof vegetation plays a vital role in protecting against wind-induced erosion and scour damage. He attributes the vegetation's roughness and permeability to creating a turbulent boundary layer across the roof surface, which aids in mitigating potentially damaging uplift pressures. Unfortunately, no studies exist which consider the plant-growth media interaction for green roof systems during high winds. However, previous ground-level plant studies exist which thoroughly investigate how wind flow around vegetation affects the surrounding soil and sediment (Burri, Gromke, Lehning, & Graf, 2011; Walter, Gromke, Leonard, Clifton, & Lehning, 2011; Kim, Cho, & White, 2000; Lancaster & Baas, 1998), as well as common wind-induced plant failure mechanisms (Jin, Fourcaud, Li, & Guo, 2010; Sposaro, Chimenti, & Hall, 2008; Berry, Sterling, & Mooney, 2006; Duan, Barkdoll, & French, 2006; Sterling, Baker, Berry, & Wade, 2003). The focus in this subsection is to review those studies

and identify how this existing knowledge can be applied to vegetation installed on green roofs.

Evidence from both field- and wind-tunnel studies focusing on the plant-erosion relationship have determined that plants protect a soil surface from erosion in the following ways: 1) providing direct coverage and sheltering of the soil, 2) “trapping” airborne soil particles, 3) providing additional soil moisture which increases the soil’s cohesiveness, and 4) reducing the air flow’s momentum via the plants’ stems and leaves (Burri et al., 2011; Kim et al., 2000; Lancaster & Baas, 1998), and is summarized by Figure 2-14. In terms of scour reduction, it was found that an exponential decrease in the soil mass transport was a combined result from both increased vegetation coverage as well as higher rates of particle impact with plants, leading to momentum reduction of the wind flow (Burri et al., 2011; Kim et al., 2000; Walter et al., 2011).

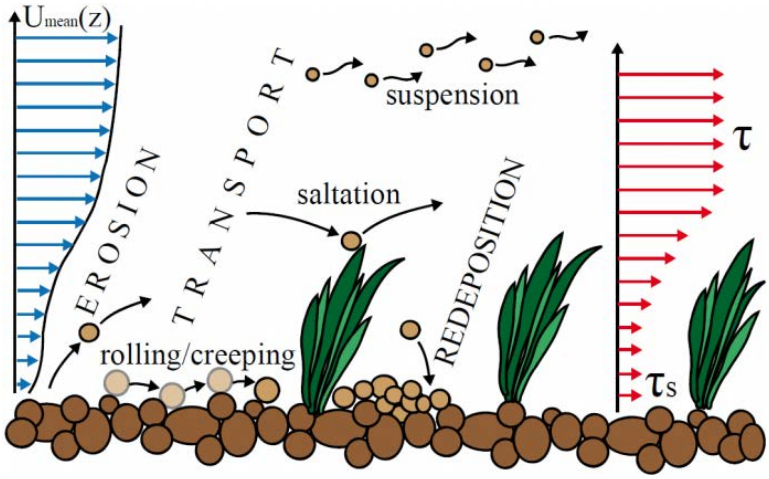

Figure 2-14. Turbulent boundary layer and aeolian processes over a vegetated surface. U_{mean} is the mean velocity, τ is the total shear stress and τ_s is the reduced shear stress acting on the ground. Figure courtesy of Walter et al., 2011.

The extent of scour protection provided by the vegetation, however, is entirely dependent upon successful performance of the vegetation itself. While the actual wind resistance of plants will vary between species and establishment age, the two main

wind-induced failure modes have been identified by the scour studies as either root or stem lodging. Stem lodging is when the plant stem is permanently displaced from the vertical, and typically occurs when the base-bending moment exceeds the failure moment of the stem base (Jin et al., 2010; Berry et al., 2006; Duan et al., 2006; Sterling et al., 2003).

Berry et al. (2006) determined that stem lodging of barley plants was a factor of the stem material strength, thickness and diameter of the stem, and can even depend on the type of fertilizer used on the soil, according to Jin et al. (2010). Root lodging occurs similarly in which the plant is permanently displaced with the vertical, but due to failures in the root base, rather than the stem (Sposaro et al., 2008). This failure mode is highly dependent upon the soil conditions, but also a factor of the plant's root structure (e.g. shape, growth, density) (Sterling et al., 2003).

Blow-off of embedded roof gravel

The ANSI/SPRI RP-14 prescribes a green roof wind design with a conservatively critical condition that the growth media is fully exposed. Although not explicitly stated, this is implied in the RP-14 by replication of the same design tables found in the RP-4, a wind design standard for ballast roof systems (ANSI/SPRI, 2008; 2010). Thus, this assumption relies on the basis that both green roofs and ballasted roof systems are primarily comprised of loosely-laid particles. However, the main distinction between these two types of systems is that ballast roof gravel typically consists of coarse-sized, inorganic, crushed stone and gravel (ANSI/SPRI, 2008) with no means of scour protection. Green roof growth media, however, is made up of both inorganic and organic material consisting of fine- and coarse-sized particles, but extensively-integrated with the vegetation's root system. This suggests that green roof growth media is not loosely-

laid on roofs like roof gravel, provided the vegetation has been well-established. Thus, if the ANSI/SPRI RP-14 is suggesting that green roofs can be treated as ballast roof systems through its reliance on the ANSI/SPRI RP-4's design tables, what led to the development of the ANSI/SPRI RP-4 and what conclusions can be pulled from its derivation and applied to green roofs?

In the 1970s, an extensive series of wind tunnel studies were conducted at the National Research Council of Canada on behalf of DOW Chemical of Canada Limited to explore the scour and blow-off failures of roof gravel due to high winds. The testing consisted of first estimating the failure wind speeds when roof gravel blow-off occurred (R.J. Kind, 1974a), performing wind tunnel tests with scale-model buildings and gravel to measure and validate the proposed estimation method (R.J. Kind, 1974b), and finally developing a design approach to mitigate roof gravel blow-off (R.J. Kind & Wardlaw, 1976). These tests provided benchmark results for all future roof gravel studies which explored the mechanics of roof gravel scour and blow-off, and formed a primary role towards the creation of the RP-4 (and hence, the RP-14).

Kind (1974b) identified four critical wind speeds at which roof gravel blow-off occurred based on their failure conditions: 1) initiation of large-scale or strong motion of stones, 2) indefinite scouring of stones, 3) initiation of blow-off over the upstream (windward) parapet, and 4) initiation of blow-off over the downstream (leeward) parapet. These critical wind speeds were measured for varying roof orientations, wind directions, building geometries and stone sizes (R.J. Kind, 1974b). The wind speeds were then reevaluated with the estimation technique presented in Kind's prior study (1974a) where the nominal diameter of the gravel was correlated with the minimum wind-induced shear

stress required to initiate gravel movement. It was found that the first three critical wind speeds (listed above) were directly proportional to the square root of the gravel's nominal diameter. Further, Kind (1974b) determined that the critical wind speeds for the gravel increased with increasing parapet height, decreased with increasing building height, and were lowest when the wind direction was set as 45 degrees. These studies were the backbone for the wind design procedure for ballast roof systems developed by Kind and Wardlaw (1976).

Scour of embedded roof gravel

Recent studies investigated the scouring patterns across the roof due to conical vortices, as well as low parapets' effects on gravel blow-off. Blessing et al. (2009) explored how different parapet configurations could mitigate conical vortices produced from critical wind directions. They were able to visually confirm the gravel scour patterns formed from these conical vortices (also described by Bienkiewicz and Sun (1992)). These conical vortices, when present, form cone-shaped, horseshoe patterns which extend from the corner of a roof when incoming winds reach their critical directions (e.g. 30 – 45 degrees). Masters and Gurley (2008) were presented with evidence of conical vortices on a number of graveled roofs which experienced scour damage following Hurricanes Francis, Jeanne, and Wilma in Florida (Figure 2-15).

Although parapets generally increase the failure wind speed for gravel, several studies have reported a critical parapet height at which increased roof uplift pressures and gravel scour occurred. A minimum parapet to building height (h/H) or length (h/L) ratio must be exceeded in order to prevent significant increases in roof suction pressures when compared to the same roof without a parapet (Pindado & Meseguer, 2003; Stathopoulos, Baskaran, & Goh, 1990; Baskaran & Stathopoulos, 1988;

Stathopoulos & Baskaran, 1988). Increases in negative pressure coefficients (Cp) due to this phenomenon were reported of up to twice the Cp values of a non-parapet roof (Stathopoulos & Baskaran, 1988). Karimpour and Kaye (2012) found that these increased suction pressures due to low parapet heights translated to lower critical wind speeds for their scale-model graveled roof study, but did not extrapolate their data to full-scale. However, Karimpour and Kaye (2013) found that while low parapets can still lead to initiation of motion for gravel at lower wind speeds, implementation of a parapet would always reduce gravel losses off of a roof when compared to a roof with none. From their 2013 study, Karimpour and Kaye defined the primary role of a parapet as to maintain the gravel on the roof, as opposed to preventing blow-off from occurring.

Figure 2-15. Horseshoe scour pattern due to conical vortices atop a Winn Dixie plaza. Photo courtesy of Dr. Forrest Masters and Whiting, 2007.

Roof paver uplift and blow-off

Aside from Retzlaff et al.'s (2009) scour study, the wind performance of modular green roof systems in realistic conditions had not been investigated prior to the study conducted at UF. The ANSI/SPRI RP-14 allows for modular green roof trays, but simply adopted the ANSI/SPRI RP-4's definitions for minimum dead loads of at least 104 kg/m^2

(22 psf) and 88 kg/m^2 (18 psf) for #2 and #4 ballast requirements, respectively (ANSI/SPRI, 2010; 2008). Like the previous subsection, the reproduction of the minimum dead load requirements in the ANSI/SPRI RP-14 suggests that green roof modules can be treated like concrete pavers, provided that protection against growth media and vegetation losses is ensured.

As with graveled roof systems, similar effort was placed in understanding how roof pavers performed in high winds, as pavers were commonly employed in perimeter and corner regions when gravel was unsuitable. Studies agree that the net external wind load which acts on a roof paver can be taken as the sum of the pressures acting underneath the roof paver (i.e. between the paver's bottom surface and roof deck) and the pressures acting on the upper surface of the roof paver; otherwise known as the differential pressure between the upper and underlying surfaces of the paver. Many of these studies have found that the underlying pressures are closely correlated with the upper surface pressures, and respond almost instantaneously to any pressure changes that occur to the upper surface (Mattacchione & Mattacchione, 1999; B. Bienkiewicz & Y. Sun, 1992; Gerhardt, Kramer, & Bofah, 1990; Bienkiewicz & Meroney, 1988; R. J. Kind & Wardlaw, 1982). This close correlation between upper surface and underlying pressures plays a major role in whether pressure equalization or net uplift of the roof paver occurs. The critical condition results in net uplift and occurs if the differential pressure between the top and underlying surfaces exceeds the weight of the paver(s). Pressure equalization is when the upper surface and underlying pressures "offset" and result in a wind load that can be significantly less than the measured wind load on an impermeable roof surface.

Following parametric studies conducted by Bienkiewicz and Sun (1997; 1992), it was determined that the permeability of and the wind flow resistance around and between roof pavers play vital roles in determining the correlation between the upper and underlying pressures. Higher pressure equalization can be achieved if the ratio between the space-between and space-underneath pavers is increased (Bienkiewicz & Sun, 1997; Bofah, Gerhardt, & Kramer, 1996; Mcdonald, Wang, & Smith, 1994) and permeable pavers are utilized (Bofah et al., 1996; Mcdonald et al., 1994).

Summary

Wind Effects on Vegetation

- Wind-induced failure of vegetation typically occurs as either root or stem lodging. These failure mechanisms are dependent of the plant's biological factors as well as the soil conditions.
- Vegetation provides protection against growth media scour by disrupting the wind flow and reducing the wind flow's momentum when upright, and sheltering substrate when prostrate. The root systems also provide extra cohesiveness to the soil.

Scour and Blow-off of Roof Gravel

- The critical wind velocity for which blow-off occurs is a function of the square root of the particle diameter.
- Conical vortices can cause significant scour damage to ballast in edge and corner locations.
- Parapets aid in mitigating scour due to conical vortices but also play a primary role in containing displaced roof gravel to the roof.

Roof Paver Uplift and Blow-off

- Paver uplift occurs when a net negative pressure differential greater than the paver weight forms between the underside and upper surface of the paver.
- Pressure equalization can mitigate potentially damaging pressure differentials, in which the increased permeability of and spacing below and between pavers promote wind flow to reach the paver's underside. If equalization can occur instantly, no net negative uplift can occur.

Discussion

The wind resistance of green roofs can be predicted at a per-component level utilizing the existing indirect wind studies reviewed in this section. This is beneficial since green roof failure would typically occur in stages. For example, the vegetation provides the primary protection against growth media scour and damage to underlying membranes. Roof gravel wind performance studies suggest that unprotected green roof growth media will fail at much lower wind speeds than typical roof gravel due to the finer, organic material, but only if the growth media is truly “loosely-laid.” Thus, the question that arises is: should the added protection provided by vegetation be considered? The reviewed ground-level plant studies reveal that vegetation coverage aids in reducing the damage potential of wind flow near a green roof surface by absorbing the wind flow’s momentum and sheltering otherwise exposed media. In regards to modular tray green roofs, the roof paver studies reviewed suggest that the same mechanics which induce paver uplift and blow-off could apply to green roof modules as well. If so, can modular tray green roof systems benefit from pressure equalization, and reduce chances of uplift failure?

Summary and Comparison

The design of green roofs against high winds is complex in comparison with traditional roofing systems. The success of a green roof is highly dependent upon the successful performance of each of its components, as a minor failure in one can cause a cascading effect that leads to catastrophic failure in the entire system. Therefore, is a holistic approach (like that described by the FLL and briefly the FM 1-35) the best method to design green roofs to be wind resistant?

Closer inspection of related studies shows that the vegetation and growth media layers have dominant roles in determining the wind resistance of a green roof system. The reviewed case-studies and existing design guidelines highlight the importance in correct installation procedures, as well as green roofs' potential susceptibility to wind-damage. Several questions and remarks arise from the presented literature:

- Should green roofs be designed as "layered" ballast roof systems in which designers must ensure the adequate wind performance of major green roof components (e.g. vegetation, growth media, and total system weight)?
- Which parameters most adversely affect the wind resistance of green roofs and how can investigators quantify them?
- Is it sufficient to only consider design uplift pressures for green roofs, and thus, only pressure chamber testing? What happens to green roofs subject to highly turbulent wind conditions (e.g. conical vortices)? If green roofs are dependent on the surrounding wind flow, chamber testing will not adequately represent what is seen in field conditions.
- What happens to green roofs in the field region of a roof? Can flow reattachment occur and still cause damage?
- Can modular tray green roof systems be treated similar to roof pavers? If so, are the same failure mechanisms present (i.e. overturning, uplift, sliding)? Which of these failure mechanisms is dominant?

These questions and remarks formed the primary motivation for the full-scale wind testing conducted at the University of Florida. It was hypothesized that wind tunnel models would only provide a general sense of how green roofs perform due to the difficulty in modeling vegetation. Thus, through full-scale testing, real plants and full-scale green roof materials could be utilized, allowing investigators to localize and identify problems at a per-component level. In doing so, the question of how green roofs perform under extreme winds can be better addressed and the current knowledge gaps between design guidelines, existing case studies, and related wind research can be bridged.

CHAPTER 3
GREEN ROOF WIND TESTING WITH UF'S HURRICANE SIMULATOR

Following the pilot study (described in Chapter 2), extensive wind testing was conducted in two phases on both built-in-place and modular tray green roof systems with UF's hurricane simulator. The parametric study was designed to account for as many factors as possible for a fixed building geometry, as their effects on the green roof wind performance were still unknown. The investigators focused on both determining a suitable plant selection and the wind performance for green roofs specifically in Florida. This chapter reviews the development and test procedures for the green roof systems in each phase. Results for both phases are presented at the end of the chapter.

Objective

The literature review presented in Chapter 2 indicated that roofs and roof systems are dependent upon many different parameters which vary based on the building geometry, type of green roof system, and incoming wind. The objective of the study was to determine the plant, structure and incoming wind parameters which most-adversely affected the wind resistance of green roof systems when subjected to simulated wind loads. The varied parameters are summarized in Table 3-1.

Description of Hurricane Simulator

Simulated winds were produced with UF's hurricane simulator (Figure 3-1). The simulator consists of four 520 kW (700 HP) diesel engines which power eight 1.5 m (5 ft.) diameter vane-axial fans. A 19000 L (5000 gal) water tanker is used to cool the engines during testing. The fans converge into a chamber where wind speeds up to 53.6 m/s (120 mph) exit a test cross-section of 3.0 m by 3.0 m (10 ft. by 10 ft.). Since the simulator was raised approximately 0.9 m (3 ft.) off of the ground, the center of the

test section was taken as 2.4 m (8 ft.) from the ground. The hurricane simulator is run by two operators: one controlling the engine throttles, and another inside a nearby instrumentation trailer monitoring the wind speeds and fan rpms. For the purpose of this study, the longitudinal turbulence intensity (I_{uu}) at the test roof height (2.4 m) was determined to be approximately 6% (F. J. Masters, Gurley, & Prevatt, 2008; Mensah, Datin, Prevatt, Gupta, & Lindt, 2011).

Table 3-1. Summary of parameters varied in both phases of wind testing.

	Phase 1	Phase 2
Number of Test Trials	6 w/ 9 modules per test[a]	8 w/ 9 modules per test 8 BIP[c]
Wind Direction	90°	45°
Parapet Height (mm)	300	0
Plants Tested[b]	A,B,C,D,E,F	A, B, C, D, E, F (retested) G, H, I, J, K, L, M, N
Plant Heights	Mixed	Mixed (retested), Tall & Short
Establishment (mo.)	3, 5, 9	6, 13 (modules) 1.5 (BIP[c])
Growth Media Depth (mm)	100, 200 (modules)	100, 200 (modules) 150 (built-in-place)
Wind Speed (m/s)	8.9, 13.4, 22.3, 31.3, 40.2, 53.6	44.7
Test Duration (min)	5	10 (typical); 20 (extended)
Moisture Level	In-situ	In-situ or Saturated

[a] Unprotected module location varied
[b] Refer to Table 3-2 for plant species

Figure 3-1. Isometric view of UF's Hurricane simulator. Photo courtesy of author.

Plant Selection

One of the primary goals of the study was to establish a selection of plants suitable for green roofs in Florida. Florida's unique climate ranges from sub-tropical to tropical, and regularly experiences a wide range of extreme weather. As such, the United States Department of Agriculture (USDA) ranks Florida's Plant Hardiness Zones range between Zones 8 through 11a (PRISM, 2012) and must account for the following considerations when selecting suitable plants: high temperatures and humidity, periods of drought, occasional freezes, periods of heavy rainfall, and hurricanes.

The study's plant selection was based on vegetation types that were most common on existing green roofs in Florida, as well as readily-available plants from regional nurseries. Good performance of plants for at least one year in an extensive green roof representative of Florida conditions was an important criterion. Criteria for plant selection included the following characteristics:

- The capacity to withstand high temperatures and humidity for extended periods of time
- The ability for moderate to fast growth rates in response to short project timeline.
- The capacity for extended drought tolerance and withstanding seasonally heavy rains
- The capacity to withstand freezes of -3.9 to 1.1°C (25 to 34°F), depending on location

Taller herbaceous ornamentals (760 to 914 mm), shorter ground covers (100 to 150 mm) and a variety of plant forms were included in the 14 species in these trials. The 14 species (Table 3-2) selected include a variety of plant forms (orthotropic vs. prostrate), leaf area (small vs. large), stem composition (hard vs. soft), and root types (short tap root vs. fibrous). Further, the list includes herbaceous perennial native plants,

ornamentals, and succulents with good track records in Florida's climate. Two varieties of Sedums and other succulents were utilized in the study as species from UF field trials that offered promise for use in Florida (T. D. Vo, Prevatt, Acomb, Schild, & Fischer, 2012).

Table 3-2. Summary of the plant selection for the green roof wind study.

ID	Species	Duration	Growth Habit	Plant Form	Leaf Area	Stem Composition	USDA Hardiness Zone(s)
A	*Aptenia cordiflolia*	Perennial	Subshrub Forb/herb	Prostrate	Large	Soft	6 to 8
B	*Delosperma cooperi*	Perennial	Groundcover	Prostrate	Small	Soft	5 to 9
C	*Dianthus gratianopolitanus*	Perennial	Herb	Prostrate	Small	Soft	3 to 8
D	*Lantana montevidensis*	Perennial	Shrub Subshrub	Orthotropic	Small	Woody	8 to 10
E	*Salvia rutilans*	Perennial	Shrub	Orthotropic	Large	Woody	8 to 10
F	*Sedum rupestre*	Perennial	Herb	Prostrate	Small	Soft	5 to 8
G	*Bulbine frutescens*	Perennial	Forb/herb	Orthotropic	Small	Soft	9 to 11
H	*Coreopsis lanceolata*	Perennial	Forb/herb	Orthotropic	Small	Soft	7 to 11
I	*Delosperma nubigenum*	Perennial	Groundcover	Prostrate	Small	Soft	5 to 10
J	*Gaillardia aristata*	Perennial	Forb/herb	Orthotropic	Small	Soft	3 to 11
K	*Lantana camara*	Perennial	Shrub/Vine	Orthotropic	Large	Woody	10 to 11
L	*Portulaca grandiflora*	Annual	Forb/herb	Prostrate	Small	Soft	5 to 11
M	*Rosmarinus officianalis*	Perennial	Subshrub/Shrub	Orthotropic	Small	Woody	8 to 10
N	*Sedum rupestre 'Angelina'*	Perennial	Herb	Prostrate	Small	Soft	5 to 8

Phase 1 Materials and Methods

The first phase of wind testing consisted of six test trials; three with 200 mm (8 in.) deep intensive modules, and three with 100 mm (4 in.) deep extensive modules. Each test trial included eight protected green roof modules, and a single unprotected module to compare the effects of both the vegetation and roof locations on the systems' wind resistance. A test matrix detailing Phase 1 of the wind testing is shown in Table 3-3. Each green roof module was planted with six plant species (IDs: A, B, C, D, E, and F

from Table 3-2) placed in a two by three array. Due to timing constraints, built-in-place assemblies were not constructed during this phase of testing.

Table 3-3. Modular tray green roof wind test matrix for Phase 1.

Test ID	Wind Testing Date	Module Depth (mm)	Establishment Period (mo.)	Parapet Configuration	Unprotected Module Location[a]
4” – T1	08/18/2011	100	3	Encompassing	9
4” – T2	08/18/2011	100	3	Encompassing	5
4” – T3	08/18/2011	100	3	Encompassing	1
8” – T1	08/18/2011	200	3	Encompassing	7
8” – T2	10/20/2011	200	5	Encompassing	8
8” – T3	02/16/2012	200	9	Leeward wall removed	8

[a] Refer to Figure 3-7 for Phase 1 location map

Preparation of Green Roof Modules

Fifty green roof modules were planted on May 5, 2011, and grown in an open field at the Alachua County Extension Office in Gainesville, FL (Figure 3-2). Twenty-five of the 50 were intensive 200 mm deep modules and the remaining half were extensive 100 mm deep modules, as differentiated in Figure 3-3Figure. Since each test trial would utilize eight protected modules and a single unprotected module, only 24 of the 25 planted modules would be tested in the six test trials planned. As a result, one protected module from both the extensive and the intensive groups of green roof modules were excluded from wind testing, and used for comparison.

These modules were filled with growth media and subsequently planted with a mixture of six plant species, as detailed above in Table. The plant selection varied between woody-stemmed and succulent species and were based on the criteria specified in the previous list. Planted green roof modules were elevated off of the ground with four tables, and a single rotating sprinkler irrigation system was installed to aid in the plant growth.

Figure 3-2. Planted green roof modules elevated from the ground at the Alachua County Extension Office. Photo courtesy of author.

Figure 3-3. Size differences of empty extensive 100 mm (left) and intensive, 200 mm (right) deep green roof modules. Photo courtesy of author.

On July 14, 2011, about one month prior to testing, the green roof modules were transported from the Extension Office to UF's Eastside Campus via moving trucks to prevent external wind damage during the transfer. The one month timeframe was to allow plants to fully recover from any stresses incurred due to the relocation process. Modules were again placed on tables and a similar single rotary sprinkler system was setup at the Eastside Campus. Erroneous disconnection of the irrigation system occurred sometime between July 30 and August 5, causing light damage to the taller, woody-stemmed plants. In response, in addition to the established irrigation, plants were hand-watered and fertilized up until the time of testing.

Description of Test Structure

A 2.4 m (8 ft.) high, three-sided wall test structure was constructed with a plan area of 2.3 m by 2.3 m (7.5 ft. by 7.5 ft.) (Figure 3-4). The structure was placed 3.6 m (12 ft.) away from the hurricane simulator opening. It was oriented so that the windward wall was normal (90 degrees) to the incoming wind flow, and the two adjacent walls were set parallel to the wind direction. The leeward side of the structure was left open so that a hydraulic lift could raise a platform which held the array of green roof modules to the desired test height. A 300 mm (12 in.) tall by 150 mm (6 in.) wide parapet (measured from the raised platform's upper surface to the top of the parapet) encompassed all four sides of the mockup roof area for five of the six test trials. The leeward parapet was removed for the final test trial due to observed wind flow reversals during testing.

Figure 3-4. Phase 1 test setup depicting the green roof and hurricane simulator location. Photo courtesy of author.

Instrumentation and Data Acquisition Methods

Wind speed monitoring

Wind speeds were monitored via an RM Young Model 05103 V wind monitor placed in front of the windward wall of the test structure (Figure 3-5). The anemometer was positioned above grade at the test roof height at 2.4 m (8 ft.), and 0.6 m (2 ft.) offset from the windward corner of the test structure. The anemometer recorded and exported the wind speed data to a text file via a LabView program for the first three test trials, but was used only to monitor the wind speeds for subsequent test trials.

Figure 3-5. RM Young Model 05103V wind monitor. Photo courtesy of author.

Visual assessment

Visual assessment of the green roof modules during the wind testing was obtained via two high-speed digital cameras, and a high-definition camcorder. Also, photographs were taken at an elevated position, towards the windward side of the green roof array immediately before and after wind testing to compare how module weight changes (detailed in following subsection) compared to their appearance. The high-speed digital cameras were enclosed in a plywood and Plexiglas case and placed approximately 3.3 m (11 ft.) away from the side of the test structure (refer to the right

side of Figure 3-4) on 3.6 m (12 ft.) tall camera tripods. These cameras were positioned to capture two profile views of the green roof vegetation during testing: an overall profile of the green roof modules, and a close-up view of the back row and leeward parapet. The high-speed cameras recorded at a resolution of 240 frames per second (fps). To provide sufficient contrast, a gridded backdrop was raised via forklift approximately 4.3 m (14 ft.) away from structure wall opposite of the high-speed cameras. In addition to the high-speed cameras, a high-definition camcorder was used to capture real-time video footage of the green roof modules as they were tested. This camcorder was positioned directly above the hurricane simulator, and had an overall view of the roof section as testing commenced. The real-time footage would serve as the primary means of identifying problematic areas of the roof section.

Pre- and post-test weight measurement

Pre- and post-test assessments were performed via weight measurement and still photography of the modules. Module weights were measured by placing individual modules onto a tray that hung off of a single frictionless bearing attached to an Omega Model LCR-200 single S-beam load cell (Figure 3-6). The load cell had a 90.7 kg (200 lb.) capacity and was accurate up to ±0.18 kg (±0.2 lb.). An NI USB-6210 data acquisition module was used in junction with a custom channel box to relay the voltage data from the load cell to the laptop in which a LabView program readout the module weights. Individual weights were recorded approximately 20 minutes before and immediately after wind testing to determine the material losses/gains on each module. Module weight changes were calculated via Eqn. 3-1.

$$\Delta\% = \left(\frac{W_{post} - W_{pre}}{W_{pre}}\right) \cdot 100\% \quad (3\text{-}1)$$

Where:

W_{post} = measured post-test green roof module weight

W_{pre} = measured pre-test green roof module weight

Figure 3-6. Omega LCR-200 S-beam load cell attached to frame and weighing tray. Photo courtesy of author.

Test Procedure

Wind testing of the intensive and extensive green roof modules was performed following the test schedule detailed by Table. Phase 1's primary goal was to obtain a qualitative assessment of how green roof modules behave to hurricane-force winds. Unprotected module locations were varied between each test trial to allow for comparisons of how protected modules perform in the same roof location and how the wind flow varies across the roof. The single unprotected and eight protected green roof modules were placed on the test roof deck and their locations were recorded in relation to the hurricane simulator, as denoted by Figure 3-7. A step-and-hold test procedure

was followed in which each wind speed for Phase 1 (Table 3-1) was run for 30 seconds before ramping up to the following wind speed. The final wind speed of 53.6 m/s (120 mph) would be held for an additional 60 seconds for a total of 90 seconds. A summary of the test procedure is as follows:

1. Weigh and record the nine green roof modules (i.e. eight protected and one unprotected)
2. Transfer modules from growth site to test structure
3. Manually load modules onto deck platform, record locations within the array (Figure 3-7), and raise to test height with hydraulic lift
4. Photograph the green roof array (i.e. pre-test photo)
5. Run wind test while recording video footage
6. Photograph the green roof array (i.e. post- photo)
7. Transfer modules back to growth site, reweigh and record the final weights

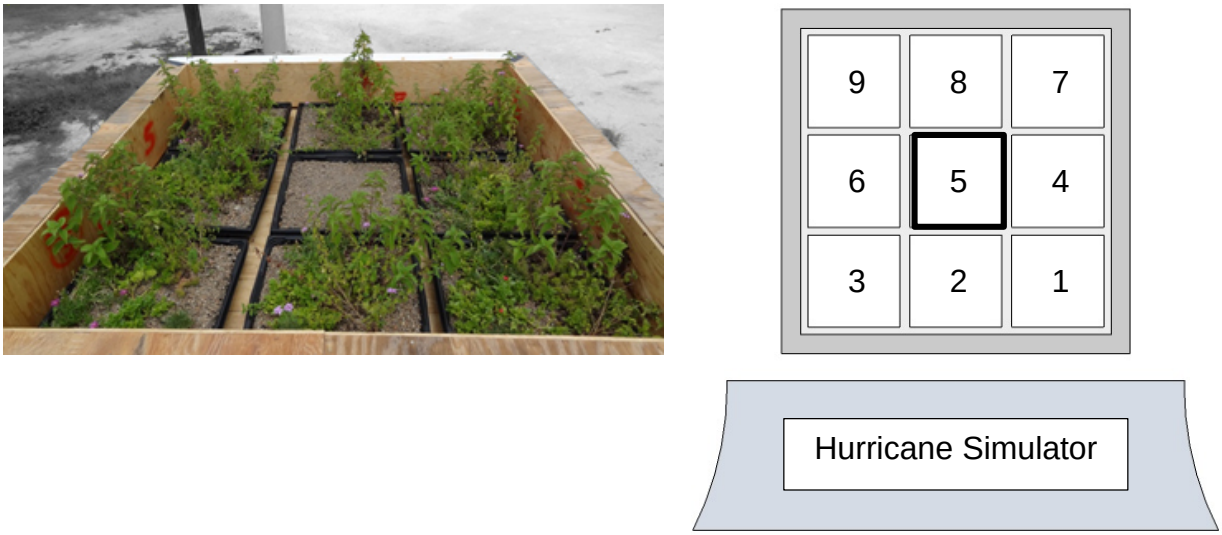

Figure 3-7. Module placement and corresponding location identification with respect to hurricane simulator position for Phase 1. Note: the heavy border indicates the unprotected module location. Photo courtesy of author.

Phase 2 Materials and Methods

The second phase of wind testing was designed to evaluate the green roof performance under more severe wind conditions by rotating the test structure 45

degrees to the wind, removing the parapet, and utilizing a constant high wind speed of 44.7 m/s (100 mph) for longer durations, as opposed to varying wind speeds. Phase 2 retested the 50 green roof modules from Phase 1 and performed testing on another 54 newly planted modules. Phase 2 also introduced 12- 150 mm (6 in.) deep built-in-place green roof assemblies for wind testing.

Preparation of Green Roof Modules

Fifty-four new green roof modules were planted at the end of December 2011 for Phase 2. Because the green roof modules tested in Phase 1 were each planted with a mixture of both tall and short plant species, the modules in Phase 2 isolated plant heights to highlight their effect on the overall wind performance. All of Phase 1's green roof modules were moved back to the Alachua County Extension Office following wind testing, where both sets (i.e. Phase 1's and Phase 2's) of modules were grown and irrigated. The single-rotary sprinkler used in Phase 1 was replaced with micro-misters for more concentrated irrigation coverage, and modules were elevated off the ground similar to Phase 1. Retested Phase 1 modules were ensured to be placed in the same roof locations for Phase 2. A summary of the modular tray green roof test matrix and plant species used in Phase 2 can be found in Table 3-4.

Construction and Preparation of Built-in-Place Green Roof Assemblies

The built-in-place green roof systems were designed and constructed on a wood deck with self-adhered waterproofing membrane according to the manufacturer's specifications (Figure 3-8). First, a drainage layer was laid atop the 2.4 m by 2.4 m (8 ft. by 8 ft.) wooden deck, followed by the filter fabric layer, and then aluminum edge restraints to form a container for the green roof. Then, a drainage cup mat was placed above the filter fabric, in which the drainage cups were filled with growth media, and

then wetted to flush any fine debris out of the drainage. The contained area was then filled with growth media and finally planted. Additional 50 mm by 250 mm (2 in. by 10 in.) wood boards were fastened to the deck along the perimeter of the edge restraints.

Table 3-4. Modular tray green roof wind test matrix for Phase 2.

Test ID	Wind Testing Date	Establishment Period (mo.)	Media Depth (mm)	Plant Height	Plant Species[a]	Test Duration (min.)
T2	06/18/2012	13	100	Mixed	A, B, C, D, E, F	10
T3	06/18/2012	13	100	Mixed	A, B, C, D, E, F	10
T5	06/20/2012	13	200	Mixed	A, B, C, D, E, F	10
T6	06/20/2012	13	200	Mixed	A, B, C, D, E, F	10
T7	06/21/2012	6	100	Tall	D, H, J, M	20
T8	06/20/2012	6	100	Short	B, F, F, I	10
T10	06/22/2012	6	200	Tall	H, J, M	20
T11	06/22/2012	6	200	Short	A, F, F, I	10

[a] A: *Aptenia cordifolia*, B: *Delosperma cooperi*, C: *Dianthus gratianopolitanus*, D: *Lantana montevidensis*, E: *Salvia rutilans*, F: *Sedum rupestre*, H: *Coreopsis lanceolata*, I: *Delosperma nubigenum*, J: *Gaillardia aristata*, M: *Rosmarinus officianalis*

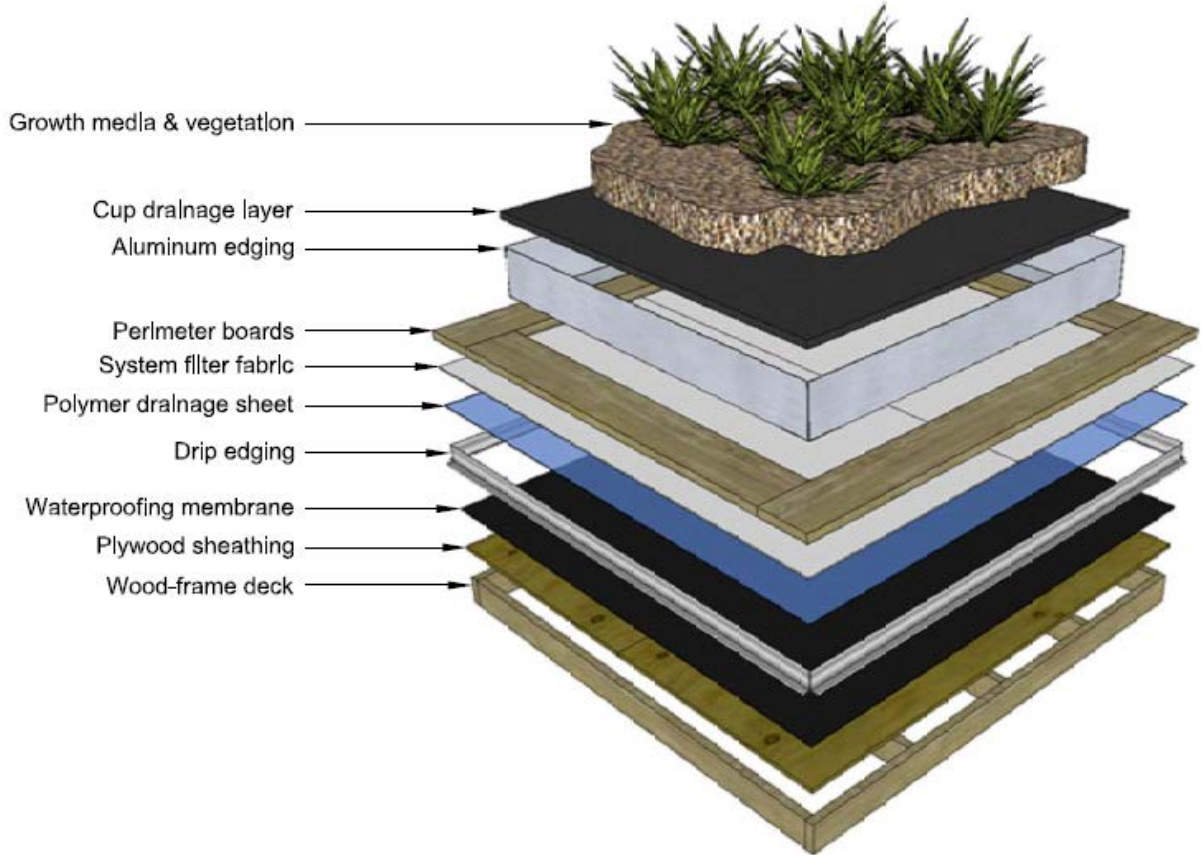

Figure 3-8. Model rendering of a built-in-place assembly's component setup. Figure courtesy of author.

The built-in-place green roof assemblies were planted as monocultures varying between tall and short plant species, and placed at a 1:12 slope to prevent ponding during irrigation. Eight built-in-place green roof trials were wind tested: four with "normal" moisture conditions and four tested immediately after irrigating the 1.8 m by 1.8 m (6 ft. by 6 ft.) green roof with 200 L (55 gal.) of water. This was done to simulate the expected heavy rainfall intensity likely to occur during a hurricane (T. D. Vo et al., 2012). A summary of the test matrix and plant species used for the built-in-place green roof assemblies is shown in Table 3-5.

Table 3-5. Built-in-place green roof assembly wind test matrix for Phase 2.

Test ID	Plant Date	Wind Testing Date	Establishment Period (weeks)	Moisture Content	Plant Species[a]	Plant Height	Test Duration (min.)
S-M1	N/A	06/12/2012	N/A	Wet	A, G, J, K, L	Mixed	10
N-S1	04/25/2012	06/12/2012	7	Normal	L	Short	10
N-S2	04/25/2012	06/13/2012	7	Normal	A	Short	10
N-T1	04/25/2012	06/12/2012	7	Normal	K	Tall	10
N-T2	04/25/2012	06/13/2012	7	Normal	G	Tall	10
S-S1	04/28/2012	06/13/2012	6.5	Wet	L	Short	10
S-S2	04/28/2012	06/13/2012	6.5	Wet	A	Short	10
S-T1	04/28/2012	06/19/2012	7.5	Wet	K	Tall	20
S-T2	04/28/2012	06/19/2012	7.5	Wet	G	Tall	20

[a] A: *Aptenia cordifolia*, G: *Bulbine frutescens*, J: *Gaillardia aristata*, K: *Lantana camara*, L: *Portulaca grandiflora*

Description of Test Structure and Test Site

Due to ongoing construction at the Powell Structures and Materials Laboratory at UF's Eastside Campus, wind testing for Phase 2 was conducted at UF's Auxiliary Library Facility located approximately 2.7 km (1.7 mi.) north of the lab. The new test site proved beneficial for the author as it was in close proximity (< 200 m) to the Alachua County Extension Office, where the modular tray and built-in-place green roofs were growing. This allowed investigators to continue wind testing of the green roof systems without introducing plant stresses that would have been incurred from a longer transport distance.

A large wooden platform raised 0.9 m (3 ft.) above grade was constructed for unrelated demonstrations with the hurricane simulator immediately prior to the green roof wind testing. Since the existing wooden platform did not obstruct the hurricane simulator's wind flow, deconstruction of the platform was not necessary. The green roof test structure consisted of two framed and sheathed walls measuring 1.5 m high by 2.4 m long (5 ft. by 8 ft.) anchored to the platform, with an elevated wooden deck that would support the green roof systems during testing. The two walls joined to form a 90 degree angle approximately 3.6 m (12 ft.) away from the hurricane simulator opening, and was oriented to replicate a cornering wind condition (i.e. 45 degrees to the incoming wind). An overview of Phase 2's test setup can be seen in Figures 3-9 and 3-10.

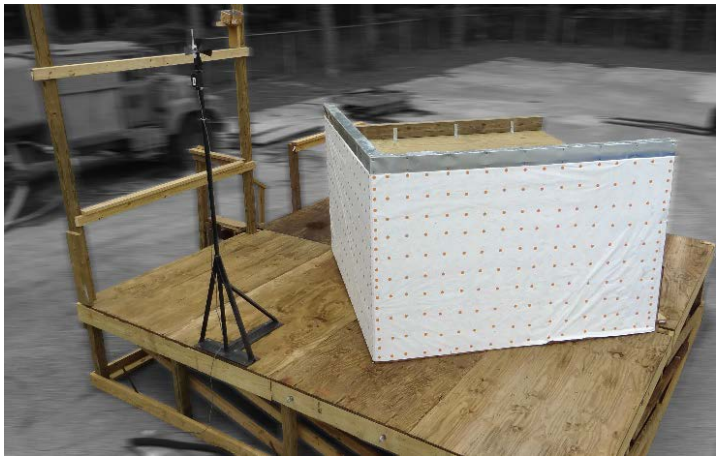

Figure 3-9. Elevated view of rotated test structure placed on wooden platform in Phase 2. Photo courtesy of author.

Figure 3-10. Profile view of wind testing setup for Phase 2. Photo courtesy of author.

Instrumentation and Data Acquisition

Wind speed monitoring

Wind speeds were again monitored by an operator with the RM Young wind anemometer described in Phase 1's description (refer back to Figure 3-5). For Phase 2, the wind anemometer was anchored to wooden deck and was situated approximately 0.9 m (3 ft.) above the test deck.

Pre- and post-test weight measurement

Pre- and post-test modular tray green roof weights were measured with a 550 mm by 550 mm (22 in. by 22 in.) Brecknell low-profile floor scale (Figure 3-11). The scale had a maximum capacity of 225 kg (500 lb.) with an accuracy of 0.1 kg (0.2 lb.), and displayed the measurements onto a digital display. This floor scale was purchased to expedite the repetitive process of weighing, and reweighing the 100 green roof modules during the second phase of wind testing.

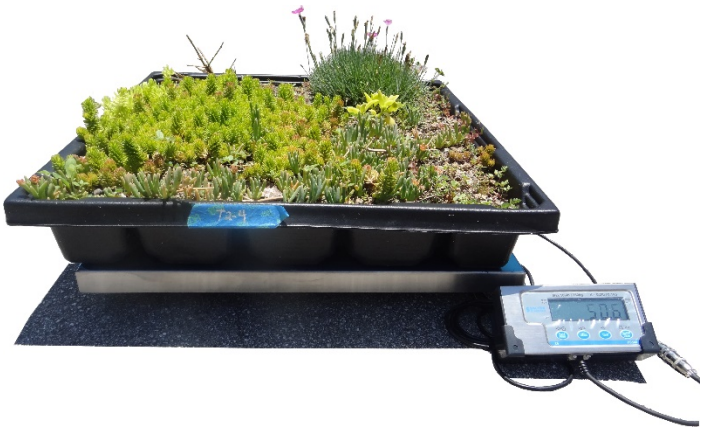

Figure 3-11. Brecknell low-profile floor scale used for weighing modular tray green roofs in Phase 2. Photo courtesy of author.

Like Phase 1, two high-speed cameras were mounted to a wooden post which extended above the test section to focus on the profile behavior of the green roof systems during wind testing. A high-definition camcorder was again used to provide overview footage of the green roof systems during testing, and was operated by

personnel elevated via a personal lift placed beside the hurricane simulator (Figure 3-10).

Visual assessment

Vegetation coverage ratios were calculated from overhead photographs taken of both built-in-place and modular tray green roof systems before, between, and after wind testing periods. Appendix B details how coverage ratios were calculated utilizing Adobe Photoshop, and the corresponding results are shown in Table B-1.

Growth media moisture content

To determine whether the growth media's moisture content has any effect on the green roof wind performance, normal "in-situ" and high saturation conditions were considered before testing the green roof systems. In-situ conditions required no additional water to be added to the green roof, and were considered for both the built-in-place and modular tray green roofs. The high saturation condition was considered only for the built-in-place assemblies, where prior to wind testing, three rain gauges (marked "L," "C" and "R" to identify their roof location) were installed across the green roof. A sprinkler with a hemispherical range was then placed on the edge of the assembly (Figure 3-12) and an irrigation pump then applied 208 L (55 gal) of water across the planted growth media (Figure 3-13). After the tanks were emptied, the three rain gauge readings were recorded.

Soil samples were collected after wind testing and overhead photographs were taken, for both green roof systems. For built-in-place assembles, soil samples were collected in five locations across the roof, and named in accordance to the convention depicted by Figure 3-14. A single soil sample was collected from the center of each tested modular tray green roof specimen. Soil samples were appropriately bagged,

labeled, and contained before being sent to the laboratory for moisture content analysis (Appendix C). The times at which the 208 L water barrel was depleted and soil samples were collected were recorded to document the total time elapsed.

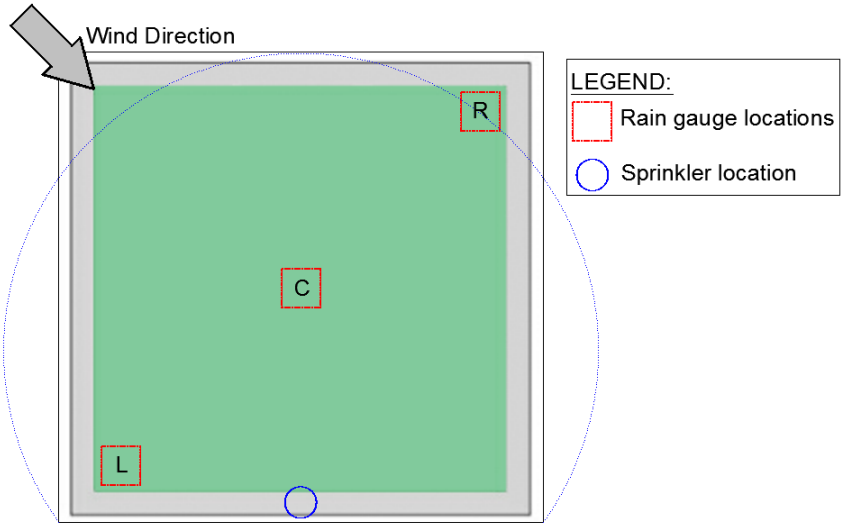

Figure 3-12. Annotated diagram detailing the sprinkler and rain gauge locations for built-in-place assemblies subject to artificial saturation. Figure courtesy of author.

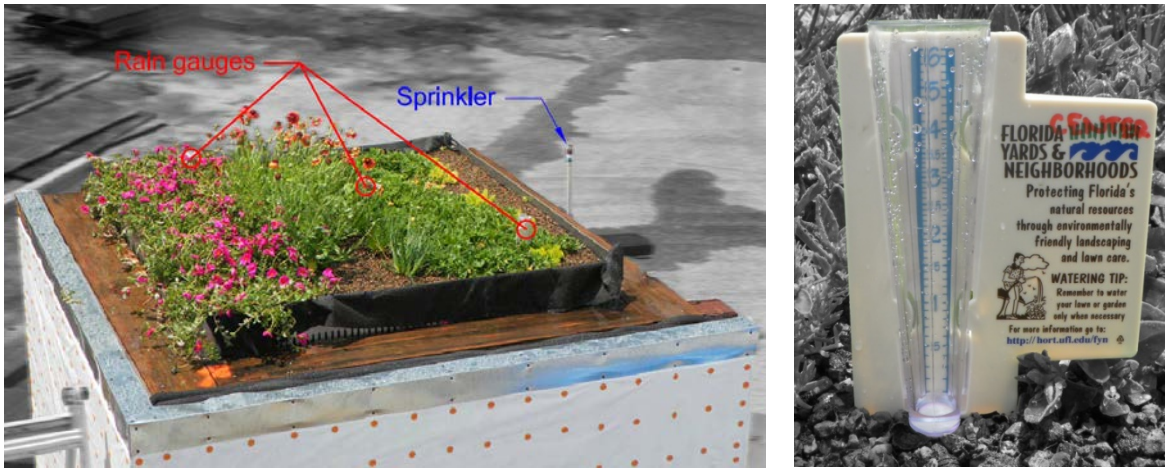

Figure 3-13. Photographs depicting the typical configuration for built-in-place assemblies subject to artificial saturation and a close-up view of a rain gauge. Photos courtesy of author.

Test Procedure

Phase 2's test procedure for both built-in-place assemblies and modular tray systems was similar to that in Phase 1, but included several additional steps unique from the procedure detailed in the previous section. The target wind speed for all test

trials was 44.7 m/s (100 mph), which limited the hurricane simulator operation to 5 minute intervals to prevent overheating. Throughout the duration of the wind testing of both green roof systems (i.e. built-in-place assemblies and modular trays), observation logs were kept to document any irregular behavior such as biomass losses. These observations were segmented into the 5 minute intervals previously described and are included at the end of this report in Appendix E. The procedures for both the built-in-place and modular tray green roof systems are separated and detailed in the following lists.

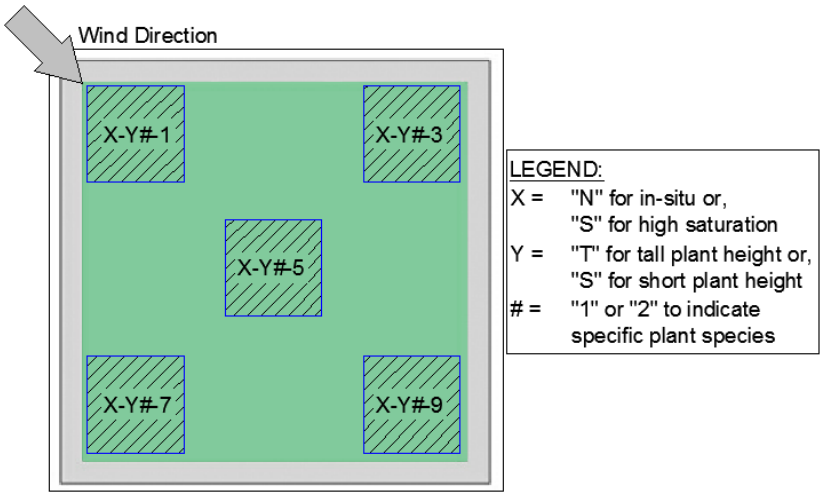

Figure 3-14. Soil sampling locations and naming convention for built-in-place assemblies as shown in Table D-1 (e.g. a sample taken from the windward corner for an in-situ, short plant height, *Aptenia cordifolia* test trial would be named “N-S2-1”). Figure courtesy of author.

For built-in-place assemblies:

1. Transfer built-in-place assemblies from the Extension Office to the test site with forklift.

2. Take overhead photo of the green roof, noting the proposed wind direction arrow and assembly ID.

3. If specified as a high saturated test trial, install rain gauges in locations as specified in Figure 3-12. Attach the sprinkler and irrigation pump to a full 208 L (55 gal.) barrel, and water BIP assembly until barrel is empty. Otherwise, skip to Step 4.

4. Raise and place the BIP assembly on the test structure deck. Seal the gaps between the walls and BIP assembly with foam backer rods and aluminum flashing.

5. Run the wind test for the first 5 minute segment and obtain video footage.

6. Take spot photos of any areas of interest

7. Run the wind test for the second 5 minute segment and obtain video footage.

8. Repeat Step 6.

9. Repeat Step 2.

10. If prolonged testing is specified (i.e. 20 minute test duration), repeat Steps 5 – 9. Otherwise, continue to Step 11.

11. Take and store soil samples, as described by Figure 3-14Figure.

For modular tray green roof systems:

1. Transport green roof modules from the Extension Office to the test site.

2. Measure the pre-test module weights with the floor scale.

3. Place modules on portable deck and take overhead photo of the green roof, noting the proposed wind direction arrow and green roof module locations, as detailed by Figure 3-15.

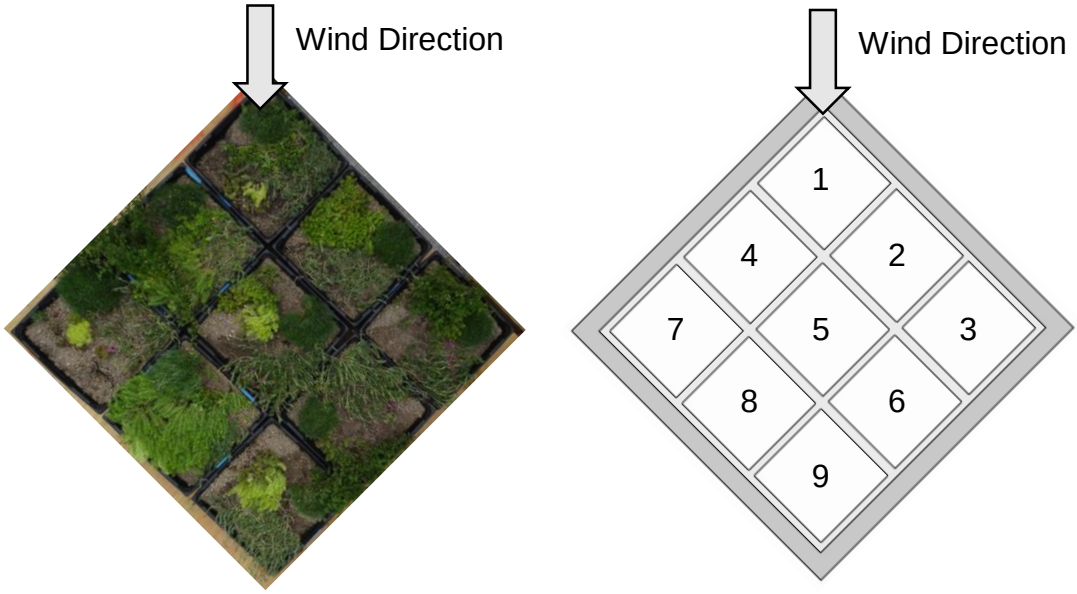

Figure 3-15. Module placement and corresponding location identification with respect to wind direction for Phase 2. Photo courtesy of author.

4. Raise and place the portable deck with green roof modules on the test structure deck. Following the blow-off failures in three test trials (later described), windward

edge modules were zip-tied to the perimeter of the portable deck (Figure 3-16). Seal the gaps between the walls and portable deck with foam backer rods and aluminum flashing.

5. Run the wind test for the first 5 minute segment and obtain video footage.

Figure 3-16. Windward edge of green roof modules zip-tied to portable deck perimeter. Photo courtesy of author.

6. Take spot photos of any areas of interest

7. Run the wind test for the second 5 minute segment and obtain video footage.

8. Repeat Step 6.

9. Take overhead photographs of the green roof modules, noting the proposed wind direction arrow and green roof module locations

10. If prolonged testing is specified (i.e. 20 minute test duration), repeat Steps 5 – 9. Otherwise, continue to Step 11.

11. Measure the post-test module weights with the floor scale.

12. Take and store a single soil sample from the middle of each tested module. Naming of the soil sample corresponds to the individual specimen name assigned prior to wind testing.

Results and Discussion

The results shown in this section are extracted from two conference papers that were published in October 2012 and February 2013 (T. D. Vo et al., 2012; T. D. Vo, Prevatt, Agdas, & Acomb, 2013) as well as a comprehensive test report written after Phase 2 wind testing in the summer of 2012 (Prevatt, Acomb, Masters, Vo, & Schild, 2012).

Phase 1 Wind Testing

A summary of the pre-test module weights and their percentage weight change (calculated by Eqn. 3-1) in Phase 1 is shown in Table 3-6, organized by their roof locations and corresponding test trials. Detailed results for each test trial conducted in Phase 1 can be found in Figures 3-18 through 3-29 located at the end of the Phase 1 subsection. For reference, the wind direction acting in those figures is from the bottom of the figure upwards.

Table 3-6. Summary of green roof module pre-test weights and post-test percentage weight changes in Phase 1

	4"-T1		4"-T2		4"-T3		8"-T1		8"-T2		8"-T3[b]	
Loc. ID[a]	Pre-test wt. (kg)	Post-%Δ wt. (%)	Pre-test wt. (kg)	Post-%Δ wt. (%)	Pre-test wt. (kg)	Post-%Δ wt. (%)	Pre-test wt. (kg)	Post-%Δ wt. (%)	Pre-test wt. (kg)	Post-%Δ wt. (%)	Pre-test wt. (kg)	Post-%Δ wt. (%)
1	23.4	-0.9	23.3	-2.3	17.0[c]	-0.6[c]	39.0	+0.8	40.3	-0.1	39.4	-0.4
2	22.7	+0.7	22.3	-1.8	19.5	-3.4	42.6	+0.2	40.0	0.0	35.3	-0.6
3	21.4	+2.9	24.4	-1.5	22.5	-2.8	39.0	-0.2	36.1	-0.1	37.2	-0.2
4	23.1	-1.1	24.0	-1.8	22.2	-2.8	40.0	+6.8	34.2	-0.1	40.7	-0.2
5	23.2	+2.5	18.9[c]	-2.0[c]	23.0	-3.0	39.6	+0.7	35.3	+1.2	38.3	-0.5
6	18.8	+12.0	24.0	-2.0	23.0	-2.5	41.4	-0.3	39.5	+0.1	36.6	+0.1
7	23.6	-3.1	21.8	-3.6	21.3	-2.8	47.9[c]	-16.0[c]	36.4	-0.4	34.5	+0.8
8	22.3	-0.1	18.3	-3.4	23.4	-2.6	42.6	-0.8	42.5[c]	-3.0[c]	49.4[c]	-1.0[c]
9	19.3[c]	-46.1[c]	23.0	-4.4	21.8	-3.8	42.6	-1.5	37.4	-0.5	37.6	+0.1

[a] Denotes module location; refer to Figure 3-7 for location in relation to wind direction
[b] Leeward parapet removed
[c] Denotes the weight or percentage weight change of an unprotected module

Variation in plant heights

Plant bending and losses were minimal up to 31.3 m/s (70 mph), but appeared to increase thereafter. Comparison of the protected and unprotected modules in the same roof locations between varying test trials confirmed findings by Retzlaff et al. (2010) who reported that protected modules can effectively bind growth media and resist scour –

even in corner regions of the roof. Due to increased exposure, taller plant species are more prone to wind damage than shorter plant species which remain low and close to the green roof surface. This was observed in Test Trials 4”-T1 and 4”-T2 in which the larger plant species (*Lantana montevidensis* and *Salvia rutilans*) was uprooted and blew off of the test roof.

Further, the 100 mm (4 in.) deep modules were seen to undergo dynamic lift in the leeward corner during testing although none of the modules actually became airborne. This lifting action was attributed to an overturning moment caused by the reversed wind flow acting (further discussed in the following paragraph) on the modules’ encompassing overhanging rim (Figure 3-3), rather than wind-induced uplift. Review of the video footage showed subtle signs of lifting of the leeward row modules once the hurricane simulator reached wind speeds of 40.2 m/s (90 mph), with increasing frequencies as the wind speeds reached 53.6 m/s (120 mph). Unprotected modules along the leeward edge of the roof experienced significant erosion of growth media and was reflected by significant losses (46% loss for the 100 mm module and 16% loss for 200 mm module). These losses were most severe when the unplanted modules were placed in the leeward corner location and led to prominent lifting of the module (as previously described) due to its decreased weight (T. D. Vo et al., 2012).

Parapet effects

When fully enclosing the roof section, the installed parapet greatly affected the wind behavior in various roof locations, as suggested by the comparison of the measured losses in the first five test trials (i.e. test trials 4”-T1 through 8”-T2). Also, the usage of the roof parapets appeared to limit the damage to plants, as minimal plant losses occurred in these five tests. However, a wind flow reversal occurred along the

leeward parapet, causing the plants to bend against the simulator's wind flow. This observation was more prominent after the hurricane simulator reached the 31.3 m/s (70 mph) threshold and beyond, as depicted in Figure 3-17. When the leeward parapet was removed in the final test trial (i.e. test trial 8"-T3) conducted in February 2012, this behavior was not observed, and losses did not exceed 1.0% of the green roof module's pre-test weights. It is expected this reversal in wind direction could occur on full-sized roofs, as wind flow reattachment along the roof dimension parallel to the wind direction is a common phenomenon. This would depend on the building's parapet height, the incoming wind speed and direction, and the roof size.

The usage of a parapet also allowed the displaced growth media to redistribute across the roof, observed in several of the test trials' modules gaining weight following wind testing (Figures 3-19, 3-25, 3-27, and 3-29). This redistribution of growth media was much more evident when unprotected modules were placed in the leeward row of modules (i.e. test trials 4"-T1 and 8"-T1 through 8"-T3) where immediately-adjacent, protected modules experienced some increase in weight after wind testing. This was not observed for the two test trials in which unprotected modules were moved closer to the windward parapet (i.e. test trials 4"-T2 and 4"-T3), in which losses were more averaged across the roof area, and aggressive growth media loss (as seen in test trials 4"-T1 and 8"-T1) and redistribution did not occur. This observation not only agrees with Karimpour's and Kaye's (2013) findings of parapets' roles in ballast containment on a roof, but also further reinforces the vegetation's role in protecting green roof modules for growth media scour.

Figure 3-17. Profile view depicting the leeward row plant behavior for different wind speeds. Shown at A) 31.3 m/s, B) 40.2 m/s, and C) 53.6 m/s. Photos courtesy of author.

Plant performance

Plant performance in Phase 1 was noted to be highly dependent upon site conditions, irrigation frequency, and the depth of growth media. Overall, intensive green roof modules showed higher plant vitality and robustness, and were often more resilient during dry conditions and irregular irrigation when compared to extensive modules. Plants also experienced dieback during the winter, effectively reducing its coverage ratio (Figures 3-28 and 3-29). However, despite the lowered vegetation coverage, the established root systems provided sufficient binding of the growth media.

19.34	22.29	23.58
18.83	23.22	23.11
21.41	22.74	22.37

Weight in kg

Figure 3-18. Test trial 4"-T1 pre-test specimen conditions and weights in kg. Photo courtesy of author.

-46.1	-0.1	-3.1
+12.0	+2.5	-1.1
+2.9	+0.7	-0.9

% Weight Change

Figure 3-19. Test trial 4"-T1 post-test specimen conditions and percentage weight change. Photo courtesy of author.

22.96	18.26	21.81
24.04	18.89	23.95
24.44	22.34	23.31

Weight in kg

Figure 3-20. Test trial 4"-T2 pre-test specimen conditions and weights in kg. Photo courtesy of author.

-4.4	-3.4	-3.6
-2.0	-2.0	-1.8
-1.5	-1.8	-2.3

% Weight Change

Figure 3-21. Test trial 4"-T2 post-test specimen conditions and percentage weight change. Photo courtesy of author.

21.80	23.41	21.29
23.08	22.99	22.20
22.52	19.50	16.96

Weight in kg

Figure 3-22. Test trial 4"-T3 pre-test specimen conditions and weights in kg. Photo courtesy of author.

-3.8	-2.6	-2.8
-2.5	-3.0	-2.8
-2.8	-3.6	-0.6

% Weight Change

Figure 3-23. Test trial 4"-T3 post-test specimen conditions and percentage weight change. Photo courtesy of author.

42.60	42.56	47.87
41.43	39.60	39.95
39.01	42.57	38.95

Weight in kg

Figure 3-24. Test trial 8"-T1 pre-test specimen conditions and weights in kg. Photo courtesy of author.

-1.5	-0.8	-16.0
-0.3	+0.7	+6.8
-0.2	+0.2	+0.8

% Weight Change

Figure 3-25. Test trial 8"-T1 post-test specimen conditions and percentage weight change. Photo courtesy of author.

37.43	42.54	36.37
39.45	35.33	34.2
36.14	40.04	40.27

Weight in kg

Figure 3-26. Test trial 8"-T2 pre-test specimen conditions and weights in kg. Photo courtesy of author.

-0.5	-3.0	-0.4
-0.3	+1.2	+0.1
-0.1	0.0	-0.1

% Weight Change

Figure 3-27. Test trial 8"-T2 post-test specimen conditions and percentage weight change. Photo courtesy of author.

37.56	49.40	34.47
36.56	38.33	40.69
37.19	35.29	39.37

Weight in kg

Figure 3-28. Test trial 8"-T3 pre-test specimen conditions and weights in kg. Photo courtesy of author.

+0.1	-1.0	+0.8
+0.1	-0.5	-0.2
-0.2	-0.6	-0.4

% Weight Change

Figure 3-29. Test trial 8"-T3 post-test specimen conditions and percentage weight change. Photo courtesy of author.

Phase 2 Wind Testing

Green roof module blow-off failures

During wind testing of the modular tray green roof systems, two sets of extensive green roof modules (test trials T3 and T8) experienced catastrophic blow-off failure of the test roof. The roof in Phase 2 represented an extreme condition where no parapets were used and green roofs were situated in otherwise commonly “non-vegetated” regions of the roof. Both test trials failed due to initial uplift of the leading corner modules (Figure 3-30), shortly after the hurricane simulator’s engines reached its 2000 RPM target (i.e. about 20 seconds after ignition). In test trial T3, once the leading corner module was lifted and moved downstream, it impacted several other modular tray specimens, causing a cascading effect which led to four additional blow-off failures, as highlighted in Figure 3-31. It appears that the blow-off failures of individual modules are easily initiated once a small degree of lift or displacement occurs.

Figure 3-30. Initial lift of the windward module in two test trials that led to blow-off failure. Shown for A) T3 (unattached modules) at 20 seconds and B) T8 (interconnected modules) at 22 seconds after target wind speed was reached. Photos courtesy of author.

Following test trial T3’s blow-off failures, the manufacturer was consulted before testing could proceed in test trial T8. It was advised that green roof modules in test trial T8 be interconnected with two 530 N (120 lbf.) tensile capacity zip-ties per edge to simulate a single three by three array system. However, due to the lack of rigidity in

both the zip-tie connections and the polymer green roof modules, the individual modular tray specimens in test trial T8 were still free to behave like the unconnected specimens in test trial T3, except a more-catastrophic failure occurred in which the whole interconnected array was blown off the roof, shown in Figure 3-32. Following the second failure case, additional anchorage to the test deck was provided for the green roof modules located on the windward edge (Figure 3-16) for all remaining tests.

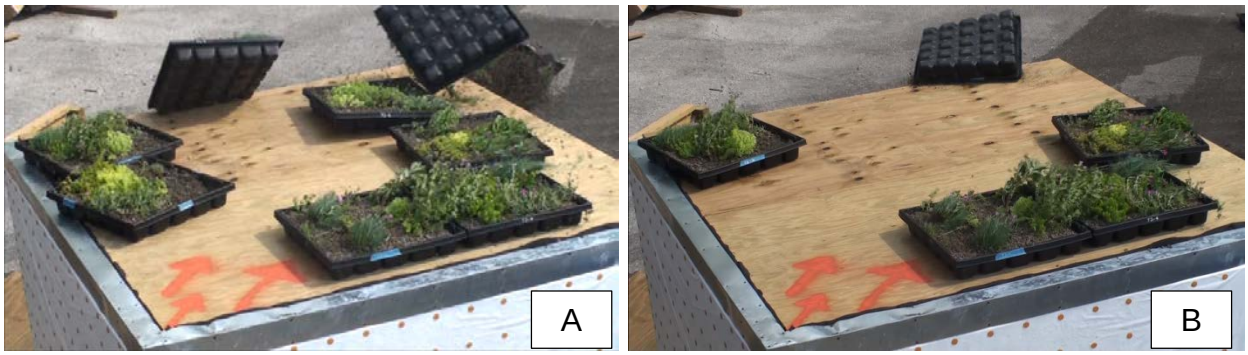

Figure 3-31. Blow-off failure in test trial T3 at two moments in time. A) After impact from the windward corner module, two modules blow off. B) Blow-off of the final windward edge module, shortly after sliding failure of leeward corner module. Photos courtesy of author.

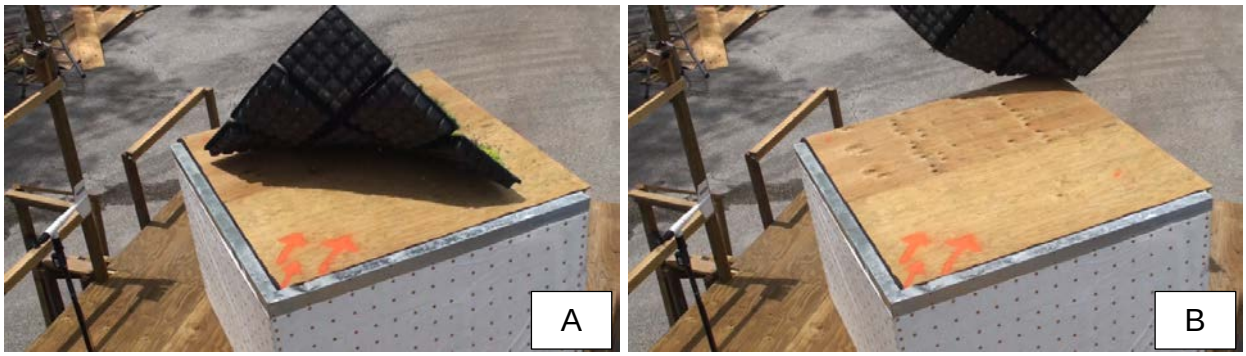

Figure 3-32. Blow-off failure in test trial T8 at two moments in time. A) Modules caught in wind flow after initial lift. B) Full system blow-off of the test roof. Photos courtesy of author.

Interestingly, blow-off failure of test trial T3 on June 18, 2012, occurred shortly after successful completion of a similar extensive module test trial (T2). Comparison between the two test trials (T2 and T3) showed that both modular tray green roof sets had similar weights (Figures 3-33 and 3-37) and were exposed to identical test

conditions (i.e. both sets of modular tray specimens were loosely-laid with no anchorage to the test deck). However, in test trial T2, a backer rod was displaced during testing, creating a gap between the leading wall and the test deck the green roof modules were placed on. While this could have attributed to the successful performance of test trial T2, the backer rod displaced midway through the second five-minute segment, long after the failure initiation time of approximately 20 seconds as observed in test trials T3 and T8.

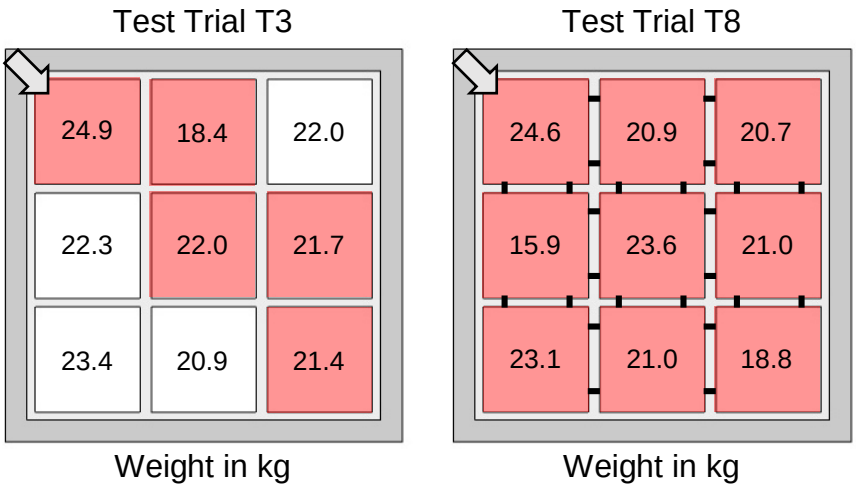

Figure 3-33. Pre-test weights for test trials T3 and T8, both of which experienced blow-off (red-shaded grids indicate blow-off failure and black links represent zip-ties). Figures courtesy of author.

Variation in establishment length and system type

Vegetation coverage ratios calculated via the procedure described in Appendix B for the wind testing conducted in Phase 2 for modular tray and built-in-place green roof systems are shown for the normal “in-situ” moisture conditions in Figures 3-37 through 3-50, and the high saturation moisture conditions (used only for the built-in-place assemblies) in Figures 3-52 through 3-54. Built-in-place assemblies were established for approximately 6.5 to 7.5 weeks before wind testing, while the modular tray systems were grown for either six or 13 months. For the modular tray specimens, additional pre-

test weights (in kg) and post-test percent weight changes were included for comparison. For all of these figures, the reference wind direction is acting from the top left corner of the figure(s), downwards at a 45 degree angle. A summary of the coverage ratio data can be found in Tables 3-7 and 3-8 for the tested built-in-place assemblies and modular tray specimens, respectively. A summary of the post-test specimen percent weight change can be found in Table 3-10.

Table 3-7. Calculated coverage ratios for built-in-place assemblies in Phase 2.

Test ID	Prior to Testing	After 10 Minutes	After 20 Minutes
N-S1	96.9%	89.1%	-
N-S2	96.2%	81.1%	-
N-T1	74.3%	43.6%	-
N-T2	50.9%	32.4%	-
S-S1	98.0%	78.9%	-
S-S2	91.8%	78.1%	-
S-T1	94.0%	68.5%	56.3%
S-T2	47.4%	35.2%	34.6%

Table 3-8. Calculated coverage ratios for modular tray systems in Phase 2.

Test ID	Prior to Testing	After 10 Minutes	After 20 Minutes
T2	64.5%	61.2%	-
T3	59.7%	-	-
T7	59.2%	49.5%	52.6%
T8	65.1%	-	-
T5	87.6%	70.4%	-
T6	72.1%	67.5%	-
T10	77.0%	70.0%	62.7%
T11	87.0%	81.0%	-

Plant coverage ratio was found to play an important role in resisting growth media erosion for both the built-in-place and modular tray green roofs (as it did in Phase 1). Five of the eight built-in-place assemblies (test trials N-S1, N-S2, S-S1, S-S2, and S-T1) achieved almost nominal vegetation coverage, measuring over 90%. Contrastingly, modular tray systems (which did not experience blow-off) all achieved slightly lower vegetation coverage prior to testing, with their average, maximum, and minimum

coverage ratios measuring 74.6%, 87.6%, and 59.2%, respectively. Overall, the built-in-place assemblies had higher pre-test coverage ratios (average 81%) than the modular tray roofs (average 72%). The coverage ratio differences following each 10 minute duration of wind testing were calculated with Eqn. 3-2 utilizing the coverage ratios shown in Figures 3-37 through 3-54 and summarized in Table 3-9.

$$\Delta C.R.\% = \left(\frac{C.R._{post} - C.R._{pre}}{C.R._{pre}}\right) \cdot 100\% \quad (3\text{-}2)$$

Where

$C.R._{post}$ = post-test coverage ratio (%) of the test trial

$C.R._{pre}$ = pre-test coverage ratio (%) of the test trial

Table 3-9. Percentage change in measured coverage ratios due to system type and establishment length

Test Trial	System Type	Age (mo.)	C.R.$_{pre}$ (%)	ΔC.R. (%) from 0 to 10 Minutes	ΔC.R. (%) from 10 to 20 Minutes
T2	Modular	13	64.5	-5.1	-
T5	Modular	13	87.6	-19.6	-
T6	Modular	13	72.1	-6.8	-
T11	Modular	6	87.0	-6.9	-
T7	Modular	6	59.2	-16.4	+6.3
T10	Modular	6	77.0	-12.6	-10.4
N-S1	BIP	1.75	96.9	-7.7	-
N-S2	BIP	1.75	96.2	-15.7	-
S-S1	BIP	1.625	98.0	-20.3	-
S-S2	BIP	1.625	91.8	-14.9	-
N-T1	BIP	1.75	74.3	-41.3	-
N-T2	BIP	1.75	50.9	-36.3	-
S-T1	BIP	1.875	94.0	-27.1	-17.8
S-T2	BIP	1.875	47.4	-24.9	-1.7

Despite having lower pretest coverage ratios, the modular tray green roofs appear to suffer a lesser average coverage ratio loss following the first 10 minutes of wind testing (-11.2%) when compared to the built-in-place systems (-23.5%). This difference in performance between built-in-place and modular tray systems remains

Table 3-10. Summary of green roof module pre-test weights and post-test percentage weight changes in Phase 2

	T2		T3		T7		T8		T5		T6		T10		T11	
Loc. ID[a]	Pre-test wt.	Post-%Δ wt.	Pre-test wt.	Post-%Δ wt.	Pre-test wt.	Post-%Δ wt.	Pre-test wt.	Post-%Δ wt.	Pre-test wt.	Post-%Δ wt.	Pre-test wt.	Post-%Δ wt.	Pre-test wt.	Post-%Δ wt.	Pre-test wt.	Post-%Δ wt.
	kg	%	kg	%	kg	%	kg	%	kg	%	kg	%	kg	%	kg	%
1	23.0	-3.6	24.9	-	21.4	-20.3	24.6	-	43.1	-1.1	45.8	-2.2	42.2	-13.5	47.5	-0.8
2	22.5	-4.2	18.4	-	19.4	-14.0	20.9	-	40.4	-0.7	41.8	-1.5	37.3	-2.7	33.7	-1.6
3	21.8	-2.6	22.0	-	22.3	+0.8	20.7	-	42.8	-0.5	40.6	-1.3	44.1	-12.0	45.3	-0.6
4	22.2	-8.6	22.3	-	24.4	-10.8	15.9	-	40.2	-0.7	41.9	-1.5	41.9	-1.7	47.6	-0.6
5	22.0	-2.1	22.0	-	20.7	-4.8	23.6	-	40.5	-0.6	42.8	-2.3	47.0	-2.3	48.7	-0.6
6	21.5	-4.0	21.7	-	21.3	-16.6	21.0	-	40.0	-0.5	39.7	-2.3	43.0	+0.2	47.4	-1.3
7	22.4	-0.8	23.4	-	23.7	-2.7	23.1	-	39.2	-0.4	42.3	-1.1	40.8	-0.7	44.0	-1.0
8	22.5	-2.8	20.9	-	19.8	-8.3	21.0	-	44.4	-0.6	47.7	-1.1	41.8	-0.4	48.0	-0.8
9	21.1	-2.5	21.4	-	20.6	-1.8	18.8	-	38.4	-1.2	42.9	-1.9	48.1	-0.9	38.8	-0.7

[a] Denotes module location; refer to Figure 3-15

apparent when considering extended, 20 minute test durations. This could be due to the modular tray systems having both substantially longer establishment for the plants, as well as higher degrees of surface roughness resulting from compartmentalized containers rather than continuous plots of growth media as seen in the built-in-place systems. Further testing would be required to determine the validity of this theory.

Growth media erosion patterns in built-in-place green roof systems

The plant bending (Figure 3-34A) growth media erosion patterns observed in Phase 2 confirmed the presence of strong suction forces below the conical vortices. For the built-in-place green roofs, it was found that most of the growth media scour occurred along the leading edges and corner of the roof. In the edge regions, the conical vortices created an inward-concaved shape among the plants in the majority of BIP assemblies with higher coverage ratios (i.e. greater than 70%) (Figure 3-34B). This led to increased wind exposure of the growth media, resulting in scour and blow-off. Growth media build-up was found to occur at the leeward corners and along the edges, further supporting evidence of vortex-induced media displacement on the tested roofs. In the highly saturated test trial S-T2, wet growth media was observed to stick to the aluminum edge restraints located on the lower left hand corner of Figure 3-34.

The erosion pattern observed in the built-in-place green roofs was not as apparent from visual inspection in the modular tray green roofs, although some localized scour was seen in individual modules. The extent of growth media scour was highly dependent upon the plant coverage ratio and location of the particular module on the roof deck. Upon reviewing the percent weight losses on the modular tray specimens tested under a normal 10 minute duration (test trials T2, T5, T6, and T11), losses appear to be spread uniformly across the modules. However, once subjected to an

extended 20 minute test duration, percent weight changes in the modular tray specimens in test trials T7 and T10 suggest that problematic areas with the most prominent growth media displacement are located in the corners and edges of the green roof module array (Figures 3-51 and 3-52). Although this observation could be due solely to the usage of tall and less established plant species in both test trials T7 and T10, the locations of the highest measured weight changes in these two test trials agree with the scour patterns observed in all of the built-in-place coverage ratios.

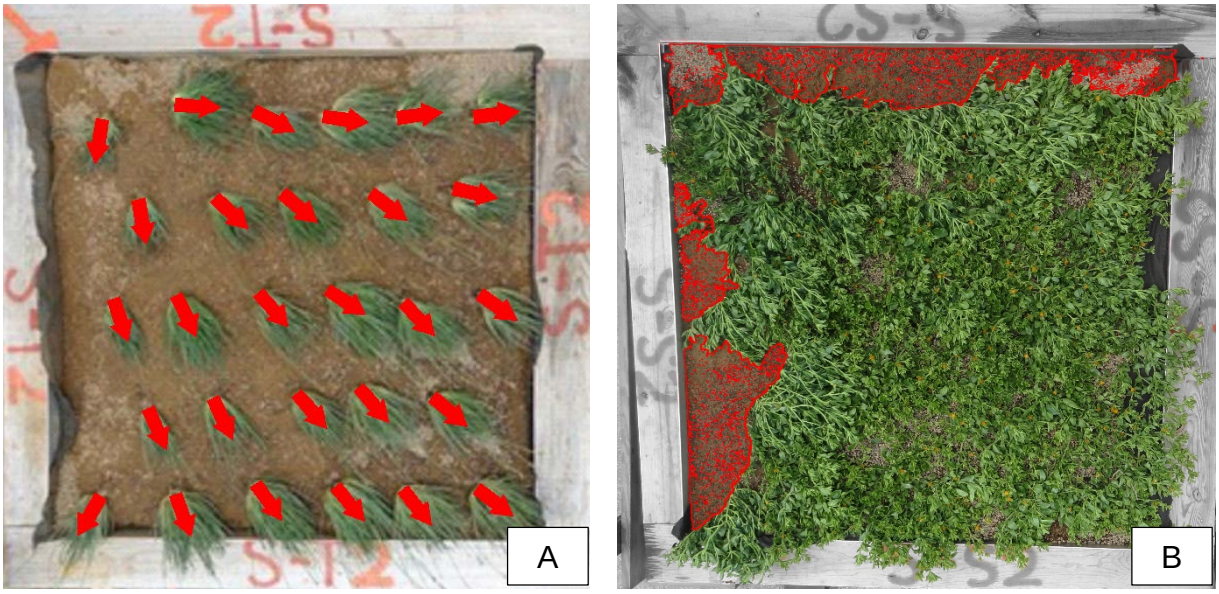

Figure 3-34. Typical scour and erosion patterns for built-in-place wind tests. A) Annotated plant bending to conical vortices in test trial S-T2. B) Inward-concaved shapes (highlighted in red) of displaced plants along edge regions in test trial S-S2. Photos courtesy of author.

Vegetation sheltering effect on loose aggregate

Closer inspection of the vegetation after wind testing show that plants do provide a roughness layer that disrupts wind flow from damaging the media surface. Spot captures taken after different 5 minute intervals of wind testing support this claim, as they showed regions within a built-in-place assembly completely devoid of coarse aggregate where plant coverage was minimal or non-existent (Figure 3-35), and other

regions where coarse aggregate appeared undisturbed by the wind flow due to protection from bent over plants (Figure 3-36).

Figure 3-35. Typical example of extreme coarse aggregate scour. A) Location of bent-over Bulbines supplying sheltering of coarse aggregate (circled in red) in test trial S-T2. A) Spot capture of the circled region in test trial S-T2. Photos courtesy of author.

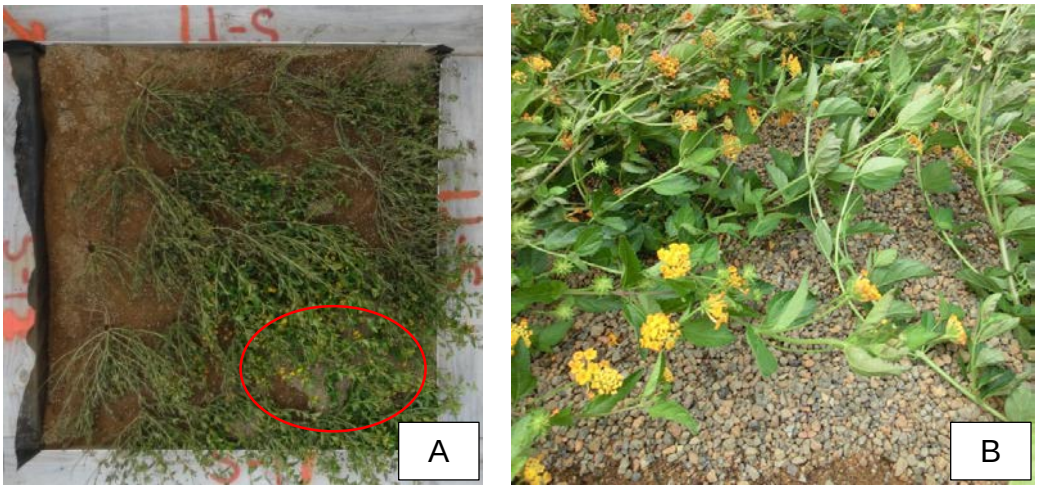

Figure 3-36. Typical example of vegetation providing sheltering of loose aggregate. A) Location of coarse aggregate sheltering from vegetation (circled in red) in test trial S-T1. B) Spot capture of the circled region in test trial S-T1. Photos courtesy of author.

Varying test durations

Coverage ratio reduction does not occur at a constant rate, as extended testing durations only resulted in minimal reductions after the first 10-minute segment (an average of a 5% difference in coverage between the first and second 10 minute

segments for test trials S-T1, S-T2, T7, and T11). The coverage ratio calculation for the modular tray test trial T7 suggests that once all of the loose and weak plant material is ejected from the roof, the remaining vegetation is quite resilient against high wind forces. This theory is further based upon the “apparent” increase in coverage ratio after 20 minutes when compared to its coverage at 10 minutes in test trial T7 (Figure 3-51). The increase in coverage ratio is not due to a higher presence of vegetation in the green roof system after testing, but rather, a reorientation of the vegetation that survived the initial 10 minutes of extreme winds.

C.R. = 64.5% Weight in kg

Figure 3-37. Test trial T2 pre-test coverage ratio and corresponding specimen weights in kg. Test trial T2 consists of 100 mm, 13 month modules. Photo courtesy of author.

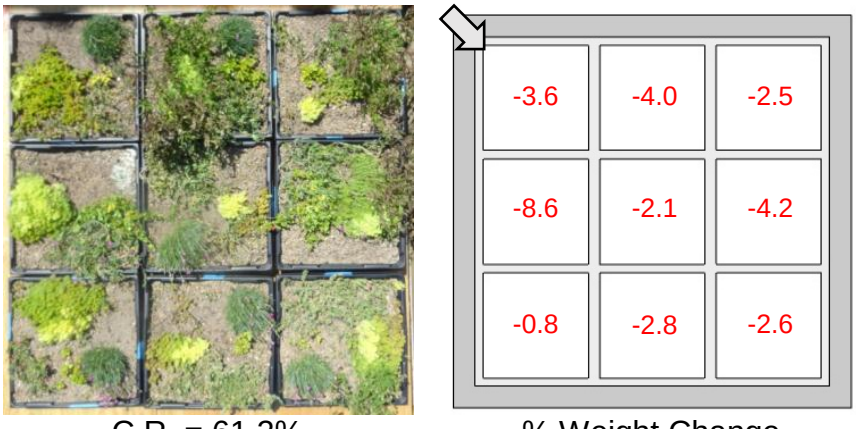

C.R. = 61.2% % Weight Change

Figure 3-38. Test trial T2 post-test coverage ratio and corresponding specimen percent weight change after 10 minutes. Photo courtesy of author.

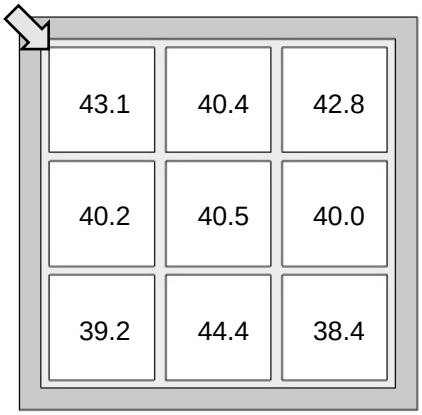

C.R. = 87.6% Weight in kg

Figure 3-39. Test trial T5 pre-test coverage ratio and corresponding specimen weights in kg. Test trial T5 consists of 200 mm, 13 month modules. Photo courtesy of author.

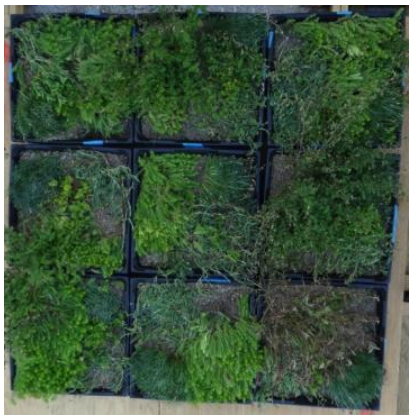

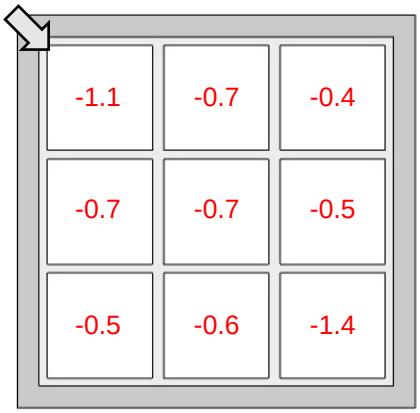

C.R. = 70.4% % Weight Change

Figure 3-40. Test trial T5 post-test coverage ratio and corresponding specimen percent weight change after 10 minutes. Photo courtesy of author.

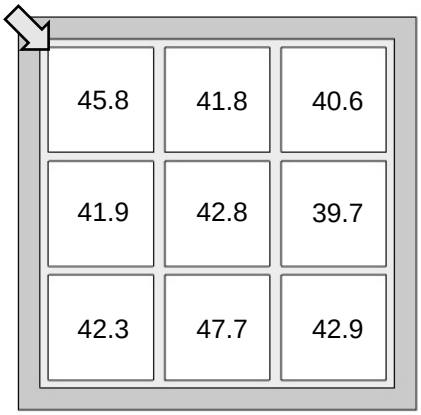

C.R. = 72.1% Weight in kg

Figure 3-41. Test trial T6 pre-test coverage ratio and corresponding specimen weights in kg. Test trial T6 consists of 200 mm, 13 month modules. Photo courtesy of author.

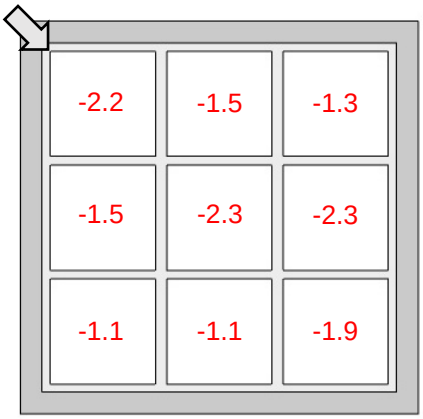

C.R. = 67.5% % Weight Change

Figure 3-42. Test trial T6 post-test coverage ratio and corresponding specimen percent weight change after 10 minutes. Photo courtesy of author.

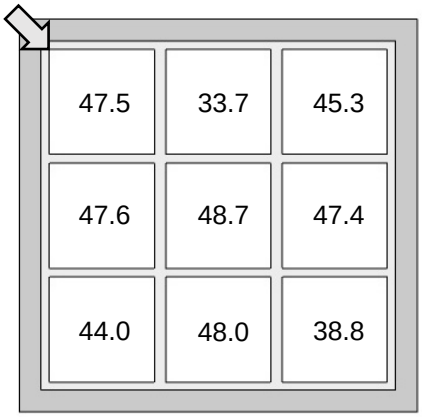

C.R. = 87.0% Weight in kg

Figure 3-43. Test trial T11 pre-test coverage ratio and corresponding specimen weights in kg. Test trial T11 consists of 200 mm, 6 month modules. Photo courtesy of author.

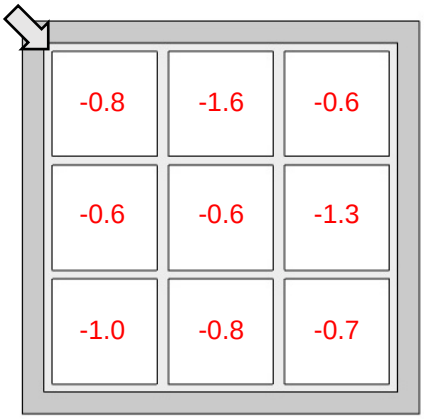

C.R. = 81.0% % Weight Change

Figure 3-44. Test trial T11 post-test coverage ratio and corresponding specimen percent weight change after 10 minutes. Photo courtesy of author.

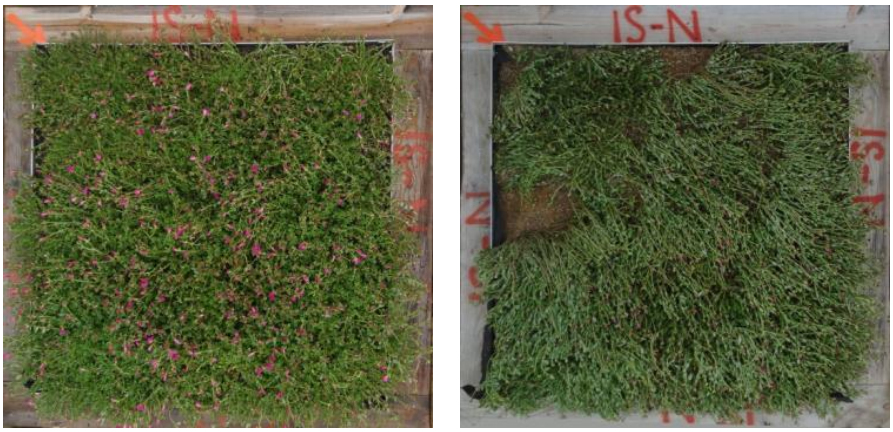

C.R. = 96.9% C.R. = 89.1%

Figure 3-45. Vegetation coverage ratios for a normally saturated BIP test trial N-S1 before and after 10 minutes of wind testing. Photos courtesy of author.

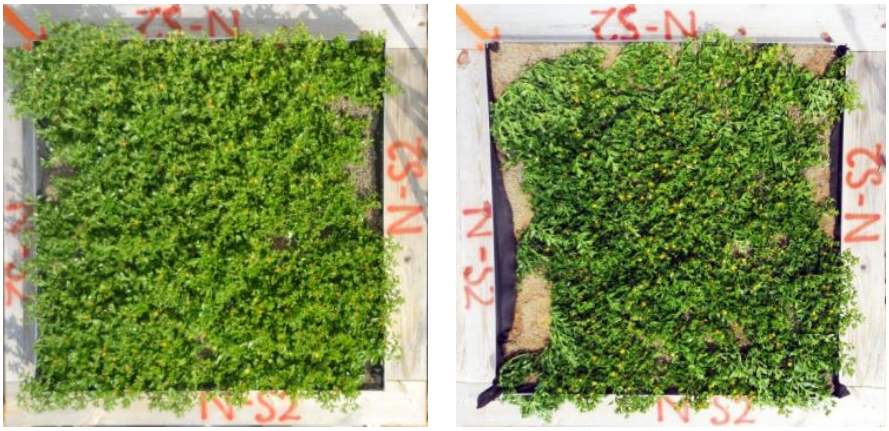

C.R. = 96.2% C.R. = 81.1%

Figure 3-46. Vegetation coverage ratios for a normally saturated BIP test trial N-S2 before and after 10 minutes of wind testing. Photos courtesy of author.

C.R. = 74.3% C.R. = 43.6%

Figure 3-47. Vegetation coverage ratios for a normally saturated BIP test trial N-T1 before and after 10 minutes of wind testing. Photos courtesy of author.

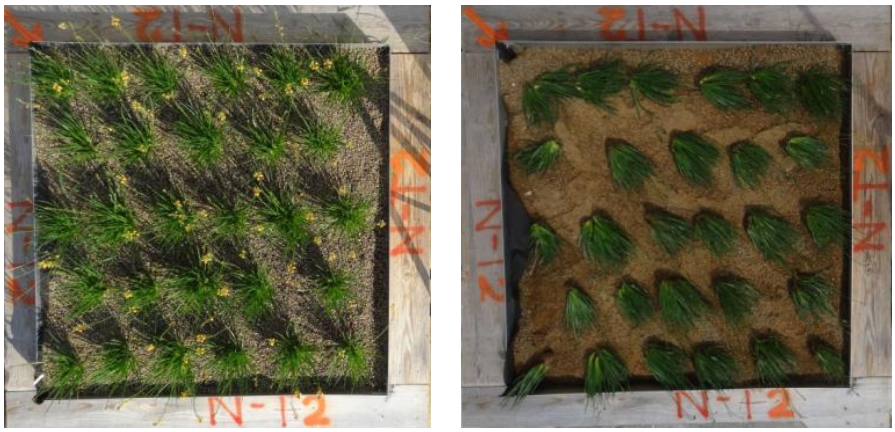

C.R. = 50.9% C.R. = 32.4%

Figure 3-48. Vegetation coverage ratios for a normally saturated BIP test trial N-T2 before and after 10 minutes of wind testing. Photos courtesy of author.

C.R. = 98.0% C.R. = 78.9%

Figure 3-49. Vegetation coverage ratios for a highly-saturated BIP test trial S-S1 before and after 10 minutes of wind testing. Photos courtesy of author.

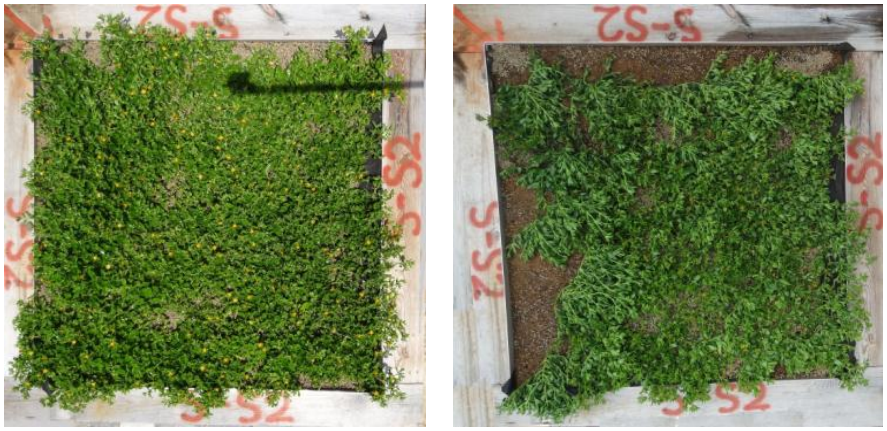

C.R. = 91.8% C.R. = 78.1%

Figure 3-50. Vegetation coverage ratios for a highly-saturated BIP test trial S-S1 before and after 10 minutes of wind testing. Photos courtesy of author.

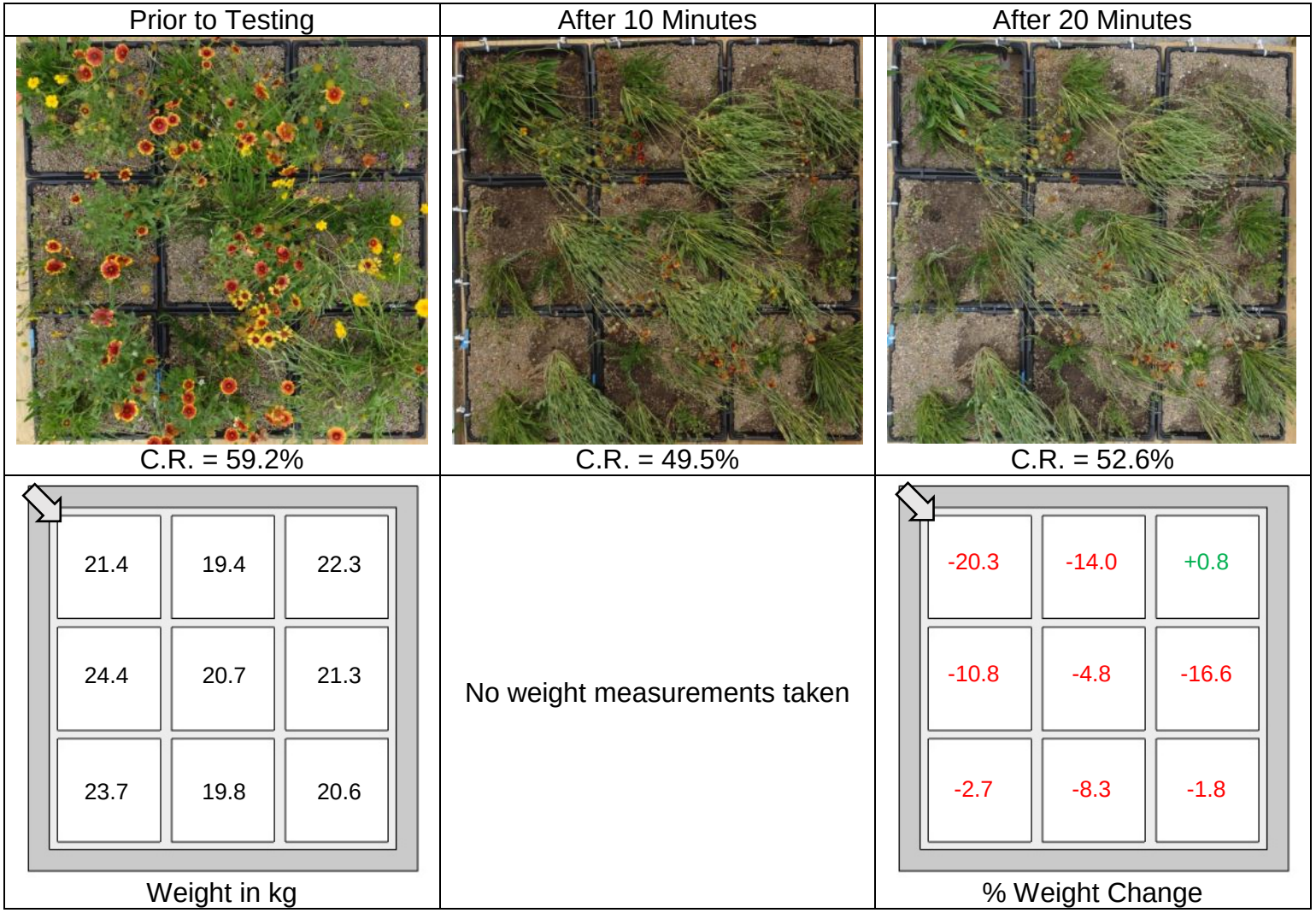

Figure 3-51. Coverage ratios and corresponding pre-test weight and post-test weight change for modular tray specimens in test trial T7 subjected to an extended 20 minute test duration. Test trial T7 consists of 100 mm, 6 month modules. Photos courtesy of author.

Prior to Testing	After 10 Minutes	After 20 Minutes
		
C.R. = 77.0%	C.R. = 70.0%	C.R. = 62.7%
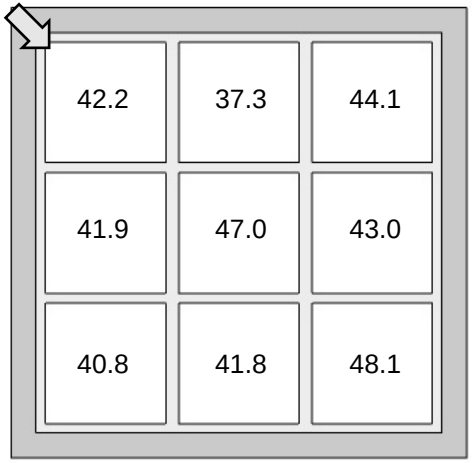	No weight measurements taken	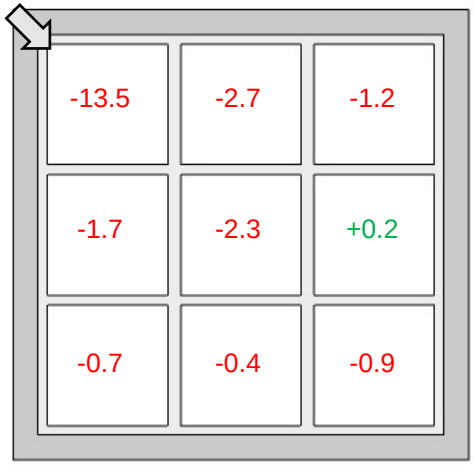
Weight in kg		% Weight Change

Figure 3-52. Coverage ratios and corresponding pre-test weight and post-test weight change for modular tray specimens in test trial T10 subjected to an extended 20 minute test duration. Test trial T10 consists of 200 mm, 6 month modules. Photos courtesy of author.

Prior to Testing	After 10 Minutes	After 20 Minutes
		
C.R. = 94.0%	C.R. = 68.5%	C.R. = 56.3%

Figure 3-53. Coverage ratios for a highly-saturated BIP test trial S-T1 subjected to an extended 20 minute test duration. Photos courtesy of author.

Prior to Testing	After 10 Minutes	After 20 Minutes
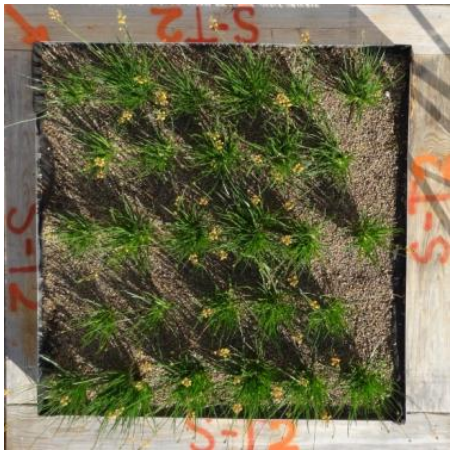	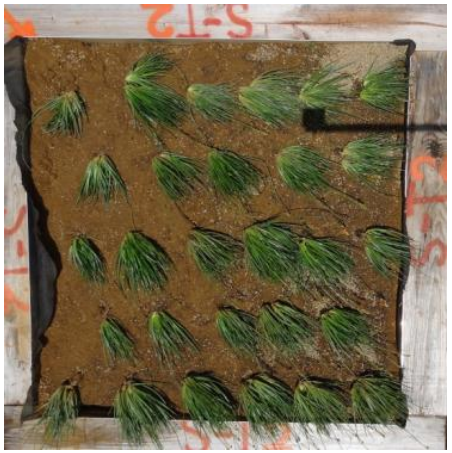	
C.R. = 47.4%	C.R. = 35.2%	C.R. = 34.6%

Figure 3-54. Coverage ratios for a highly-saturated BIP test trial S-T2 subjected to an extended 20 minute test duration. Photo courtesy of author.

Growth media moisture content effects

All moisture contents obtained in Phase 2 were calculated in three separate batches, sent to an independent laboratory, and shown in its basic form in Appendix C. To separate the moisture contents between the wind tests and plant uproot tests, these data were further summarized for the wind tests only, in Appendix D.

A summary of the moisture content data for the built-in-place assemblies is shown in Table D-1. In addition, to determine if the moisture content had any effect on the measured weight changes, the moisture content was plotted against the recorded weight loss (e.g. weight gain is taken as negative) in Figures D-1 through D-5. Because regular rainfall occurred during Phase 2 wind testing, a record of the daily rainfall on each day that wind testing was performed is shown in Table D-2.

Besides specimens which utilized the Portulaca species (N-S1 and S-S1), tests on built-in-place assemblies showed no significant difference in coverage ratio results between trials that were artificially saturated immediately before wind testing and those that had normal growth media moisture condition. For test trials N-S1 and S-S1, there was a noticeable reduction in wind resistance (i.e. -20.3% loss vs. 7.7%) when artificial saturation was applied (Table 3-9). However, despite the extensive wetting, the roofs drained quickly, resulting in moisture contents varying from 21% to 30% (Table D-1). The high variation in the elapsed time between the pre- and post-test soil sample collection times for the built-in-place assemblies was due to a combination of uncontrollable factors, including: irregular operation of the irrigation pump, duration of the wind test, or stalled simulator operation.

From Figures D-1 through D-5, the modular tray specimens, which were tested with in-situ moisture conditions, appear more prone to weight changes based on

changes in roof location rather than measured moisture content. Because isolation of one effect over another is not possible with this current study, further extensive testing is required to determine the true effects of how moisture content affects green roof systems.

Variation in plant heights

Similar to Phase 1, a clear difference in wind performance was observed between tall and short plant species. Because the plant selection for the green roof systems were isolated to include only tall or short species in Phase 2, their effect on the green roof wind resistance could be better understood. With no parapet present in Phase 2, the windward regions of the tested roofs were not protected and the wind flow reversal present in Phase 1 was not observed. For both built-in-place and modular tray green roof systems, the shorter plant species experienced less scour damage than the taller plant species as reflected by lower post-test coverage ratios for systems with tall plant species. This is again due to the taller plants being fully exposed to the incoming wind which cause a higher degree of biomass losses (e.g. leaves) and plant bending, as shown in the comparison in Figure 3-55. As a result, extreme coarse aggregate blow-off was observed during wind testing of systems containing tall plant species.

Figure 3-55. Profile view comparing the plant performance after wind testing. Shown for A) short plant test trial, N-S2 and B) tall plant test trial, N-T1. Photos courtesy of author.

Variation in module depths

For modular green roof systems, comparison between extensive and intensive modules showed that similar effects on the plant vitality were observed as in Phase 1. The pre-test coverage ratios obtained for the modular tray specimens tested in Phase 2 (including the failed test trials T3 and T8) showed that extensive green roof modules averaged a coverage ratio of 62% while intensive green roof modules averaged 81%. Since the wind performance of a green roof system is directly correlated with the vegetation coverage of the system, this quantified observation might provide sufficient evidence of the requirement of growth media depths that surpass 100 mm (4 in.) for modular tray green roofs in Florida.

When comparing the post-test weight changes between extensive and intensive green roof modules, intensive modules appear to perform favorably in terms of the averaged percentage change of their original weight when compared to extensive modules. However, due to the failure of two extensive module test trials (i.e. T3 and T8) combined with the small sample size, these observed trends should be further explored through more isolated test procedures (e.g. uniform plant species and establishment with varying growth media depths, etc.).

Vegetation damage

As recorded in the observation logs transcribed into Appendix E, wind-induced losses primarily consisted of coarse aggregate and leaf blow-off. Observed losses involving uprooting of entire plants and occurrences of stem lodging were minimal, but present. The most common plant failure observed was root lodging. As previously defined in Chapter 2, root lodging is the failure means in which stresses cause collapse of the plant structure at the base, exposing the root system, and stem lodging is where

the stem itself breaks close to the base. The modular green roof assemblies, tested after 13 months establishment showed no signs of root lodging following each test trial, while those grown for 6 months had a several cases. This could be attributed to the more-established root systems effectively binding all of their surrounding media, further described in Chapter 4. The built-in-place green roof assemblies, on the other hand, were grown for 1.5 to 2 months and had occurrences of root lodging after each test trial.

Root lodging was limited to the individual plant specimens that were fully immersed in the wind flow; i.e. taller, woody-stemmed plants were more prone to root lodging over a greater widespread area than shorter plants in built-in-place tests (Figure 3-56). Short plant species in the built-in-place tests (Portulaca and Aptenia) only displayed root lodging failure in the high scour regions previously described. In general, the taller plant species (Gaillardia, Lantana, Bulbine, & Coreopsis) all exhibited higher signs of stress (desiccation) after wind tests on both built-in-place and modular tray green roof systems.

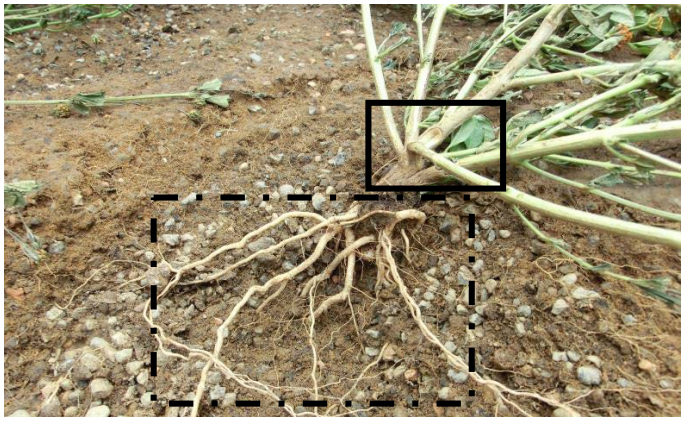

Figure 3-56. Lantana plant displaying both root (dashed square) and stem (solid square) lodging after a wind test on built-in-place green roof. Photo courtesy of author.

Statistical Analyses

To assess the impact of different environmental settings and green roof properties, comparative statistical analyses through different strata of project settings

were completed on successful test trials with modular tray green roof specimens. The uncontrolled factors between test trials (i.e. wind test duration, plant type, usage of unprotected module, etc.) in combination with the small number of experimental tests presented a limited sample pool for conducting a statistical analysis. Therefore, non-parametric comparative analyses were conducted for two cases: specimen weight differences' relation to corresponding experimental means and overall weight differences between test trials of similar variables. Test scores for different exercises will indicate different significance thresholds, thus standardized with the p-values shown in Tables 3-12 and 3-13. For both sets of comparative assessments, the null hypothesis (i.e. no difference exists between test samples) is rejected if the probability is less than 5% (i.e. p-value < 0.05). The Test IDs from Phase 1 and Phase 2 were standardized to share a common naming convention for the Stat IDs, as shown in Table 3-11.

Table 3-11. Naming convention used between Wind Test IDs and Stat IDs

Phase	Wind Test ID	Stat ID	Phase	Wind Test ID	Stat ID
1	4"-T1	1.1	2	T2	2.1
1	4"-T2	1.2	2	T5	2.2
1	4"-T3	1.3	2	T6	2.3
1	8"-T1	1.4	2	T7	2.4
1	8"-T2	1.5	2	T10	2.5
1	8"-T3	1.6	2	T11	2.6

Table 3-12 presents the first set of comparative assessments used to determine the significance of the differences between the pre- and post-test weights of individual modules in each test trial. In other words, the sample population is obtained from taking the nine pre-test weights and comparing them with their corresponding post-test weights. The concluding p-values will describe whether or not statistical differences exist between the test samples in each experiment. Refer to Tables 3-3 and 3-4 for further details on the differences between test trials.

Table 3-12. Comparison of statistical data between specimens within each experiment.

Stat ID	Statistical Test	Test Score	p-value	Stat ID	Statistical Test	Test Score	p-value
1.1	Wilcox	24	0.91	2.1	Wilcox	45	0.009[a]
1.2	Wilcox	45	0.004[a]	2.2	Wilcox	44	0.008[a]
1.3	Wilcox	45	0.004[a]	2.3	Wilcox	45	0.009[a]
1.4	Wilcox	26	0.73	2.4	Wilcox	45	0.004[a]
1.5	Wilcox	26	0.29	2.5	Wilcox	44	0.008[a]
1.6	Wilcox	34	0.20	2.6	Wilcox	45	0.009[a]

[a] Null hypothesis rejected

Because the overall weights were not independent of each other (i.e. gains from one specimen as a result of the losses from another), a paired analysis of the pre- and post- weights is more suitable for the data set under consideration. Non-parametric Wilcoxon signed rank-sum tests were used to test the specimen weights. Non-parametric analyses, unlike more common parametric statistics, do not rely on assumptions such as normality and are therefore more flexible, and considering the smaller sample size of the data points, they were adopted over more traditional parametric statistics.

The results from Table 3-12 state that significant differences *were* present between pre- and post- test weights for Tests 1.2, 1.3, and 2.1 – 2.6. When these results are compared against results in Figures 4 and 5, it is apparent that test trials which experienced net losses (i.e. test trials where more growth media blow-off occurred than redistribution) resulted in statistically significant differences between their specimens' pre- and post- test weights. Thus, the usage of a parapet during testing resulted in less significant differences in specimens' weights, and further reinforces Karimpour's and Kaye's (2013) findings that state the role of rooftop parapets is to contain loose material from ejecting from the roof, rather than control displacements altogether.

Table 3-13 presents results from the second set of comparative tests conducted to assess the differences in observed soil losses for similarly-constructed test trials (i.e. same wind speeds and test durations, etc.). Provided the test setups had consistent treatments, it was assumed that there should be no statistically significant difference in the soil loss observed between the experiments for specimens placed in the same roof locations. The Kruskal-Wallis Method, which can be considered a non-parametric one-way ANOVA, was used to conduct statistical analyses among tests with more than two subgroups. Analyses with only two subgroups utilized the non-parametric Wilcox rank test. Table 3-13 presents eight cases tested in order to isolate treatment (i.e. factors changed between test trials) effects on weight changes. Pairwise (i.e. ad-hoc) comparisons were done to complement the Kruskal-Wallis test results.

Table 3-13. Comparison of statistical data between experiments with similar treatments.

Case	Stat IDs Considered	Treatment Varied	Statistical Test	Test Score	p-value
1	1.1, 1.2, 1.3	Unprotected module location	Kruskal-Wallis	6.03	0.05[a]
2	1.1, 1.4	Module depth, unprotected module location	Wilcox	42.0	0.93
3	1.4, 1.5, 1.6	Unprotected module location	Kruskal-Wallis	0.27	0.88
4	2.1, 2.2	Plant types, test duration in 2.2	Wilcox	57.5	0.14
5	2.2, 2.5	Module depth	Wilcox	26.5	0.23
6	2.3, 2.4, 2.5, 2.6	Plant types, test duration in 2.5	Kruskal-Wallis	13.3	0.004[a]
7	2.3, 2.4, 2.6	Plant types	Kruskal-Wallis	15.7	0.0004[a]
8	2.3, 2.4	None	Wilcox	78.5	0.001[a]

[a] Null hypothesis rejected

The test results presented in Table 3-13 varied greatly in terms of rejection or acceptance of the null hypothesis. While cases 2 – 5 resulted in statistical confirmation

of the initial hypothesis that similar test conditions produced no significant differences in weight changes within a 5% confidence, other cases appear to contradict that hypothesis. For example, in case 8 where the treatments were identical, the resulting p-value states that the weight changes between Tests 2.3 and 2.4 were statistically different. Due to high variability between test trials (i.e. multiple treatments in an experiment), reliable conclusions from the second set of comparative tests cannot be made at this time (T. D. Vo et al., 2013).

Summary

Green roof systems were subjected to realistic wind loads and their performance was observed. The results obtained from both phases of wind testing provide reasonable guidance towards the proper wind design for a green roof system. This can be summarized as follows:

1. Green roofs are highly susceptible to wind-induced damage if placed in corner or edge regions of a roof. Current design guidelines are correct in prohibiting green roof placement in these roof regions, as a breach in the vegetation can eventually escalate to green roof failure.

2. Blow-off failure of modular tray green roofs can occur, if subjected to critical conditions. However, small changes to the current design or utilization of anchorage may be sufficient in preventing catastrophic failures from occurring.

3. Roof parapets provide two vital roles to the well-being of a green roof: reducing uplift pressures and forcing potential conical vortices upwards, and containing and preventing displaced green roof growth media from roof blow-off. Utilization of parapets can also protect taller plants that would otherwise receive the blunt wind forces.

4. High vegetation coverage provides an effective means of preventing growth media scour and erosion damage. However, simply having a high coverage ratio does not imply that the green roof is completely wind-resistant as coverage ratios can be expected to greatly reduce during a storm event. Utilizing resilient vegetation that has a low and dense growth spread (i.e. limiting tall plants) can combat this problem.

5. Green roof vegetation is highly variable and dependent upon its surrounding conditions (e.g. climate, growth media depths, etc.), depending on the species. It is

therefore the responsibility of the green roof designer or horticulturalist to understand which types of vegetation best suits a given project.

6. Plants need to be provided a sufficient establishment period, regulated irrigation, and sufficient room to grow (in growth media depth and surrounding widths), as these were all factors which affected the vitality of the green roof vegetation used in this project. It appears that for modular tray green roofs, intensive depth modules provided sufficient room for plants to grow. Further, combining plants with different root spreads showed an effective method of fully-binding otherwise loose growth media (given a long enough establishment).

The results from this study represent a nonconservative account as damages measured here should be minimal in comparison to what should be expected during real hurricanes, which can last up to ranges of three to 24 hours of strong winds. Thus, more studies are required to calibrate the results obtained from these short-duration tests (five to 10 minutes in length), to longer test durations. Further, since the turbulence intensities in actual hurricanes can be expected to be much higher, greater degrees of dynamic movement in plants are expected. Despite these limitations, the study reinforces the importance of the vegetation's role in the green roof wind resistance. It highlights how future green roof designers can possibly put effort towards fortifying the plant design to increase the overall wind performance of a green roof.

CHAPTER 4
PLANT UPROOT TESTING

Plant uproot testing was conducted during Phase 2 of the full-scale wind testing utilizing a custom-developed Plant Uproot Device. The testing was conducted to evaluate the effects of various parameters (plant species, growth media depth, establishment time, growth media moisture content, and wind-induced scour losses) on the resistive capacity of plant roots, which could describe the soil-stabilization capacity of a green roof module. This chapter will review two existing laboratory plant uproot studies, describe the development of the Plant Uproot Device, and summarize the results found. The development of a Plant Uproot Device is described and the experimental procedure and results presented in this chapter.

Background and Objectives

Little is known about the uproot potential of commonly-used plant species in green roof systems, and even less of how field-grown plants in modular green roof systems react to mechanical uplift loads. This section reviews two laboratory plant uproot studies conducted by Bailey et al. (2002) and Hamza et al. (2007).

2002 – Bailey et al. – The Role of Root System Architecture and Root Hairs in Promoting Anchorage Against Uprooting Forces in *Allium cepa* and Root Mutants of *Arabidopsis thaliana*

Baily et al. (2002) determined the effect of the number of roots, lateral coverage, and root hairs on the anchorage to the soil during mechanical loading. The authors compared the performance of a thick, unbranched, uniform width *Allium cepa* plant species against a multi-branched *Arabidopsis thaliana* plant species to determine whether a deeper and more uniform root system (the former species) would increase root anchorage.

Plants were grown in a controlled laboratory environment while the amounts of light and water they received were recorded. Prior to uproot testing, the soil was saturated and then allowed to drain for approximately 30 to 90 minutes. The plant specimens were then clamped with a corrugated metal grip, lined with thin pieces of rubber, and then uprooted at a rate of 100 mm/min for the *Arabidopsis thaliana* species and 500 mm/min for the *Allium cepa* species with a universal testing machine (UTM). Stems that broke (not roots) during uprooting were discarded from the results.

Of the 93 uprooted *Allium cepa* plants tested, 83 broke at or near the clamp. The authors found that breakage of an *Allium cepa* root was indicated by a sharp drop (≤ 0.15 N) in the load in the load vs. displacement plot (Figure 4-1). This force drop to root breakage relationship was consistent for the number of roots broken on a single plant. Further, they found that the closer the distance between two force drops (i.e. time between two individual broken roots), the better chance that the two roots added to the peak uproot resistance (termed as root cooperation). If this distance increases, the first root does not contribute to the peak uproot resistance of the plant.

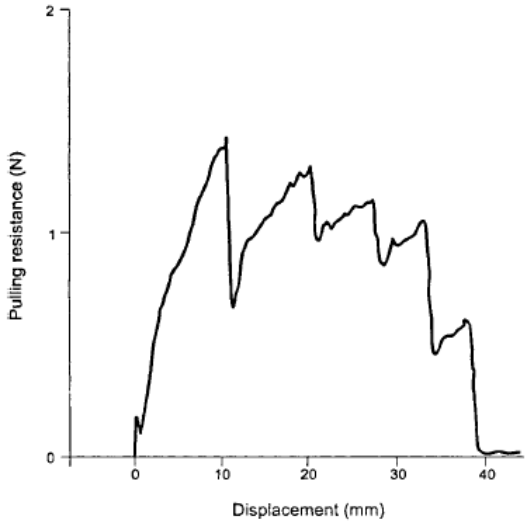

Figure 4-1. Uprooting force trace for a single *Allium cepa* in which five roots broke, indicated by five force drops in the plot. Figure courtesy of Bailey et al., 2002.

In testing the *Arabidopsis thaliana*, the authors observed a 14% increase in peak uproot force, supporting their hypothesis of lateral roots contributing to soil anchorage. When comparing two variations of *Arabidopsis thalianas*, the authors found that the inclusion of roots hairs in one variation did not contribute to a higher peak uproot load. Thus, root hairs were concluded to not have any contribution to anchorage.

2007 – Hamza et al. – Mechanics of Root-Pullout from Soil: a Novel Image and Stress Analysis Procedure

Hamza et al. (2007) studied the uproot mechanics of four different root models (termed as analogue-roots) made of Viton rubber. The purpose of their study was to gain a better understanding of the root-soil interaction (Figure 4-2) during mechanical loading with controlled variation of root properties. The authors also utilized a novel image analysis approach using Particle Image Velocimetry (PIV) to measure root and soil movements prior and after uproot testing.

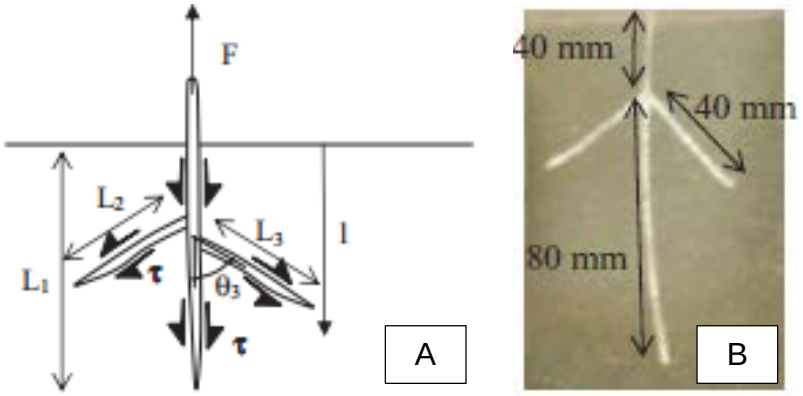

Figure 4-2. Applied mechanical loadings to plant root systems. A) Forces resisting pull-out (system with lateral roots). B) Artificial Viton-rubber root with three branches. Figure and photo courtesy of Hamza et al., 2007.

The authors utilized analogue-roots as opposed to real root systems to control the inherent high variability in biological factors (e.g. root size, branching, etc.) as well as have a uniform material strength (E = 7 MPa for Viton rubber). Two of the roots consisted of single tap systems with varying root lengths, while the other two were more

representative of actual root systems being made up of a single tap with either two or four additional branches. The analogue-roots (or live seedlings used for comparison) were placed in a transparent box packed with soil with a water content of 12%. Similar to Bailey et al.'s (2002) study, the free ends of the roots were clamped with a screwthread grips with hard rubber surfaces. Both the artificial roots and two species of planted seedlings (Pea and Maize species) were then uprooted with an Instron model 5540 universal testing machine (UTM) at a displacement rate of 3 mm/min. Digital photographs were taken prior to and after testing for image analysis using PIV (not described in this report).

Analogue taproots with no laterals had the lowest pull-out capacities whereas the analogues with two laterals had the highest (~2.5 N avg.). Further, for small vertically applied displacements (< 4 mm), all root analogues displayed negligible differences in behavior. This was attributed to the root analogue deformations being restricted in the unbranched zones for displacements less than 4 mm. Axial forces diverged after this 4 mm threshold.

Uproot testing of the live Pea and Maize plants resulted in expectedly higher uproot loads. Specifically, the Pea plant (unbranched root system) did not experience root breakage, and showed that its fine root hairs affect the deformation field around the root and result in larger displaced body of soil. For the Maize plant, which consisted of a more complex root system, the uproot load gradually increased until a peak load of 5 N was reached at which a sudden drop occurred after 13 mm displacement. In general, they found that root system response to uplift varied between pull-out of the entire root

system, root breakage near the stem, or breakage within the root system with possible attachment of the soil plug.

Summary

Two laboratory uproot studies were conducted by Bailey et al. (2002) and Hamza et al. (2007). Both studies performed mechanical pullout tests on plants with simple root structures. The studies reviewed found that the inclusion of laterals in the root system increased the peak uproot loads due to better anchorage to the soil. Bailey et al. (2002) were able to identify when root breakage occurred from a load vs. displacement plot from the presence of sudden load drops, as well as when root cooperation occurred. Root cooperation was determined to directly add to the peak uproot capacity. The role of finer root hairs was determined to be negligible towards the peak uproot capacity in Bailey et al.'s (2002) study, while Hamza et al. (2007) showed that they caused a larger displaced soil area. Further, several unique uproot conditions (e.g. pull-out of soil plug, etc.) were found to occur for following mechanical pull-out of plants (Hamza et al., 2007).

Discussion

Although the field-uproot testing described in this chapter shares some similarities with the two laboratory studies reviewed, several differences distinguish them from one another. Although there was more control of plant growth and loading conditions in laboratory settings, the plants tested for this research were grown in-field and species were mixed within the green roof modules. This offers a realistic representation of how green roof modules are planted on actual roof decks. Because plant species were mixed within modules, their root growths are dependent of each other (due to intertwining). It is believed that interspecies root interactions are important

in stabilizing the growth media, and should offer a factor of safety for measured peak uproot capacity when compared with individually-tested plants. In addition, plant species tested in this study were multi-stemmed with spreading form root systems. This resulted in attachment of small, residual roots when the rare instances of stem failures occurred. These results were chosen not to be omitted as the load prior to breakage still represented some measure of the root capacity.

From the reviewed studies, two parameters which appeared to affect the peak uproot capacities of tested plants were identified:

- Moisture content of the soil/growth media
- Root spread (number of laterals which extended horizontally)

Research Objective

A plant's pull-out capacity has a direct relationship to its anchorage to soil and therefore, the soil/growth media stability. With increased growth media stability, wind-induced scour of growth media is lessened, thereby reducing the uplift potential of a modular green roof system. Thus, the purpose of this study was to determine the important parameters which affected the pull-out capacity of five plant species. The hypotheses formed for the study were as follows:

1. Modules which experience higher scour losses from wind testing will yield plants with lower uproot capacities (i.e. plants with poor uproot capacities provide poor scour protection).
2. One-hundred (100) mm deep modules will yield plants with lower uproot capacities than 200 mm deep modules due to less space for roots to grow.
3. Higher interspecies root interactions will increase uproot capacities when comparing same plant species (i.e. 13 month, six plant mixes will have higher uproot capacities than six month, four plant mixes)

Materials

Plant Species Tested

Plant species selected for uproot testing were based on availability to provide a sufficient sample size to adequately consider the test parameters identified in the previous subsection. Thus, a total of five plant species with varying repeats were tested over a span of 63 individual uproot tests. A summary of the uproot test matrix and plant parameters can be found in Table 4-1 and Figure 4-3, respectively.

Table 4-1. Plant uproot test matrix detailing count, plant species and varied parameters.

Module Age	Moisture Content	Count	100 mm Deep Modules[a]	Count	200 mm Deep Modules[a]
6 months	Normal	3	DE	3	AP
		3	GA	3	DE
				6	GA
	High[b]	3	GA	3	AP
				3	GA
13 months	Normal	3	AP	3	AP
		3	DI	3	DI
		3	LA	3	LA
	High[b]	3	AP	3	AP
		3	DI	3	DI
		3	LA	3	LA

[a] Plant ID shown for clarity; see Figure 4-3 for full species name
[b] Modules were artificially saturated prior to uproot testing

Development of the Plant Uproot Device

A Plant Uproot Device was developed at the Powell Structures and Materials Laboratory, located at the University of Florida Eastside Campus. This device was developed in lieu of usage of a Universal Testing Machine (UTM) since the green roof modules could not fit beneath the uplift area of the UTM, and any alteration to the modules would prevent meaningful comparisons with existing field-installed modules. The device consisted of: a custom-designed foam and rubber insert clamp, an Omega

LCR-200 S-shaped hanging load cell with a 90.7 kg (200 lb.) capacity, 1.6 mm (1/16 in.) diameter steel cable, and a 150 mm (6 in.) linear electric actuator. The actuator's displacement rate was determined to vary from 900 to 1900 mm/min (36 to 75 in/min). This variability was attributed to the relative weight of the uplifted material to the actuator's capacity, and could not be manually controlled. However, fine resolution of the load vs. displacement plots was not required due to the mix plants' root interactions in each tested module.

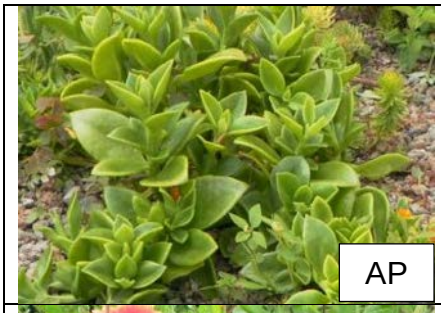

ID	Species	Plant Growth Property
AP	*Aptenia cordifolia*	Soft stems with wide, low-lying cover
DE	*Delosperma nubigenum*	Soft stems with moderate, low-lying cover
DI	*Dianthus gratianopolitanus*	Soft stems with concentrated, low-lying cover
GA	*Gaillardia aristata*	Soft and slender stems with heavy flowers that provide wide cover
LA	*Lantana montevidensis*	Woody stems with moderate cover

Figure 4-3. Uproot-tested plant species and summary of their growth properties. Photos courtesy of author.

Both the actuator and load cell were connected to a National Instruments USB-6218 data acquisition device, which was connected to a portable laptop for data collection and system operation. Utilizing two 100 mm (4 in.) U-bolts, the actuator was

vertically mounted to a 50 mm by 200 mm by 2.5 m (2 in. by 8 in. by 96 in.) piece of pressure treated lumber placed on-end horizontally between two, tripod supports (Figure 4-5).

Test Methodology

The author predicted that the growth media moisture content will affect the uproot resistance of the green roof modules' plants. As such, for several sets of plant species tested, selected modules were artificially saturated prior to uproot testing to compare the uproot resistance of "in-situ" and highly saturated modules. After the necessary plants were uprooted from module specimens, a single soil sample was taken from the green roof module and stored for moisture content analysis (raw data in Tables C-1 through C-3).

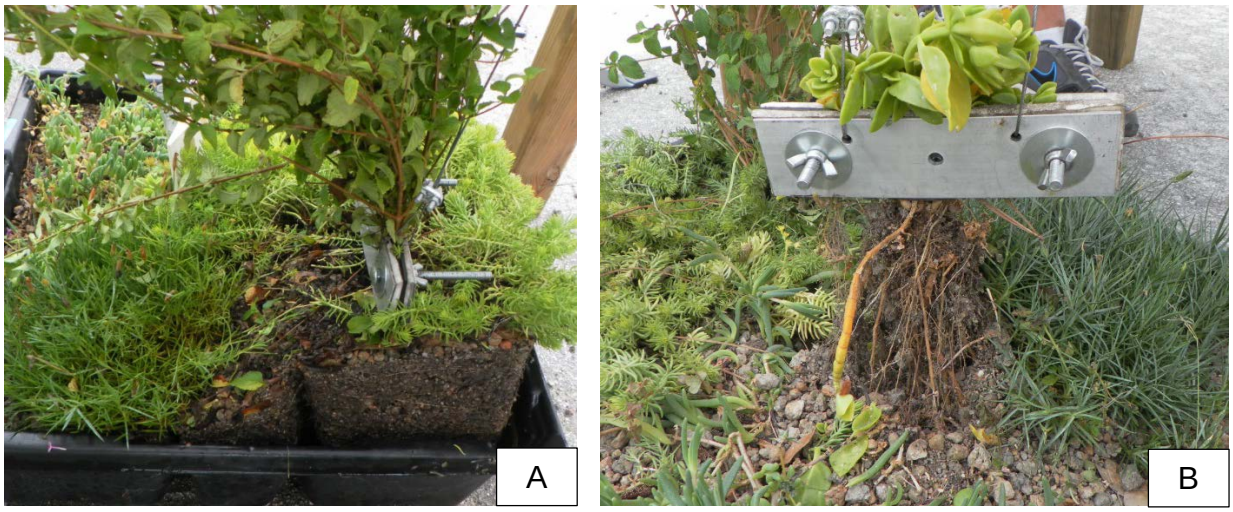

Figure 4-4. Examples of typical uproot test outcomes. A) Lifting of fully-bound growth media for a Lantana uproot test and B) root separation from growth media for an Aptenia uproot test. Photos courtesy of author.

Uproot testing was performed by attaching the corresponding foam and rubber insert clamp to the base of the selected plants and retracting the actuator upwards until either of two conditions occurred: a full 150 mm extension of the actuator lifted the root system mostly intact with growth media still fully attached (Figure 4-4A), or

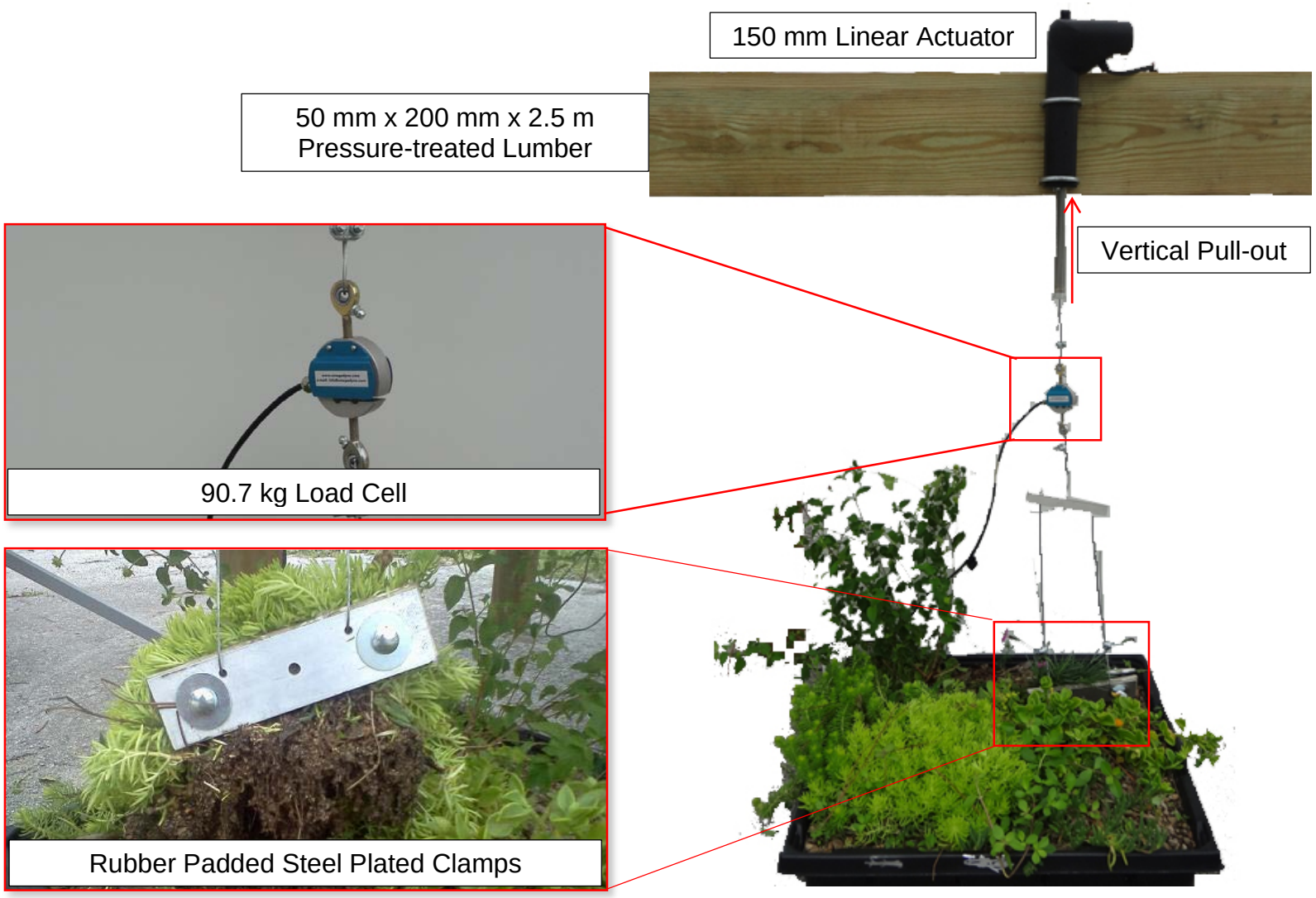

Figure 4-5. Component overview of the Plant Uproot Device. Photos courtesy of author.

root/stem separation from the growth media prior to full actuator extension (Figure 4-4 B). Two unique cases of root/stem separation exist: “catastrophic” separation from the growth media where a sudden load drop is recorded as a result of a collective root breakage from the growth media or progressive root/stem separation. The latter case can be best demonstrated by the top-left plot in Figure F-7, whereas the former case can be described by the top-left plot in Figure E-5.

Because the Plant Uproot Device consisted of a separate load cell and linear actuator, a Labview program was created to record the separate time histories for the actuator’s displacement and the load cell’s force reading at a 50 Hz frequency. The data were then exported to text files which were later merged within MatLAB to create load vs. displacement plots for each test trial, shown in Appendix F.

Results

A summary of the 63 uproot tests can be shown in detail in Tables F-1 and F-2 for both the 200 mm and 100 mm deep modules, respectively. This data was plotted, and then organized by the plant species, establishment period, and module depth, in Figure F-1.

Statistical comparisons are used to determine the significance of the results when considering the effects of the varying factors (e.g. plant type, module depth, etc.). The significance of two quantifiable variables (e.g. moisture content and uproot force) will be determined via their correlation factor. For comparisons between categorical variables (e.g. module age and root interaction, plant type) and quantifiable variables, non-parametric Wilcox rank tests will be performed. The Wilcox rank test was chosen because normality of the data was not known, and comparisons made were typically between two samples (e.g. Aptenia, 200 mm deep vs. Aptenia, 100 mm deep). The null

hypothesis assumes that no differences exist between the two sample sets, and is rejected when the p-value is less than 0.05.

Visual Ranking of Root Systems for Given Plant Species

Visual inspections were performed on tested root systems as well as of the modules' growth media following the uproot testing. Inspection of the growth media in both 100 mm and 200 mm deep modules showed that the root systems completely bound the growth media into a single unit (Figures 4-6 and 4-7). This observation confirmed that both 6 and 13 months of establishment were sufficient establishment lengths for roots to fully spread throughout the modules in a North Florida climate.

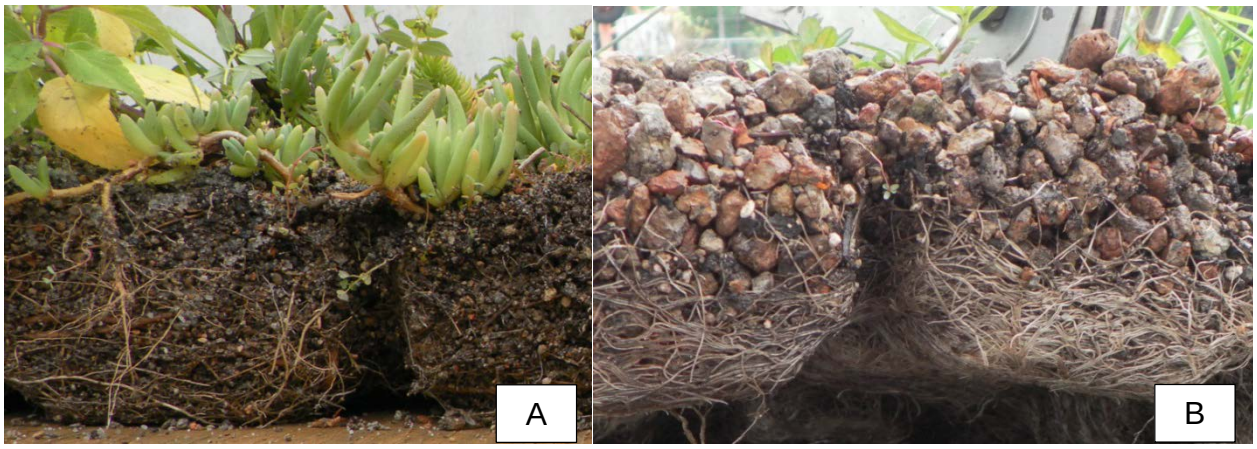

Figure 4-6. Example root spread into growth media for different-aged 100 mm modules. Shown for A) 13 month and B) 6 month modules. Photos courtesy of author.

Figure 4-7. Example root spread into growth media for a 13 month, 200 mm module. Photo courtesy of author.

A review of several of the uprooted plants' root structures allowed for relative rankings of their root spread to be made. These qualitative rankings classified the root structure of a species based on the root length and spread, described as either extensive, moderate, or shallow as summarized in Table 4-2. Example root spreads for individual Lantana, Delosperma and Aptenia species are shown in Figure 4-8 A, B, and C, respectively (plants not shown at the same scale). Following this subsection, the results and analyses shown will determine the adequacy of the root spread rankings presented.

Table 4-2. Qualitative root spread rankings for uproot test species

Aptenia cordifolia	*Delosperma nubigenum*	*Dianthus gratianopolitanus*	*Gaillardia aristata*	*Lantana montevidensis*
Shallow - Moderate	Shallow - Moderate	Shallow - Moderate	Moderate	Moderate - Extensive

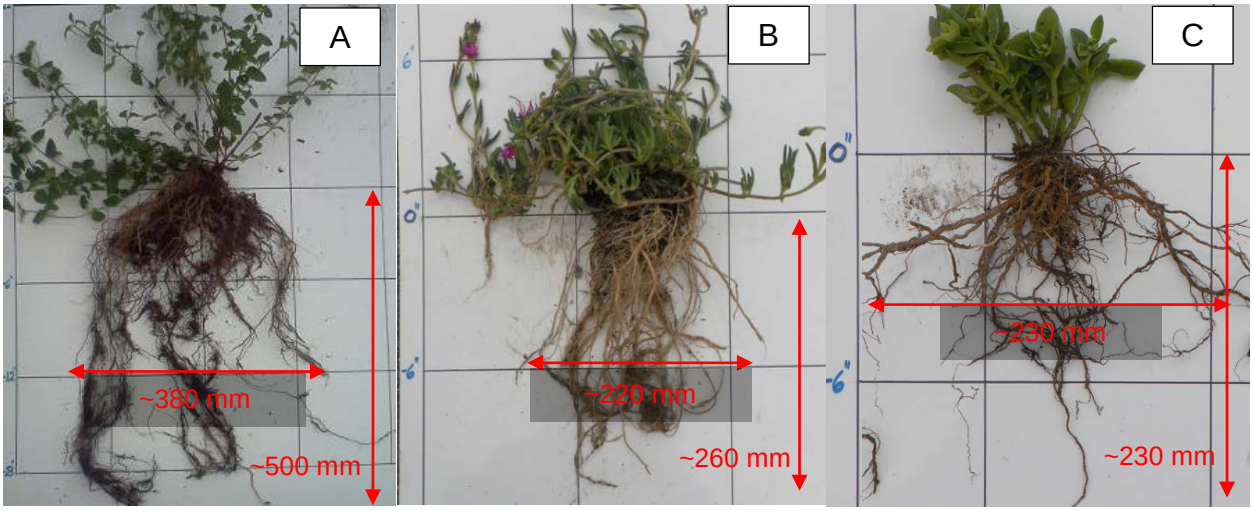

Figure 4-8. Annotated root spreads for three plant species. Shown for A) *Lantana montevidensis*, B) *Delosperma gratianopolitanus*, and C) *Aptenia cordifolia*. Photos courtesy of author.

Variation of Plant Species

A boxplot of the measured peak loads for varying plant species is shown with the annotated medians as well as the outliers (less than 150 N) in Figure 4-9. The boxplot relaxed the varied parameters that were identified (e.g. moisture content, age and root

interaction, etc.) to generalize the uproot resistance of individual plant species used in the uproot study.

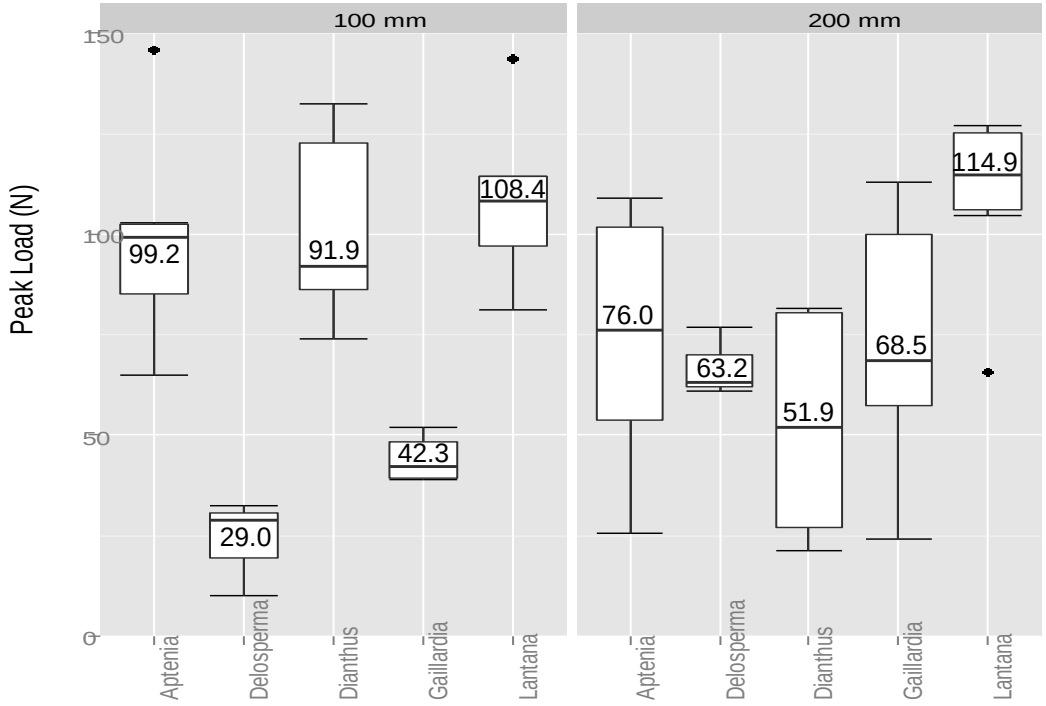

Figure 4-9. Boxplots summarizing the peak measured uproot for each plant species in either 100 mm or 200 mm deep modules.

Several observations can be made for individual plant species from Figure 4-9:

- The Lantana species has the most reliable root and plant structure, and most consistent uproot performance for both module depths. This is reflected by the relatively small interquartile ranges (IQRs) in Figure 4-9, and minimal occurrences of root/stem separation from the growth media. This appears to agree with its assigned root ranking of moderate – extensive in Table 4-2.

- The Aptenia species performs better in 100 mm deep modules than 200 mm modules, reflected from its lower spread (smaller IQR) and higher median peak. Closer inspection of the load-displacement plots for the Aptenia species showed several occurrences of root/stem breakage prior to full actuator displacement for both module depths. This suggests that its uproot performance in mixed-planted modules is well-bounded by the test data obtained.

- The Dianthus species had wide spread in both module depths, but displayed higher uproot capacities in 100 mm deep modules.

- The Gaillardia species had low spread and an overall low uproot capacity in 100 mm modules but opposite conditions in 200 mm modules.

Effect of Module Depth on Test Outcome and Uproot Capacity

To determine whether the variation in module depth affected the peak uproot loads, the all parameters except the module depths were relaxed, and two histograms of the peak loads were plotted against the module depths in Figure 4-10. From Figure 4-10, both module depths are consistent in that most of the measured uproot loads ranged between 0 to 150 N (33.7 lbf), if outliers are ignored. It can be seen that both module depths showed no strong signs of skewness in the peak uproot loads. However, if outliers were ignored, the 200 mm modules showed a more symmetric distribution than the 100 mm modules.

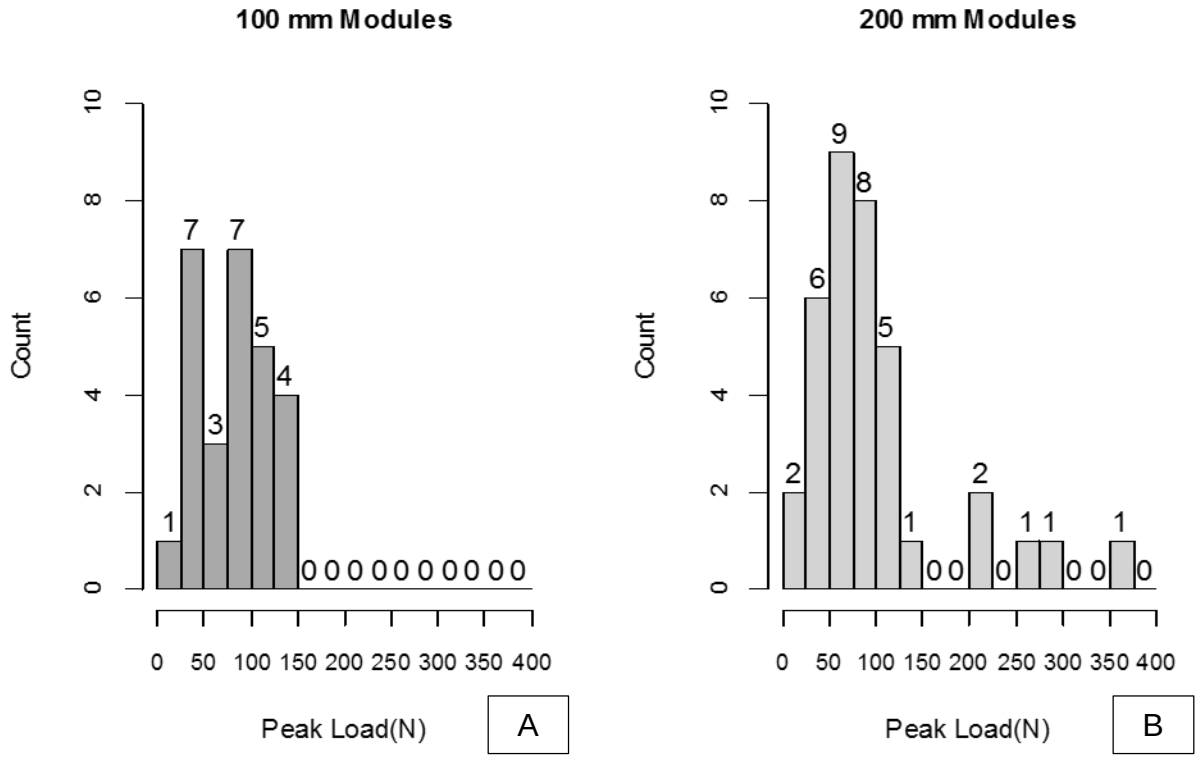

Figure 4-10. Histograms of peak uproot loads for either varying module depths. Shown for A) 100 mm deep modules and B) 200 mm deep modules.

However, when taking plant species into account, Figure 4-9 suggested that plants 100 mm modules yielded more consistent and favorable uproot test outcomes. To determine the favorability of outcomes between 100 mm and 200 mm deep modules, the load vs. displacement plots in Figures F-2 through F-12 were reviewed by the author. Favorable outcomes were defined as either when the load vs. displacement plot showed minimal counts and magnitudes of load drops (e.g. a small load drop occurring at the end of the load curve was acceptable) or when the load curve plateaus, but experiences no sudden load drops before full actuator extension (e.g. mid-displacement plateau with maximum load, but no further load drops). A summary of the favorable uproot test outcomes is shown in Table 4-3, in which the ordering for each species' rankings follows the order of their plots in Appendix F (left to right for each row, then top to bottom of each page). From Table 4-3, 74% (20/27) of the 100 mm and 39% (14/36) of the 200 mm modules resulted in favorable outcomes.

Table 4-3. Observed favorable uprooting outcomes from load-displacement plots.

Plant ID	Age (mo.)	100 mm Modules[a]	# of F	Total	200 mm Modules[a]	# of F	Total
AP	6	-	-	-	F, U, F, F, U, U	3	6
AP	13	F, U, F, U, U, F	3	6	U, F, U, U, U, U	1	6
DE	6	F, F, U	2	3	U, U, U	0	3
DI	13	U, F, F, U, F, F	4	6	U, U, F, U, U, F	2	6
GA	6	U, F, F, F, F, F	5	6	U, F, U, U, U, U, F, U, F	3	9
LA	13	F, F, F, F, F, F	6	6	F, F, F, F, F, U	5	6
		Totals (100 mm)	20	27	Totals (200 mm)	14	36

[a] F = Favorable; U = Unfavorable

Statistical comparisons were then made between the Aptenia (13 month sets), Delopserma, Dianthus, Gaillardia, and Lantana plant species (assuming relaxation of the moisture content and wind-induced weight changes effects) to determine whether the varying growth media depth caused any significant differences within the individual

plant species' peak uproot capacities, as summarized in Table 4-4. The Wilcox test results from Table 4-4 suggest that no statistical differences exist between all data sets of varying module depths except the Gaillardia species. Further, the *Gaillardia aristata* were the only annual species tested (i.e. all others were perennials), meaning that its life cycle occurs within a single growing season, and likely resulted in a weaker stem/root structure. This reinforces the observations made from Table 4-3 and Figure 4-9 for the Gaillardia species, in that they are more susceptible to differences in peak uprooting capacities when subject to changes in growth media depth than other tested plant species within this study.

Table 4-4. Statistical data for uproot samples with differing module depths.

ID	Depth (mm)	Sample Size, n	Mean (N)	SD	Wilcox Test Score, W	p-value
AP	200	6	135.03	91.32	16.0	0.8182
	100	6	98.85	27.17		
DE	200	3	67.00	8.65	0.0	0.1000
	100	3	23.77	12.04		
DI	200	6	75.70	75.77	28.0	0.1320
	100	6	101.28	24.93		
GA	200	9	100.34	99.14	10.0	0.0496[a]
	100	6	44.05	5.68		
LA	200	6	131.82	68.11	14.0	0.5887
	100	6	108.45	21.30		

[a] Null hypothesis is rejected

Planting Density and Age Effects on Peak Uproot Capacity

Since the peak uproot loads were determined to be well-bounded between the ranges of 0 to 150 N (33.7 lbf) for varying module depths, it was deemed suitable to relax the effects due to varying module depths and plant species, and determine how varying the establishment age and planting densities affected the peak uproot loads. Thus, the peak uproot loads were separated between either six month, four plant mixes or 13 month, six plant mixes, and two histograms were created in Figure 4-11.

A comparison of the histograms in Figure 4-11 show a clear difference in skewnesses for the peak uproot loads in different establishment and planting densities. While the six month, four plant mix is positively skewed to the left, the 13 month, six plant mix, contrastingly, is negatively skewed to the right. This makes a strong indication that peak uproot loads tend to be higher when plants are grown for longer periods of time in higher planting densities.

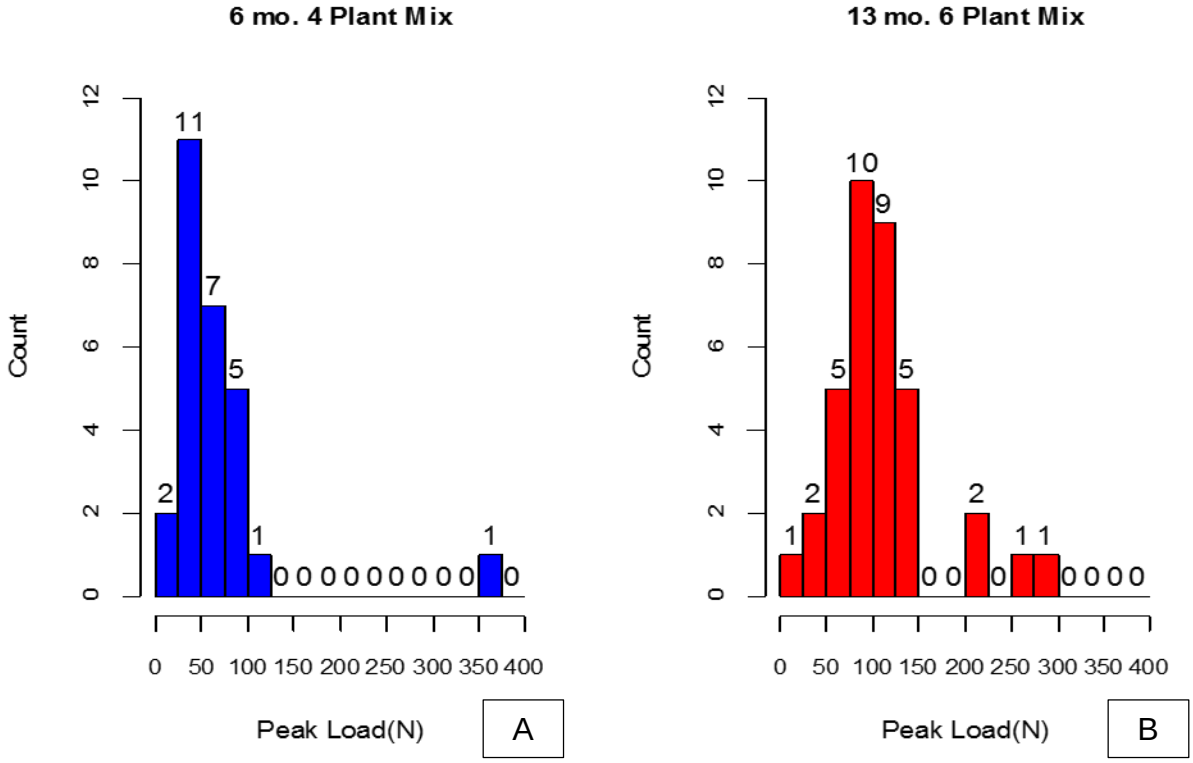

Figure 4-11. Histograms of peak uproot loads for varying module ages and planting densities. Shown for A) six month, four plant mixes and B) 13 month, six plant mixes.

A single comparison was made with the Aptenia species since they were the only plant species in the study to have varied the planting density and module age within the same module depth. The peak load-displacements were plotted with linear fits for Aptenias planted in six month, four plant modules and 13 month, six plant modules in

Figure 4-12. The R-values are 0.811 and 0.515 for the six month, four plant mix and 13 month, six plant mix, respectively. The resulting p-value for the Wilcox test is shown below in Table 4-5 and suggests that the variation in age and planting densities caused no statistically significant differences between peak uproot loads within a 5% confidence level. Despite this, the observations made from Table 4-5 and Figure 4-12 for the *Aptenia cordifolia* plants in 200 mm modules, show weak agreement to the finding from Figure 4-11, reinforcing that Hypothesis #3 is true.

Table 4-5. Summary of statistical data for *Aptenia cordifolia* plants with varying module ages and planting densities.

ID[a]	Age (mo.)	Sample Size, n	Mean (N)	SD	Wilcox Test Score, W	p-value
AP	13	6	135.03	91.32	30.0	0.0649
	6	6	57.20	29.22		

[a] See Table 4-2 or 4-3 for plant species name

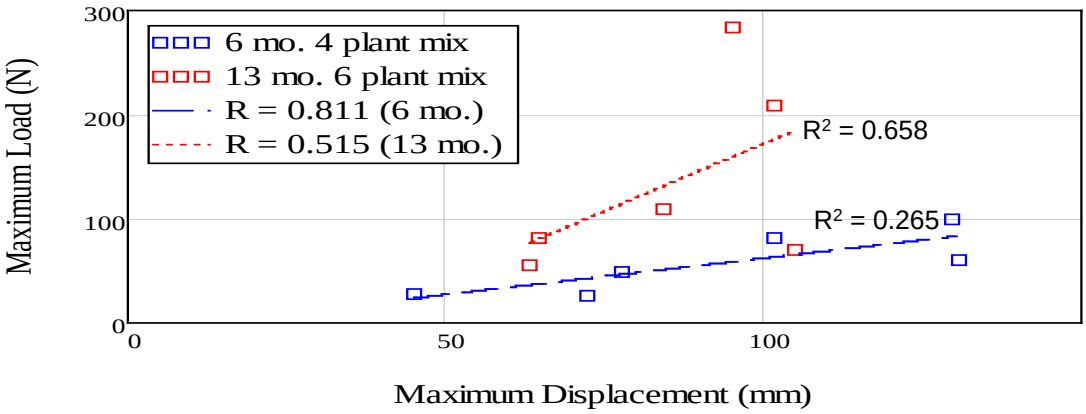

Figure 4-12. Load vs. displacement scatterplot for 6 and 13 mo. Aptenias in 200 mm modules.

Effect of Growth Media Moisture Content on Peak Uproot Loads

Plots summarizing the maximum load vs. measure moisture content for 200 mm and 100 mm deep modules are shown in Figures 4-13 and 4-14, respectively. No observable trends exist between the moisture content and uproot resistance for the plant species tested in the 200 mm deep modules, while both a positively and a

negatively linear correlation can be seen to exist in the Aptenia and Gaillardia species planted in 100 mm deep modules, respectively. Still, correlation (R) and R^2 values were calculated between the moisture content and measured uproot loads for each plant species in both 200 mm and 100 mm deep modules in Table 4-6. The weak and opposing trends in correlations between the data suggests that moisture content played a minimal role in the uproot capacity of the plants.

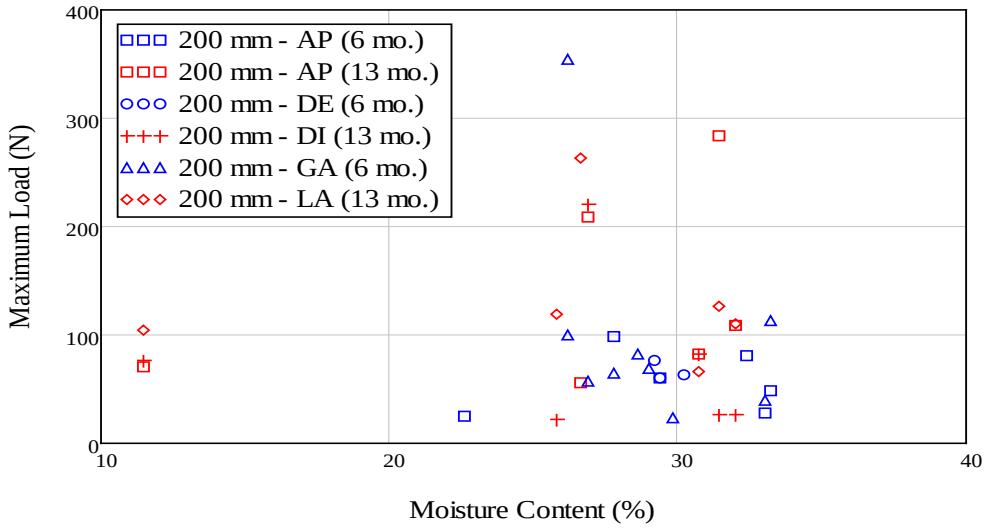

Figure 4-13. Maximum load vs. growth media moisture content percentage scatterplot for 200 mm deep modules.

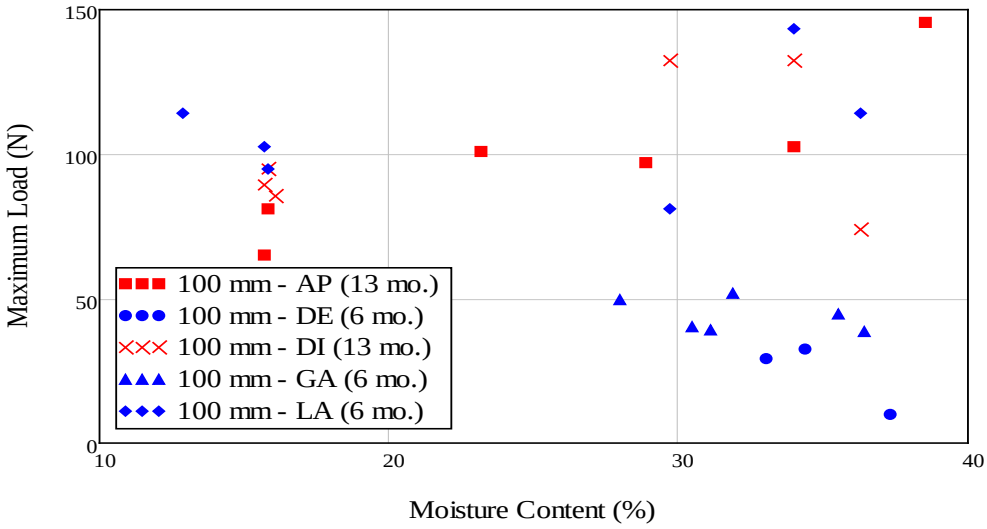

Figure 4-14. Maximum load vs. growth media moisture content percentage scatterplot for 100 mm deep modules.

Table 4-6. Summary of Pearson correlation coefficients between moisture content and uproot resistance for varying plants in 200 mm and 100 mm deep modules.

Plot ID	Depth (mm)	Age (mo.)	Sample Size, n	R^2	R-value	Plot ID	Depth (mm)	Age (mo.)	Sample Size, n	R^2	R-value
AP	200	6	6	0.019	0.139	AP	100	13	6	0.785	0.886
AP	200	13	6	0.147	0.384	DE	100	6	3	0.801	-0.895
DE	200	6	3	0.300	-0.548	DI	100	13	6	0.125	0.353
DI	200	13	6	0.019	-0.137	GA	100	6	6	0.146	-0.382
GA	200	6	8[a]	0.003	-0.056	LA	100	6	6	0.106	0.326
LA	200	6	6	<0.001	0.003						

[a] Omitted outlier

Effect of Wind-Induced Losses on Peak Uproot Loads

It was hypothesized that higher measured losses from the wind testing in a modular tray green roof specimen would result in lower uproot capacities for the plants. Therefore, it should be expected that a negative correlation would exist between the two variables. With the moisture content effects relaxed, maximum load vs. percentage weight change plots were created for wind-tested 200 mm and 100 mm deep modules in Figures 4-15 and 4-16, respectively. Plants which were not wind-tested were omitted from these plots.

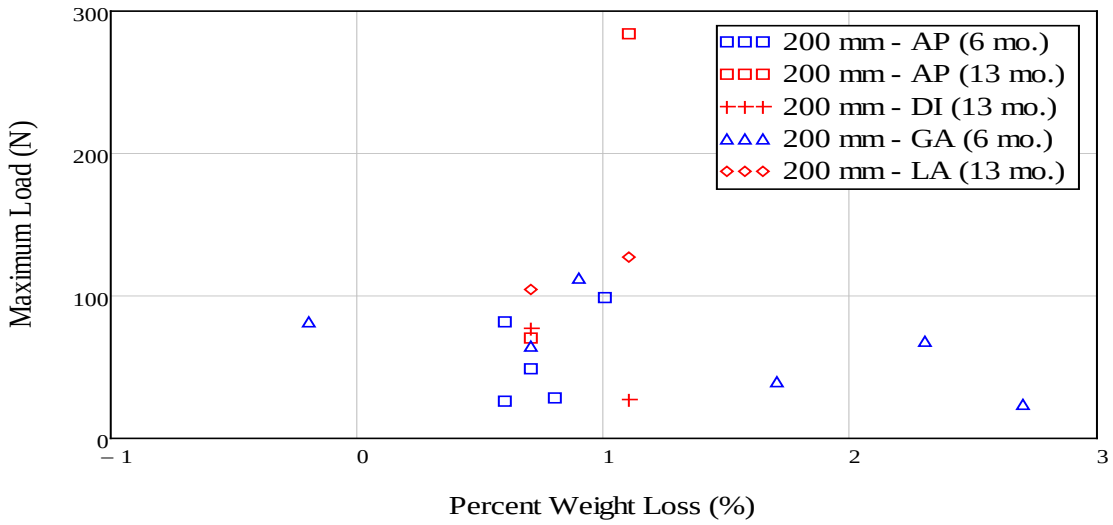

Figure 4-15. Maximum load vs. percentage weight change scatterplot for 200 mm deep modules.

From Figures 4-15 and 4-16, no discernable trends can be identified within all but the Gaillardias planted in 200 mm deep modules. For those plants, a negative linear correlation with an R-value of 0.636 (R^2 = 0.404) was calculated (Figure 4-17). All of the wind-tested Gaillardias shown came from the same wind test trial in Phase 2 (T10) and had varying roof locations. Further, all of the uprooted Gaillardias from the plot separated from the growth media prior to full extension of the linear actuator.

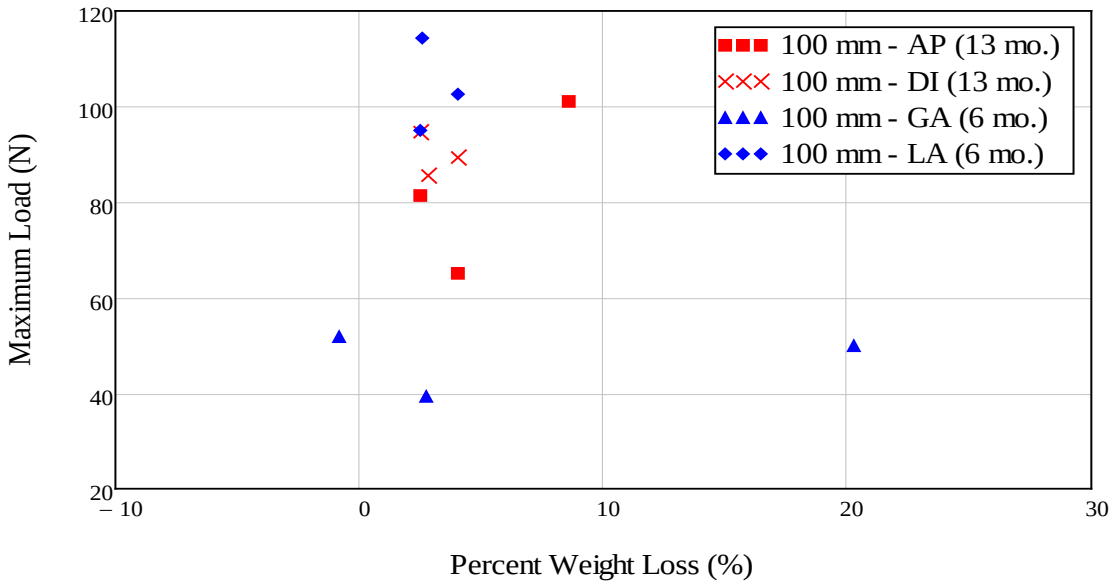

Figure 4-16. Maximum load vs. percentage weight change scatterplot for 100 mm deep modules.

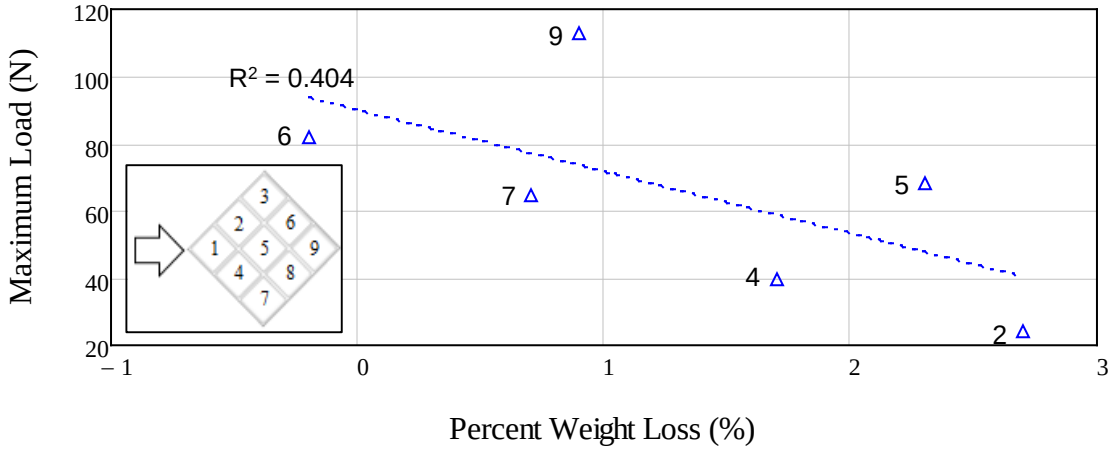

Figure 4-17. Maximum load vs. percentage weight change scatterplot for wind-tested Gaillardias in 200 mm deep modules with annotated module roof locations.

The lack of observable trends in Figures 4-15 and 4-16 does not necessarily translate to wind-induced losses having no relationship to the root anchorage to the growth media (i.e. uproot capacity of a plant). It suggests that for the current study, the wind-induced losses are more dependent upon the module's roof location during wind testing. If modules were placed under the same wind loading conditions (i.e. identical test duration, roof location, etc.), better comparisons could be made between wind-induced weight changes and the root anchorage.

Summary

A Plant Uproot Device was developed to conduct uproot testing on field-planted modular green roof systems consisting of varying mixtures of plants. When compared to laboratory tests, the study reflects more realistic conditions expected on actual green roofs, since plant species are typically varied for design with less-refined control in their establishment. A total of 63 uproot tests were performed on a total of five plant species: 1) *Aptenia cordifolia*, 2) *Delosperma nubigenum*, 3) *Dianthus grantianopolitanus*, 4) *Gaillardia aristata*, and 5) *Lantana montevidensis*. Both visual and statistical comparisons were made for the plant uproot performance. The findings can be summarized as follows:

- Establishment periods of six to 13 months were adequate in the Florida climate for full root growth in extensive and intensive modules. Low-lying plants had mostly shallow to moderate root spreads while taller plants had moderate to extensive root spreads.
- The *Lantana montevidensis*, a perennial species, had the highest uproot capacities (medians: 108 N for 100 mm modules and 115 N). This reinforces its strong root anchorage as only one of the 13 tested plants experienced premature separation with the growth media. All of these findings were consistent with its relative root ranking of moderate to extensive spread.
- Larger module depths yield plants with more scatter of uproot capacities and resulted in more occurrences of root separation from the growth media. However,

only the *Gaillardia aristata*, an annual specie, appears to show a statistically significant difference in their uproot capacities when the module depths were varied.

- The combined effect of higher planting density and longer establishment resulted in greater uproot capacities.
- No observable trends could be identified between growth media moisture content and uproot capacities for all tested plant species except the *Aptenia cordifolia*, a perennial species, which exhibited a strong, positive correlation.
- Wind-induced weight losses in the modules did not affect the uproot capacities for four of the five plants tested in this study. The *Gaillardia aristata* species grown in the 200 mm deep modules displayed a negative correlation between uproot capacity and percent weight loss.

Discussion

The three hypotheses made at the beginning of this study are reassessed as follows:

Hypothesis 1. Modules which experience higher scour losses from wind testing will yield plants with lower uproot capacities (i.e. plants with poor uproot capacities provide poor scour protection).

This was not proven in this study for all plant species, due to lack of sufficient sample size. The negative correlation between the *Gaillarida aristata* species grown in 200 mm modules appear to agree with this hypothesis. However, it was identified in Chapter 3 that weight losses were more reliant on the module's roof location during the wind testing experiment. Thus, a more-refined study should be conducted in which modules are subjected to identical wind conditions.

Hypothesis 2. One-hundred (100) mm deep modules will yield plants with lower uproot capacities than 200 mm deep modules due to less space for roots to grow.

Grouping the modules by their growth media depths showed that with omitted outliers, peak uproot capacities were well-bounded between 0 to 150 N (33.7 lbf).

Closer inspection showed that the hypothesis was true for only two of the five tested plant species (*Gaillardia aristata* and *Delosperma nubigenum*). The other three plant species behaved opposite of the proposed hypothesis. A Wilcox rank test determined that only the *Gaillardia aristata* species showed significant differences between uproot capacities for varying module depths. Comparing individual plant species' uproot capacities and frequency of "favorable" root to soil attachment showed that 100 mm deep modules resulted in lesser spread of peak uproot loads and occurrences of root separation from the growth media when compared to 200 mm deep modules.

Hypothesis 3. Higher interspecies root interactions will increase uproot capacities when comparing same plant species. It should be noted that 13 month modules yield six plants per module while six month modules only have four plants per module.

From the histograms in Figure 4-11, a strong indication exists which suggests that the combined effect of increased age and root-interactions leads to slightly higher uproot capacities. Closer study of the *Aptenia cordifolia* species, showed a weak correlation that agreed with this indicator. A better comparison (outside the limits of this study) would be to test the uproot capacity of a single plant against the same plant in varying-sized plant mixtures.

Summary

The results and findings shown in this study offer a limited view on how plant uproot capacities could be used to determine suitable wind-resistant plant selections for green roof systems in a given climate. Previous studies by Bailey et al. (2002) and Hamza et al. (2007) have shown that plant uproot capacities are directly related to soil

stability (root anchorage). However this was the first study to investigate the uproot capacities from field-planted vegetation in realistic green roof conditions.

While it was expected that individual plant species would vary in uproot capacities, the strong indication that uproot capacities could be increased through higher planting densities and longer establishment offers significant stipulations for future green roof wind designs. If this hypothesis holds true, laboratory studies conducted on individual plants would provide conservative results, thus allowing green roof designers to provide mixed planting options to introduce factors of safety against wind-induced uprooting.

It was of high interest to observe the *Lantana montevidensis* species portray the most consistent uproot capacities out of the five species tested. Recall from Chapter 3, the Lantanas' tall plant heights had contributed to visibly high wind-induced bending stresses, and was therefore deemed as unsuitable plant species for green roofs with low parapets. However, following this uproot study, the author proposes that in combination with a sufficiently high parapet, a wind-resistant plant design for green roofs should consist of low-lying, widespread plants to protect and contain loose aggregate from blow-off and scour, and taller plants with higher root-anchorage capacities to increase the sublayer growth media stability.

CHAPTER 5
PRELIMINARY DESIGN WORKSHEETS FOR MODULAR TRAY GREEN ROOFS

This chapter will review the work completed in the development of the wind design worksheets used to calculate design wind loads and failure wind speeds based on ASCE 7 provisions. The chapter will first review the motivation and background literature which resulted in development of the design worksheets. Then, the worksheets' methodologies are detailed, and a comparison is made between the predicted worksheet values with the full-scale failures observed with the modular tray specimens tested in Chapter 3 for validation. A typical calculation for an example building and hypothetical green roof array size is then presented, and the chapter concludes with a proposed envelope design procedure for efficient green roof wind designs. The bulk of the information presented in this chapter was extracted from a recent ACWE conference paper by the author and his colleagues (T. Vo, Prevatt, Acomb, & Masters, 2013).

Background and Motivation

Following the wind-induced failures of the green roof modules described in Chapter 3, the author observed several failure mechanisms (sliding, uplift and overturning) exhibited by the modules from the test footage. Due to lack of instrumentation on the test deck, only the roof-height wind speed was known (~44.7 m/s). This section reviews two recent studies, similarly focusing on the wind effects on rooftop pavers by: Aly et al. (2012) and Irwin et al. (2012).

2012 – Aly et al. – Full-scale Aerodynamic Testing of a Loose Concrete Roof Paver System

In 2012, Aly et al. conducted full-scale wind testing on concrete paver systems to determine the aerodynamic wind loads acting on a concrete roof paver. Their study

aimed to further investigate how underside and upper surface wind pressures affect ballasted roof systems, and offer methods of mitigation.

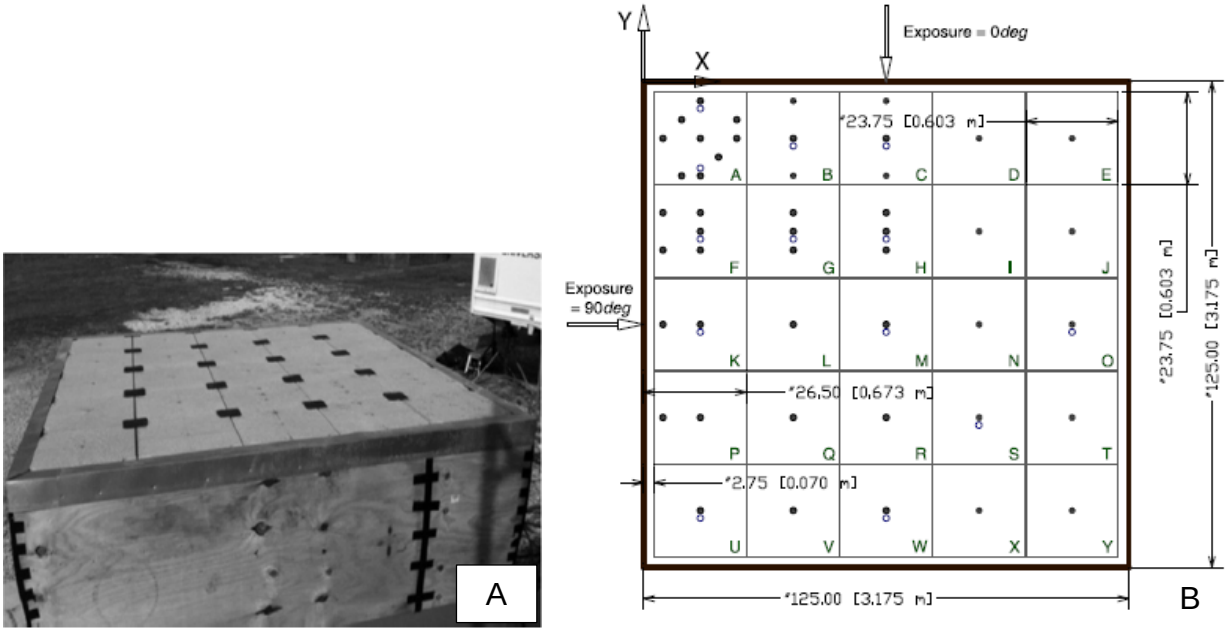

Figure 5-1. Wind testing configurations detailing paver and pressure tap locations. A) Paver array set-up on the test building and B) pressure tap mapping in relation to incoming wind directions. Photo and figure courtesy of Aly et al., 2012.

Wind testing was conducted utilizing a six-fan “Wall of Wind” located at Florida International University (similar to UF’s eight-fan hurricane simulator). The Wall of Wind has a test opening of 6.7 m wide by 4.9 m high (22 ft. by 16 ft.) and is capable of producing category 1 Saffir-Simpson Scale hurricane wind speeds. The researchers constructed a test building measuring 3.2 m by 3.2 m by 2.1 m high (10.4 ft. by 10.4 ft. by 7 ft.), had no parapet, and was placed 6.6 m (21.7 ft.) away from the Wall of Wind’s test opening. Twenty-five concrete pavers, each measuring 61 cm by 61 cm by 5.1 cm thick (2 ft. by 2 ft. by 2 in.), were equipped with a total of 63 pressure taps placed on either the upper surface or underside of the pavers , and installed atop the building’s roof as a five by five array (Figure 5-1A). A higher density of pressure taps was allocated towards the windward corner of the paver system (Figure 5-1B). Pavers were

placed on 30 cm (1 ft.) pedestals to allow for a uniform underside gap. A Cobra Probe was installed at eave height to measuring the incoming wind speed. The Wall of Wind produced a 3-second gust of about 28.5 m/s (63.7 mph) with a turbulence intensity of about 27% at the eave height. The test building was tested for five wind directions (0, 22.5, 45, 67.5, and 90 deg) and pressure times histories were collected at a frequency of 100 Hz for three minute durations. Mean, RMS, and peak pressure coefficients on the upper surface (Cp_{ext}) and underside (Cp_{int}) of the pavers were obtained for each wind direction.

The researchers found that the most critical wind directions occurred at 22.5 and 67.5 degrees. The differential pressure coefficient time histories were calculated by Eqn. 5-1 for all pavers.

$$Cp_{tot}(t) = [Cp_{ext}(t) - Cp_{int}(t)] \tag{5-1}$$

Where:

$Cp_{ext}(t)$ = external pressure coefficient (upper surface)

$Cp_{int}(t)$ = underside pressure coefficient

The net differential pressure coefficients were then applied to their corresponding pressure tap's tributary areas to obtain uplift forces via Eqn. 5-2,

$$F_A(t) = \frac{1}{2}\rho {U_3}^2 \left[\frac{1}{n_a}\sum_{i=1}^{n_a} Cp_{tot,i}(t) \cdot A_i\right] \tag{5-2}$$

and overturning moments via Eqn. 5-3

$$M_{A,o-o}(t) = \frac{1}{2}\rho {U_3}^2 \left[\frac{1}{n_a}\sum_{i=1}^{n_a} Cp_{tot,i}(t) \cdot A_i \cdot d_i\right] \tag{5-3}$$

Where:

ρ = air density assumed as 1.25 kg/m^3

U_3 = peak 3-s wind speed in m/s

n_a = total number of external pressure taps on the paver

A_i = tributary area of the tap, i

The investigators then considered two cases for analysis: the single paver in the wind ward corner, a two by two and a three by three grouped paver system. The forces and moments were calculated utilizing an assumed design wind speed of U_3 = 65.3 m/s (146 mph) corresponding to the Miami region (ASCE 7-05 code) from both a capacitive and design standpoint (i.e. ASCE 7-05 MWFRS). Moments were assumed to act about the leeward edge of the paver/paver system.

The investigators found that for the single paver case, only considering the external, upper surface pressure overestimated the net differential pressure by as much as 15%. Further, the uplift forces were higher when closer to windward edge of the paver, which would result in higher overturning moments than the resistive moment due to the weight of the paver alone. As such, they determined that a single paver's resistive capacity (weight of 472 N) could not withstand the applied uplift and overturning forces corresponding to a 65.3 m/s (146 mph) wind speed.

While two by two paver arrays (total weight of 1886 N) could not withstand the estimated peak uplift forces produced by the design wind speed of 65.3 m/s (146 mph), three by three paver arrays (total weight of 4244 N) showed sufficient capacity. For grouped paver arrays, the authors stated that rigid connections were required for modules to act as a single rigid body. Thus, maintenance of the paver systems was

recommended to prevent fatigue of the rigid connections and build-up of debris between the paver gaps.

2012 – Irwin et al. – Wind Tunnel Model Studies of Aerodynamic Lifting of Roof Pavers

A 1:10 scale wind-tunnel study was conducted in RWDI's wind tunnel by Irwin et al. (2012) to investigate the rooftop behavior of pavers during high winds. This investigation was performed following wind-induced paver movement on a rooftop terrace during a storm with peak gusts of 40.2 – 49.2 m/s (90 – 110 mph), as shown in Figure 5-2. Those displaced rooftop pavers measured 61 cm by 61 cm (2 ft. by 2 ft.), weighed 422 N (95 lbf.), and were installed on the roof terrace with a gap of 1.6 cm (5/8 in.) between the pavers' underside and roof deck. It was noted that the two rows of pavers nearest the roof edge were strapped together.

Figure 5-2. Displaced roof pavers on a rooftop terrace following storm event. Photo courtesy of Irwin et al., 2012.

Pressure equalization of ballast roof systems (e.g. rooftop pavers) typically occurs very quickly (< 0.1 s). This is due to very small air volume exchanges between the underside and top surface of a paver required for equalization. However, for roof regions where conical vortices can significantly increase the external uplift pressures, this pressure equalization may not occur quickly enough, resulting in the net uplift of the

roof paver. They determined that the critical wind speed at which lift-off of a single paver occurs (i.e. the uplift force equals the paver weight) could be calculated from Eqn. 5-4.

$$U_{CRIT}(t) = \sqrt{\frac{W}{\frac{1}{2}\rho C_z A}} \tag{5-4}$$

Where:

W = paver weight

ρ = air density

C_z = vertical aerodynamic force coefficient

A = paver area

Based on similar studies, Irwin et al. (2012) approximated the C_z value of an individual paver to be equal to 1/3 of the magnitude of the peak negative external pressure coefficient on the upper surface of the paver (i.e. $C_z = -(1/3)C_{p,peak}$). For strapped (or interconnected) pavers, the authors state that the uplift loads are generally shared across pavers, increasing the critical lift-off speed of the paver system by a factor of 1.4 to 1.7. They claimed that straps should be transverse to the axes in which conical vortices act. Full strapping in both orthogonal directions would therefore be the most conservative approach.

Wind testing was conducted in RWDI's boundary layer wind tunnel measuring 4.8 m long by 2.4 m wide (16 ft. by 8 ft.). A 1:10 scale model of the corner of the roof terrace was constructed and two roof-wall configurations were considered: an isolated roof corner and the roof corner with a back wall. High density Styrofoam models of the pavers (each weighing 0.68 g) were installed. A mean velocity profile for an urban area (Exposure B) was simulated with a roof-top turbulence intensity of 15%. The

investigators tested four paver setups: without straps, edge straps only, full strapping of the array, and full strapping with steel angle edge restraints. Their results are shown in Table 5-1. Speed improvement ratios are compared to the edge strapping configuration.

Table 5-1. Model roof paver wind tunnel test results (Irwin et al., 2012).

Paver system configuration	Roof/wall model configuration	Model lift-off speed (m/s)	Speed improvement ratio	Predicted full scale lift-off speed (m/s)
Without straps	Isolated flat roof	2.2	0.88	44
	Roof w/ back wall	2.0	0.88	41
With straps along first two rows of pavers	Isolated flat roof	2.5	1.00	50
	Roof w/ back wall	2.3	1.00	46
With full strap system	Isolated flat roof	3.3	1.32	65
	Roof w/ back wall	3.1	1.36	63
With full strap system and steel angles in place	Isolated flat roof	>6.1[a]	>2.41	119
	Roof w/ back wall	-	-	-

[a] Pavers did not actually lift-off the roof; only hovered in place.

The lift-off speeds determined for the edge strapping configuration were indicative of the assumed failure wind speeds seen on the roof terrace, validating their study. The authors concluded that the introduction of any type of strapping system would increase the lift-off speed of a paver system. An extreme condition of utilizing steel angle edge restraints showed that paver systems showed no movement for full-scale equivalent wind speeds greater than 119 m/s.

The authors identified that accurate scaling of the Reynolds number must be considered when performing wind tunnel tests on pavers subject to high conical vortices. While the localized effects from conical vortices are averaged out over larger tributary areas typical of larger roof systems, pavers have smaller tributary areas and are more susceptible to peak uplift loads caused by conical vortices. It was

approximated that peak negative pressure coefficients would grow more negative by -0.5 for each factor of 10 increase in the Reynolds number.

Discussion

Both Aly et al.'s (2012) full-scale paver study and Irwin et al.'s (2012) wind tunnel study concluded that grouping pavers together resulted in higher lift-off wind speeds than when compared to individual pavers. Further, Aly et al. (2012) specified that rigid attachment between pavers was required for grouped systems to behave as single units. Both studies attributed pressure equalization to play a small role in reducing the overall uplift of pavers (Aly et al. documented upwards of a 15% reduction in uplift).

Both studies investigated comparable-sized pavers (in full scale), and demonstrated the blow-off potential of concrete pavers weighing approximately 422 – 472 N. The question that arises is how do green roof modules relate to these two reviewed studies? The author of this report documented both overturning and sliding failures indicative of the failure mechanisms defined by Aly et al. (2012). For example, the absence of rigid connections (i.e. utilization of zip-ties) between green roof modules in the three by three array led to a similar blow-off failure that was observed for a single green roof module. If green roof modules are hypothesized to behave similar to rooftop pavers, then it should be expected that extensive (100 mm) green roof modules would fail at lower wind speeds due to lower weights (e.g. green roofs typical 18 – 22 kg vs. pavers typical 41 – 45 kg).

Objective

Current design guidelines only compare zone uplift pressures with corresponding green roof dead loads, and offer no method of mitigation of the three failure modes identified by the investigators. Further, the overturning of rigid roof array systems can

easily be calculated, given the design roof pressures and array size. While the current limitations of the project prevent the ability to determine green roof overturning and uplift capacities, it is proposed that the design demand loads could be defined for design.

The purpose of this study was to develop a preliminary method of efficiently determining design uplift forces, overturning moments, and failure wind speeds for any given building geometry and green roof array configuration, utilizing ASCE 7 Components and Cladding provisions.

Methodology

Idealized Model for a Typical Green Roof Module

An idealized representation of a typical green roof module was developed, as shown in Figure 5-3. The predicted forces affecting the module's wind performance were then superimposed on the figure. It should be noted that frictional forces are shown to exist in the diagram despite the module pivoting about a corner and not in contact with the surface.

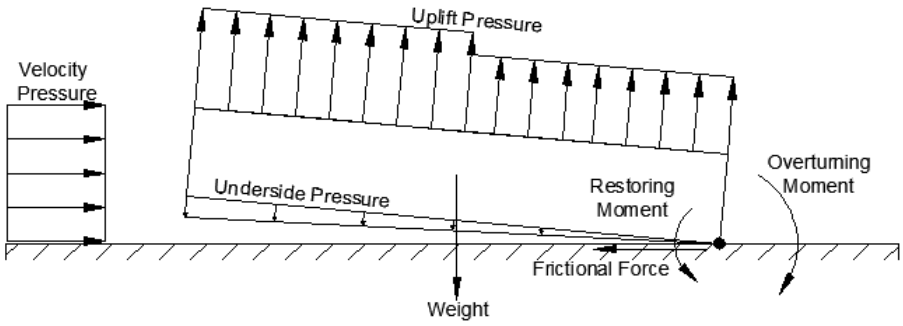

Figure 5-3. Free body diagram of a single 610 mm by 610 mm by 100 mm deep (24 in. by 24 in. by 4 in.) idealized green roof module.

Because the wind load provisions in ASCE 7 provide roof pressures for any given building geometry and design wind speed, localized wind effects due to module imperfections, unevenness, drainage cavities, and over-hanging edges (as detailed

earlier in Figure 3-3) shall be ignored. Therefore, any pressure equalization effects due to the air permeability of the green roof systems will be effectively ignored for the preliminary design approach presented in this study.

Definition of Wind-Induced Failure Modes

Three possible wind-induced failure modes were identified for the green roof module(s) from the experimental footage: sliding, uplift, and combined overturning. The external forces that contribute to these failure modes are summarized in Figure 5-3. In order to determine the ASCE 7-calculated wind load effects on each of these failure modes, the failure criteria are defined.

Sliding

Sliding of several modules was observed on the test roof before blow-off occurred. Sliding of the system due to the velocity pressure is a function of the wind direction and array size (which determines the projected area) and incoming velocity pressure. This failure mode was defined as when the lateral force due to the velocity pressure acting on the modular array is greater than the static friction force, as expressed by Eqn. 5-4:

$$F_{vel} \geq \mu_s N \tag{5-4}$$

Where

μ_s = coefficient of static friction between the deck material and the modular tray material

N = normal force acting upwards perpendicular to the deck (assumed to equal the weight of the modular system due to low roof slopes);

F_{vel} = force due to velocity pressure from Eqn. 5-5

$$F_{vel}(V) = q_h(V)A_{proj} \tag{5-5}$$

Where

q_h = velocity pressure from Eqn. 5-6 (ASCE 7 velocity pressure)

A_{proj} = exposed projected area of the modular array system from Eqn. 5-7

$$q_h(V) = 0.613K_zK_{zt}K_dV^2(N/m^2) \tag{5-6}$$

(In US) $$q_h(V) = 0.00256K_zK_{zt}K_dV^2(lb/ft^2)$$

If $h_m \geq h_p$: $$A_{proj} = (h_m - h_p)l_{proj} \tag{5-7a}$$

Otherwise: $$A_{proj} = 0 \tag{5-7b}$$

Where

K_z = velocity pressure exposure coefficient

K_{zt} = topographic factor assumed as 1.0

K_d = wind directionality factor assumed as 0.85

V = design wind speed in m/s

h_m = depth of the modular array system

h_p = height of the parapet

l_{proj} = projected length of array transverse to wind direction.

As shown by Eqn. 5-7b, the authors of this paper made the assumption that only the exposed depth of the modular green roof system experiences the direct velocity pressure, q_h (i.e. when the depth of the green roof system is greater than the parapet height). Otherwise, it was expected that the modular array system experienced no external lateral forces from the wind. While this assumption may be valid for arrays placed in close proximity behind any given parapet height, it is probable that by increasing the distance between the windward edge of the green roof system and the

parapet, the projected area exposed to the velocity pressure also increases. The distance at which this exposure increases is not explored within this study, as the author predicted that due to the relatively small module heights of 100 mm and 200 mm (4 in. and 8 in.), failures resulting from strictly lateral forces would not be the controlling failure mode of modular green roof systems.

Uplift

Uplift of the modules was identified as a possible mode of failure. The total uplift of an array is a function of the approaching velocity pressure, external roof pressure coefficients (based on building's geometry), and the array's size. Appropriately, the total array weight can be defined as the system's dead load multiplied by its total area. Failure can be defined as when the total uplift force acting on the modular array exceeds the total weight of the array, Eqn. 5-8:

$$U_{tot}(V) \geq W_{tot} \tag{5-8}$$

Where

U_{tot} = total uplift from Eqn. 5-9

W_{tot} = total weight from Eqn. 5-10

$$U_{tot}(V) = \sum_{j=1}^{n} q_h(V)\, A_j\, GC_{p_j} \tag{5-9}$$

$$W_{tot} = \sum_{j=1}^{n} wA_j \tag{5-10}$$

Where

n = total number of modular trays in the array

q_h = velocity pressure from Eqn. 5-6

A_j = area of module *j*

GC_p = j[th] module's corresponding external pressure coefficient

W = dead load of selected system (as specified by manufacturer)

Overturning

The sliding and uplift failure modes assume that once the limit conditions are met or exceeded, modular array failures occur. Following the full-scale failures described in Chapter 3, the author hypothesized that a more plausible failure mode results from the external forces defined in Eqn. 5-5 and Eqn. 5-9 combining to "overturn" the array system about a moment arm dependent upon the incoming wind direction. Failure is defined as when the wind-induced overturning moment meets or exceeds the restoring moment created by the dead load of the system array, described by Eqn. 5-11:

$$M_{over}(\mathrm{V}) \geq M_{res} \tag{5-11}$$

Where

M_{over} = overturning moment from Eqn. 5-12a or Eqn. 5-12b

M_{res} = restoring moment from Eqn. 5-13

If $h_m \geq h_p$: $$M_{over}(V) = \left[F_{vel}\left(\frac{\left(h_m - h_p\right)}{2} + h_p\right)\right] + \sum_{j=1}^{n}\left(q_h\, A_j\, GC_{p_j}\bar{y}_j\right) \tag{5-12a}$$

Otherwise: $$M_{over}(V) = \sum_{j=1}^{n}\left(q_h\, A_j\, GC_{p_j}\bar{y}_j\right) \tag{5-12b}$$

$$M_{res} = W_{tot}\bar{Y} \tag{5-13}$$

Where

F_{vel} = lateral force due to velocity as determined by Eqn. 5-5

W_{tot} = total system weight found by Eqn. 5-10

$\bar{y}_j$ = moment arm from system pivot point's axis transverse to the wind

direction and the location of the j^{th} module's centroid

$\bar{y}$ = moment arm from system pivot point's axis transverse to the wind direction and the location of the system centroid.

Inspection of Eqn. 5-12a shows that the first term in the equation is simply the lateral force due to the velocity pressure (via Eqn. 5-5) multiplied by its vertical moment arm. Like before, this assumes that parapet heights larger than the module's depth result in the lateral component of Eqn. 5-12a equaling zero, which yields Eqn. 5-12b. The magnitude and number of the moment arms included in the evaluation of Eqn. 5-12a and 5-12b are solely dependent upon the size and placement of the green roof module array in relation to the plan roof area, and the incoming wind direction.

Worksheet Assumptions and Limitations

The design assumptions and limitations that the investigators made in developing the Wind Load Determination and its supplementary Failure Wind Speed Calculation worksheets are summarized in this subsection.

Building properties

Buildings heights can range anywhere between 0 – 152 m (500 ft.), with taller buildings requiring wind tunnel modeling and testing as recommended by ASCE 7. The considered buildings must be rectangular in shape (Figure 5-4), with impermeable, flat (sloped at less than 7 degrees) roof decks. Parapet widths will not reduce the total roof plan area. Parapet heights will be measured from the growth media surface of the green roof array to the top surface of the parapet.

ASCE 7 wind loads

ASCE 7-10's Components and Cladding (C&C) wind load provisions detailed in Chapter 30 were used to determine the negative pressures on the roof. The C&C

approach was chosen over the Main Wind-Force Resisting System (MWFRS) approach because modular green roof systems were assumed to behave as ballast systems which provide no support or stability to the building, although this preliminary design approach may overestimate the wind loads since pressure equalization effects are ignored. The worksheets' code derives from Chapter 30 Parts 1 and 3 for low rise ($h \leq 18.3$ m) and medium to high rise ($h > 18.3$ m) buildings, respectively. Depending on the user's input, the worksheets automatically determine the appropriate method to calculate the roof pressures and resulting forces and moments which act on the defined roof system. Roof pressure zones are defined according to the pressure coefficient zone width (*a*) as shown in Figure 5-5.

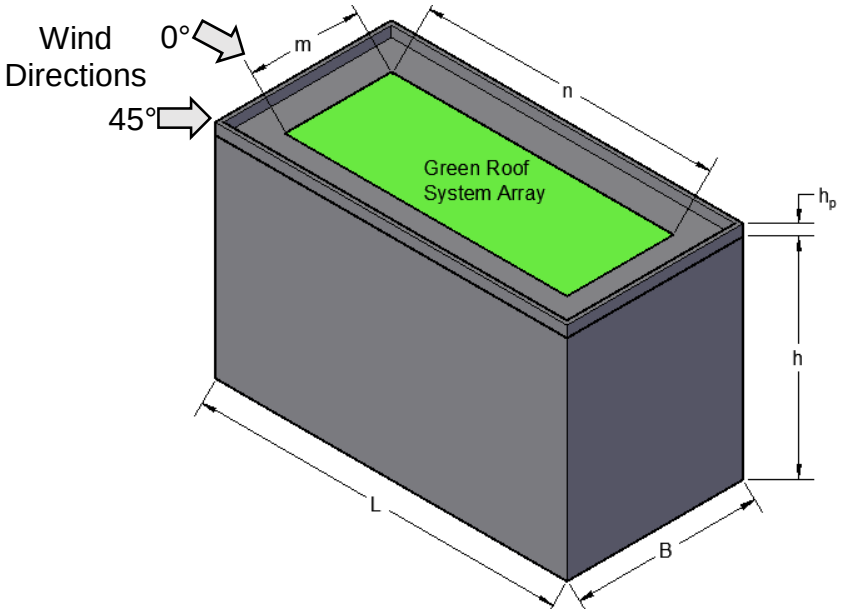

Figure 5-4. Typical building and green roof dimensions with considered wind directions. Figure courtesy of author.

Flow charts describing the Building Parameter selection procedure and Design Failure Wind Speed worksheet are shown in Figures 5-6A and 5-6B, respectively.

Several assumptions were made to adjust the ASCE 7 methodology (ASCE, 2010) for use in the design worksheets:

- Internal pressure coefficients (GC_{pi}) are taken as zero. The roof deck is assumed to be impermeable and therefore offers no contribution to the total uplift load of the roof system. Until better documentation of pressure equalization effects, underside pressures on green roof arrays shall not be considered.

- Wind directionality (K_d) and topographic factors (K_{zt}) shall be taken by default as 0.85 and 1.0, respectively. Users interested in a detailed calculation of K_{zt} can refer to ASCE 7-10's Section 26.8.

- Overhang external pressures are currently not considered.

- While users can utilize wind speed maps in ASCE 7-10 Chapter 26, the author recommends obtaining design wind speeds via the Applied Technology Council (ATC) Wind Speed by Location online tool (Applied Technology Council, 2013). This tool accurately interpolates site-specific wind speeds to the nearest 0.5 m/s (1 mph), based on the building's GPS location.

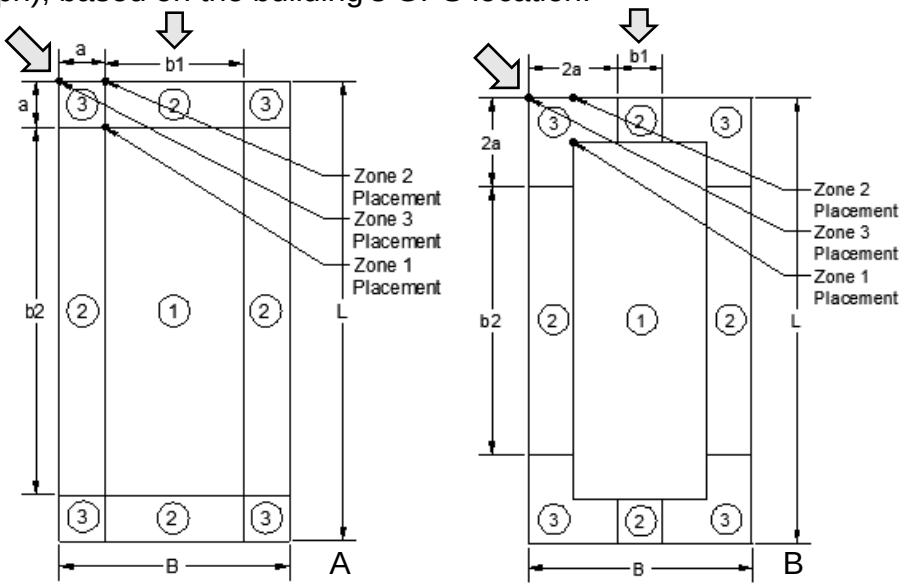

Figure 5-5. Diagrams describing the defined pressure zones and array placement locations. Shown for A) low-rise (h ≤ 18.3 m) buildings and B) medium to high rise (h > 18.3 m) buildings. Figures courtesy of author.

Users of the design worksheets should consider the calculated loads with discretion, as the design loads and failure wind speeds are not necessarily the most conservative values obtainable. The worksheets automatically incorporate ASCE 7-allowed reductions to uplift pressures when appropriate:

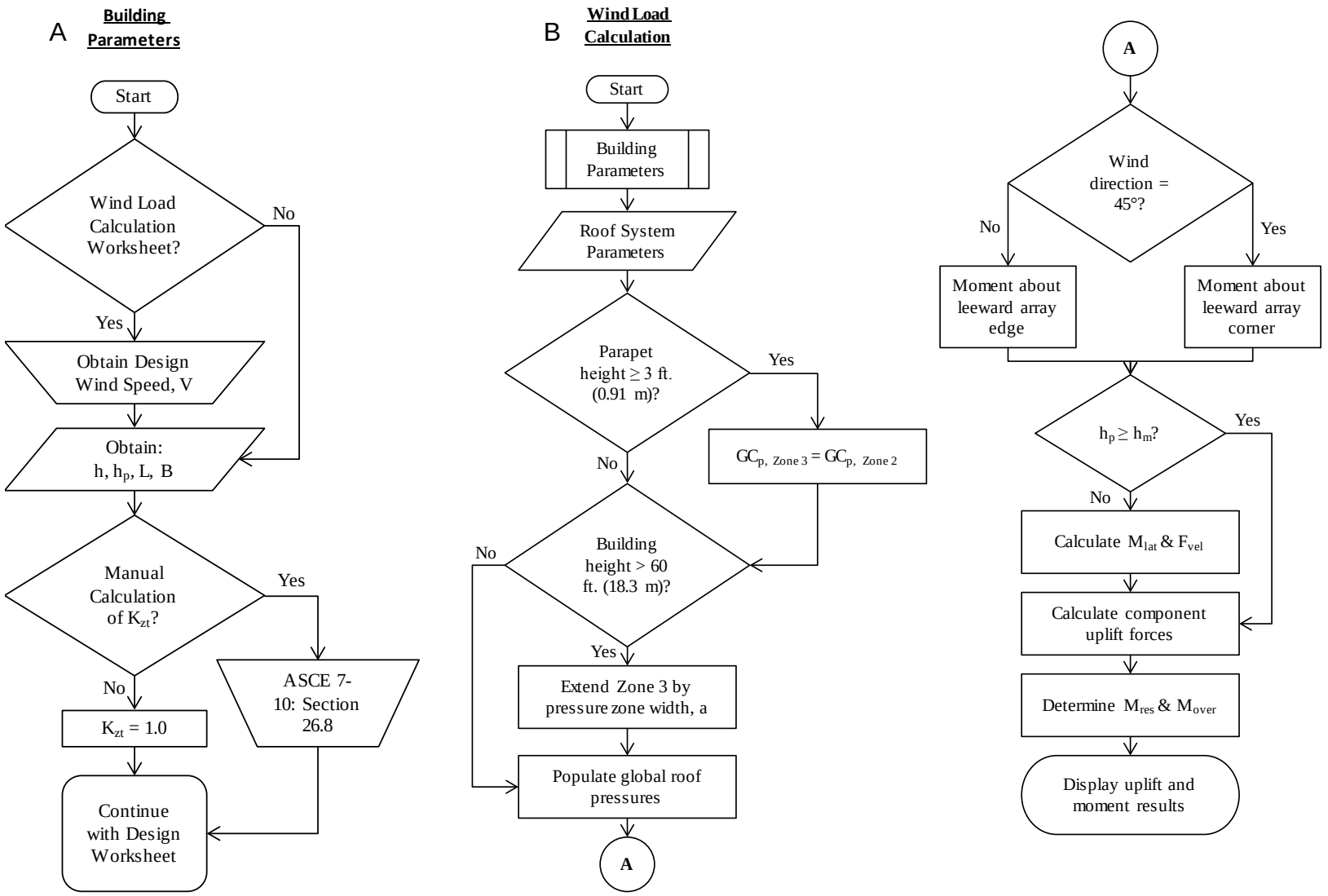

Figure 5-6. Design worksheet flow charts. A) Describing the building parameter selection and B) the Wind Load Calculation worksheet

- Larger effective wind areas (i.e. larger array sizes) lead to larger reduction factors to pressure coefficients (Figure 5-7).

- Zone 3 pressures can be taken as Zone 2 pressures when parapet heights are at least 0.91 m (3 ft.) in height. As previously described, parapet heights are measured from the growth media surface to the top surface of the parapet.

Modular tray green roof system

The following requirements must be met in the construction of the user-defined green roof system to ensure that the roof system exhibits the moment behavior described in Eqn. 5-11 through Eqn. 5-13:

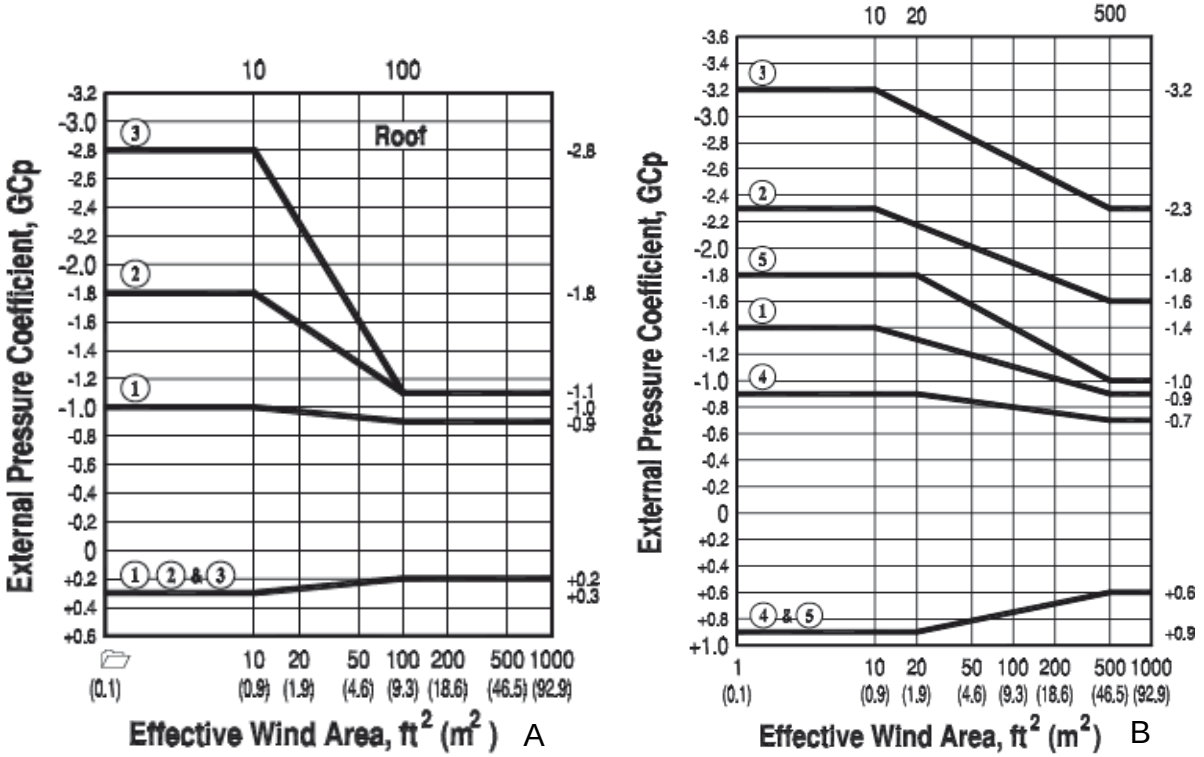

Figure 5-7. Diagrams for external pressure coefficients utilizing ASCE 7's C&C method for a given effective wind area. A) For low-rise (h ≤ 18.3 m) buildings and B) medium to high rise (h > 18.3 m) buildings. Figures courtesy of ASCE, 2010.

- Based on the green roof module blow-off failures described in Chapter 3 and Aly et al.'s (2012) recommendations for grouping concrete pavers, when considering modular tray green roof systems which are larger than a single module, rigid connections must be provided between each module.

- Array dimensions are limited to square shapes.

- The windward corner location of the array, specified as either a Zone 1, Zone 2, or Zone 3 placement, must be selected by the user, as detailed in Figure 5-5. The windward corner locations are relative to the pressure zone width (*a*).

- Users must specify either a 0 degrees or 45 degrees wind direction. Therefore, horizontal moment arms used in Eqn. 5-12 and Eqn. 5-13 are taken parallel to the wind direction, and act from the Uplift Force (Eqn. 5-9) point of application (i.e. centroid of the tributary area) to a pivot line that either passes through the leeward edge of the module array for a 0 degree wind direction or passes through the leeward corner, transverse to the 45 degree wind direction.

Purpose of Design Worksheets

Primary Design Wind Load worksheet

The primary Design Wind Load worksheet was created to allow users efficiently determine and compare design wind loads (i.e. uplift, sliding, and overturning) with system capacities, for varying-sized buildings and roof systems. This design worksheet provides green roof designers and manufacturers a direct path to determining whether the specified green roof system would meet or exceed the design loads specified by ASCE 7-10.

Supplementary Design Failure Wind Speed worksheet

The supplementary Design Failure Wind Speed worksheet utilized the same code from the primary worksheet, but varied the design wind speeds to obtain an overturning moment curve. When plotted against the restoring moment curve for the user-inputted roof system, a design failure wind speed could be back-calculated. This failure wind speed represents the upper limit for the design 3-second gust wind speed measured at 10 m (33 ft.) in Exposure C conditions – the same wind speed extracted from ASCE 7-10 wind maps.

This provides green roof designers and manufacturers a powerful method of selecting ASCE 7-appropriate green roof systems by inputting building and green roof information, backing out a failure wind speed, and directly comparing it with the

building's design wind speed. If the back-calculated failure wind speed exceeded the building's design speed, the green roof system must be redesigned.

Results and Discussion

Both the primary and supplementary design worksheets described previously have been manually evaluated to ensure that the results reflect ASCE 7-10 values for both low-rise and medium- to high-rise building conditions. This portion of the paper will summarize the observations from two module roof blow-off failures, and utilize the worksheets to evaluate the expected design loads and compare the expected failure wind speed against the actual speed.

Comparison of Observed Blow-Off Failures and Worksheet Predictions

As previously mentioned in Chapter 3, two cases of blow-off failures were observed when testing extensive green roof modules atop a test roof at the University of Florida. Extensive green roof modules in these two test trials weighed approximately 47.9 – 57.5 N/m^2 (10 – 12 psf). The approximated measured wind speed at roof height was 45 m/s (100 mph). As such, for the comparison in this section, the input 3-second gust wind speed will also be taken as 45 m/s, and the pressure exposure coefficient, K_z, was taken as 1.0.

The input parameters for the design worksheets are shown in Table 5-2. The predicted design loads for the estimated input wind speed of 45 m/s is shown in Table 5-3. The overturning vs. restoring moment plots produced from the Design Failure Wind Speed worksheet are shown in Figures 5-8 and 5-9 for 1x1 and 3x3 green roof module arrays, respectively. Design failure output values from both design worksheets are shown in Table 5-4.

Table 5-4 suggests that depending on the array placement and size relative to the roof area, failure of the green roof system could still occur due to the overturning moment, even if uplift pressures are still smaller than the system weight. It also shows that with perfectly rigid arrays, failure wind speeds could be increased by increasing array sizes.

Table 5-2. Input parameters for primary and supplementary design worksheets for verification with wind test blow-off failures.

Building Parameters		Array size	1x1	3x3
Height, h (m)	2.4	Array depth, h_m (mm)	100	100
Length, L (m)	2.4	Array length, n (mm)	600	1830
Width, B (m)	2.4	Array width, m (mm)	600	1830
Parapet height, h_p (mm)	0			
Wind speed at h (m/s)	45[a]			
Array dead load (N/m^2)	57.5			
Array placement	Zone 3			
Wind direction (deg)	45			

[a] Only used for Design Wind Load worksheet; results shown in Table 5-3

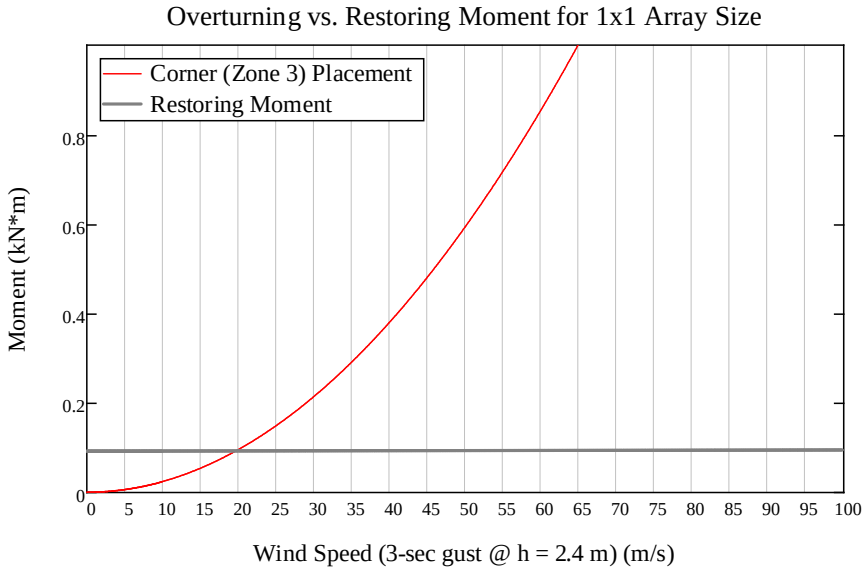

Figure 5-8. Overturning vs. restoring moment curves for a 1x1 green roof module array.

As can be seen between Tables 5-3 and 5-4, the approximated failure wind speed of 45 m/s was roughly twice the predicted failure wind speeds calculated from the Design Failure Wind Speed worksheet for both 1x1 and 3x3 array sizes. As such, a 45

m/s wind speed led to significantly greater uplift forces and overturning moments than the resisting weights and moments (Table 5-3).

Table 5-3. Output values from the primary design worksheet for 1x1 and 3x3 arrays utilizing the estimated failure wind speed of 45 m/s.

	Total uplift kN	Total weight kN	Overturning moment kN-m	Restoring moment kN-m
1x1 Array	0.921	0.214	0.401	0.092
3x3 Array	5.462	1.922	7.366	2.485

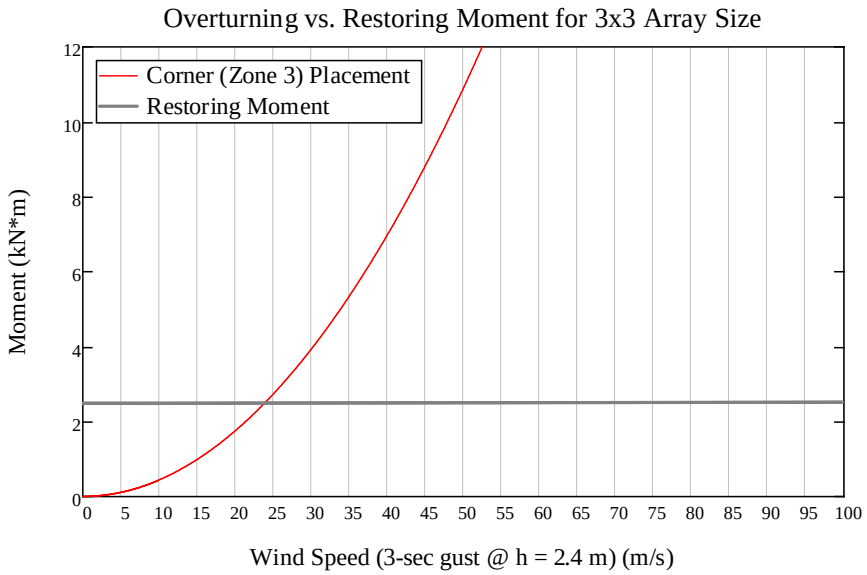

Figure 5-9. Overturning vs. restoring moment curves for a 3x3 green roof module array.

Table 5-4. Output values from the primary and supplementary design worksheets for 1x1 and 3x3 arrays utilizing failure wind speed input parameters.

	Failure wind speed[a] (m/s)	Result Uplift[b] (N)	Total Weight[b] (N)	Resulting Overturning Moment[b] (N-m)	Restoring Moment[b] (N-m)
1x1 Array	19.7	211	214	92	92
3x3 Array	23.9	1840	1920	2480	2480

[a] Back-calculated from the Design Failure Wind Speed worksheet
[b] Calculated from the failure wind speed shown in the 2nd column

The upshot of the large discrepancy between the observed and predicted failure wind speed is that the supplementary design worksheet predicted more conservative failure wind speeds. Therefore, the developed worksheets should provide reasonable

design values derived from ASCE 7-10 load provisions, given that the assumed module behavior is correct.

Example Green Roof Design Envelope Procedure via Worksheet Calculations

To demonstrate the worksheets' effectiveness in efficiently developing a design envelope for suitable green roof configurations, this section will highlight how to select a suitable green roof array size and placement configuration by comparing failure wind speeds with ASCE 7-10 design wind speeds.

Example Problem Statement:

For a typical "Big Box Retail" building measuring 7.62 m high (25 ft.), 137.2 m long (450 ft.), and 76.2 m wide (250 ft.) with no parapet, located in Chicago, IL, determine the appropriate sized array and placement configuration for both extensive and intensive depths utilizing ASCE 7-10 design provisions. Assume an Exposure B category, 45 degree wind direction, and that the individual module plan dimensions are 600 mm long by 600 mm wide (24 in. by 24 in.). Extensive and intensive modules will be assumed to weigh 718 N/m^2 (15 psf) and 1.436 kN/m^2 (30 psf), respectively. Module depths for extensive and intensive systems will measure 100 mm (4 in.) and 200 mm (8 in.) in depth, respectively. The maximum-sized rigidly linked array will be limited to 10 modules by 10 modules. Building input parameters for the "Big Box Retail" building are shown in Table 5-5.

Procedure:

1. Obtain design wind speed, V, for a Risk Category II building located in Chicago, IL from either ASCE 7-10 wind speed maps or ATC's Wind Speed by Location tool.
2. Input building geometry to Failure Wind Speed worksheet, summarized in Table 4.
3. Input desired array sizes, depths, and weights.

4. The Design Failure Wind Speed worksheet outputs speeds for each exposure category and placement location for the specified array configuration. Extract values into Table 5-6.

5. Repeat steps 3 – 4 until sufficient failure wind speeds are obtained. These values represent design 3-second wind gusts measured at 10 m high in Exposure C conditions.

6. Compare the list of wind speeds obtained in Step 5 to the design wind speed obtained in Step 1. Wind speeds smaller than the design wind speed from Step 1 are rejected.

Table 5-5. Big Box Retail building design worksheet input parameters.

Height (m)	Length (m)	Width (m)	Parapet height (m)	Pressure zone width (m)	Design wind speed (m/s)
7.62	137.2	76.2	0	3.05	51.4[a]

[a] Obtained via the ATC online tool (2013)

Table 5-6. Big Box building output of failure wind speed envelope for extensive and intensive modules in Exposure B conditions.

	Extensive, 100 mm deep, 718 N/m^2			Intensive, 200 mm deep, 1436 N/m^2		
Placement	Zone 3 (m/s)	Zone 2 (m/s)	Zone 1 (m/s)	Zone 3 (m/s)	Zone 2 (m/s)	Zone 1 (m/s)
1x1	26.4	32.8	43.8	36.8	45.4	59.5[a]
2x2	27.0	33.4	44.4	38.1	47.0	62.1[a]
3x3	29.2	35.1	44.9	41.2	49.4	63.3[a]
4x4	33.2	37.7	45.7	46.9	53.3[a]	64.5[a]
6x6	42.3	42.7	46.7	59.8[a]	60.3[a]	66.0[a]
8x8	42.5	43.3	46.8	60.1[a]	61.2[a]	66.1[a]
10x10	42.8	43.8	46.8	60.5[a]	61.9[a]	66.1[a]

[a] Design failure wind speeds which exceed the building's design wind speed shown in Table 5-5

The bolded wind-speeds shown in Table 5-6 highlights the envelope of acceptable design failure wind speeds for the different array configurations. It can be seen that extensive green roof modules weighing 0.718 kN/m^2 would not be suitable in any array configuration for the example Big Box Retail building.

The selection of a suitable intensive green roof system, on the other hand, is more flexible. In order to place an array consisting of intensive green roof modules in

the Zone 3 region of the roof, a minimum array size of six modules by six modules must be met before the system can withstand the overturning moments caused by the design wind speed of 51.4 m/s for Chicago, IL. Intensive modules consist of any array size if placed in a Zone 1 location.

For both extensive and intensive systems, the increase in failure wind speeds due to the increase in array size is limited by the pressure zone width calculated for the building. This is due to the averaging effect of zone pressures on larger array sizes. For example, a small array experiencing only a Zone 3 pressure will fail before a larger array which averages Zones 1, 2 and 3 in its uplift and overturning moment calculations. As such, the increase in the design failure wind speeds reduces with increasing array sizes.

Summary

Two design worksheets were developed for calculating Design Wind Loads and Design Failure Wind Speeds, derived from ASCE 7-10's Component and Cladding load provisions. The developed worksheets allowed for efficient determination of ASCE 7 wind loads but also an alternative method of designing green roofs for a given site's design wind speed. The findings from this study can be summarized as follows:

- A failure wind speed envelope procedure was introduced as a new, efficient method of designing green roof systems according to ASCE 7 provisions.
- Green roof arrays must be rigidly attached for failure mechanisms to apply.
- Overturning failures control the three failure mechanisms identified.
- The developed worksheets produce conservative results when compared to the blow-off failures described in Chapter 3's wind testing. However, since pressure equalization effects were not considered, the design wind loads may be overly conservative.

- There are diminishing returns for increasing the array size to increase design failure wind speed.

The last bullet of the summary highlights the limitations of this design approach to mitigating potentially damaging wind uplift forces. Fortunately, edge restraint and racking systems have been explored by both Irwin et al. (2012) and Fischer (2013) show promise as effective methods of securing ballast roof systems from blow-off.

CHAPTER 6
KEY FINDINGS AND RECOMMENDATIONS

This document described extensive research on the wind resistance of green roof systems conducted at the University of Florida. It presented an in-depth literature review that described the current state of knowledge and perception of green roofs in high winds. It also detailed the full-scale wind testing of built-in-place and modular tray green roofs, and the uproot testing conducted on field-planted vegetation. It concluded with an alternative and preliminary wind design approach for green roofs utilizing ASCE 7 wind provisions. To summarize the document, the following key findings and recommendations are made:

There still exists a knowledge gap between the actual green roof wind behavior and how current design guidelines address it. While existing guidelines and standards provide a good start towards the wind design for green roof systems, the lack of direct research has left an industry that has green roofs concentrated to non-hurricane-prone regions, while still susceptible to wind-induced damage (Fischer, 2013). Since guidelines and standards exist to disseminate research findings for effective practice in industry, future wind investigations are required and encouraged by the author to promote more wind-resistant green roof systems.

It is proposed by the author that green roofs subject to high winds will experience progressive failure, thus requiring better understanding of their wind resistance on a per-component level. Existing ground-level plant wind studies have proven that vegetation disrupts and absorbs potentially damaging wind flow. Further, established knowledge of roof gravel wind behavior states that its roof blow-off wind speed is proportional to its size. However, when this same knowledge is applied to green roofs

(e.g. ANSI/SPRI RP-14), the added benefit of the vegetation's root-anchorage is not addressed, treating green roof growth media as loosely-laid particulate – a condition that is unacceptable for an established green roof system.

From the full scale wind testing conducted it was determined that wind-induced rooftop pressures and airflow can be very damaging to green roofs. While uplift pressures alone may not disturb growth media or vegetation to high degrees, the presence of highly turbulent conical vortices can significantly damage green roofs in edge and corner regions, confirming current design guideline restrictions. Further, the usage of parapets was found to not only protect windward edge vegetation from wind-induced stresses, but also play a vital role in containing growth media on the roof, agreeing with Karimpour's and Kaye's (2013) study. More importantly though, it confirmed that the presence of vegetation *alone* plays a vital role in preventing catastrophic growth media scour, as shown in Phase 1 testing. In other words, simply having an established root system may provide sufficient scour and erosion resistance.

That said, can focus be shifted towards selecting a plant that can resist turbulent wind conditions not often seen at ground level? Proper wind design of green roofs should initiate with the proper selection and installation of its vegetation, thus making a holistic approach like the FLL (2008) appropriate. In that sense, perhaps the first step to forming a region's wind resistant plant selection for green roofs is through extensive uproot testing. It has been shown that the uproot (pullout) capacity of a plant is directly related to its root anchorage to the soil (Bailey et al., 2002; Hamza et al., 2007). The uproot testing determined that a combined effect of greater establishment and planting density could increase the plant's peak uproot capacity. The *Lantana montevidensis*

species yielded the most reliable and highest median uproot performance (resisting over 100 N of uproot force). It is therefore recommended that plant mixes should consist of low-lying vegetation with extensive spread to protect loose aggregate, and taller, resilient plant species with strong root systems. If the findings from the study hold true, the proposed mixed planting configurations would provide some factor of safety to wind-induced uprooting in comparison to laboratory testing. Further refined tests are required to assess the moisture content and wind-induced damage effects on uproot capacities.

But until the necessary research has been conducted, the question of whether or not current green roof design guidelines adequately address the wind issue still exists. Catastrophic blow-off failures of extensive green roof modules were documented in the full-scale wind tests, and exposed the controlling failure mechanism to be overturning of the system, rather than pure uplift. Since the FLL and FM 1-35 already require usage of external wind load provisions, the two ASCE 7-based design worksheets developed offered efficient methods of selecting modular tray green roof systems with rigid interconnections that not only meet the ASCE 7 design requirements for wind, but also incorporate the identified failure modes. Further, the Design Failure Wind Speed worksheet allows for a quick and refined envelope design procedure specific for the green roof size and building site. In comparison to the full-scale failures described in Chapter 3, the design worksheets produce conservative values. However, until further green roof testing is conducted, by not incorporating the pressure equalization effects that have been documented in previous literature, the design loads may be overly conservative. Either way, edge restraint and racking techniques studied by Irwin et al. (2012) and Fischer (2013) offer additional methods of blow-off failure mitigation.

The findings presented in this report offer a single record of how green roofs potentially perform in more realistic conditions (i.e. perpendicular wind direction with parapet and extreme cornering wind with no parapet), and can hopefully provide a reference point for future full-scale testing studies on green roofs. While the project's findings and procedures presented do not necessarily provide definite answers to the current wind issue, they certainly provide necessary considerations for future wind testing. With the recent developments in testing facilities, such as FIU's new 12-fan Wall of Wind and the Institute for Business and Home Safety's (IBHS) 105-fan facility, further testing utilizing larger green roofs is recommended to investigate how flow reattachment and rack systems (as described by Fischer, 2013) affect green roofs subject to high wind. Further, with a HAPLA system being developed at UF, chamber pressure testing is proposed to investigate whether modular tray green roof systems are capable of withstanding 9.58 kPa (200 psf) uplift pressures. Replication of the study will require the formation of a pressure differential to form between the upper and underside surfaces of the green roof module, in less than 0.1 seconds, as suggested by Irwin et al. (2012). Once full understanding of how green roofs behave under high winds is achieved via additional controlled test methods, dissemination of the future research findings can proceed, eventually leading to tools and guidelines which designers, manufacturers and code officials can use for hurricane-prone regions.

APPENDIX A
PLANT SELECTION GUIDANCE FROM FLL

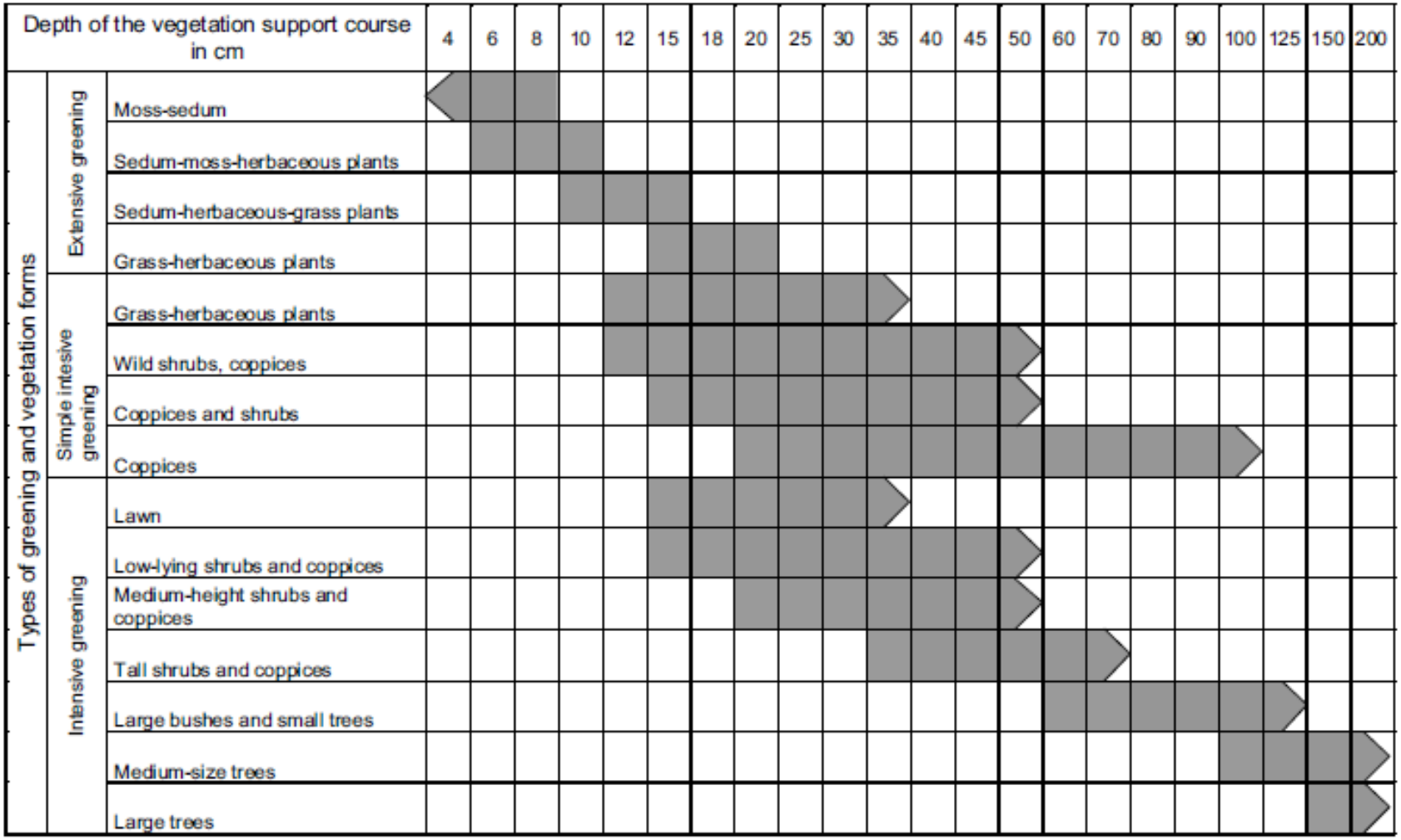

Figure A-1. Vegetation requirements for given substrate depths. Figure courtesy of FLL, 2008.

APPENDIX B

PROCEDURE FOR CALCULATING COVERAGE RATIOS IN ADOBE PHOTOSHOP

1. Select the Polygonal Lasso tool (in tool palette to left of workspace).	
2. Make selection of area of interest.	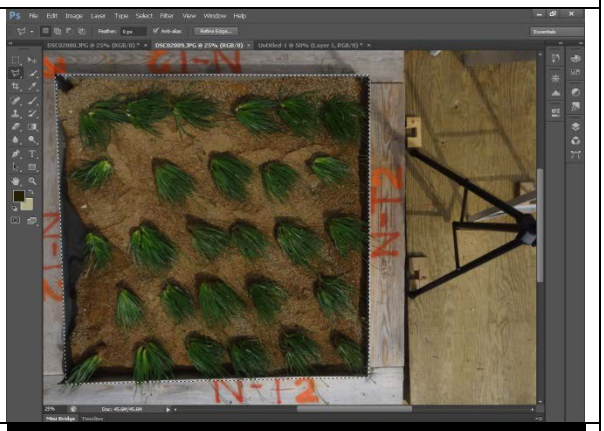
3. Choose Select > Color Range. Then: i. Click the Selection radio button ii. Selection Preview to Black Matte (the entire photo will turn black) iii. Click Add to Sample Button	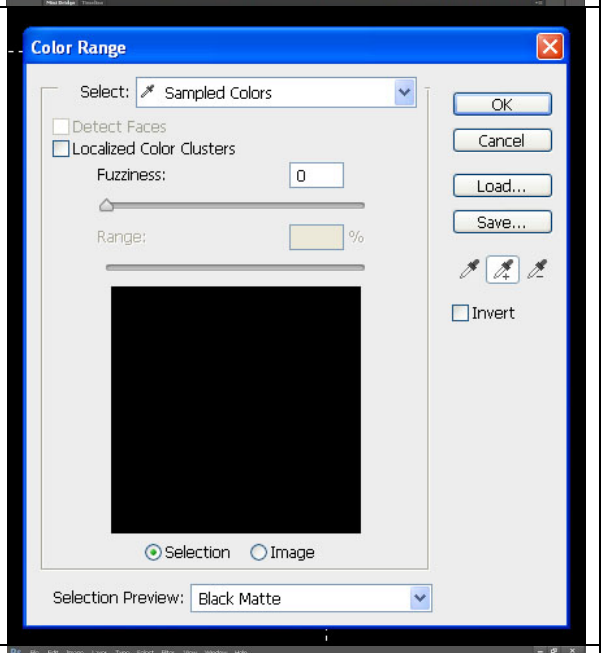
4. Click the plant(s) by making selections (as you make these selections the plant should become more visible	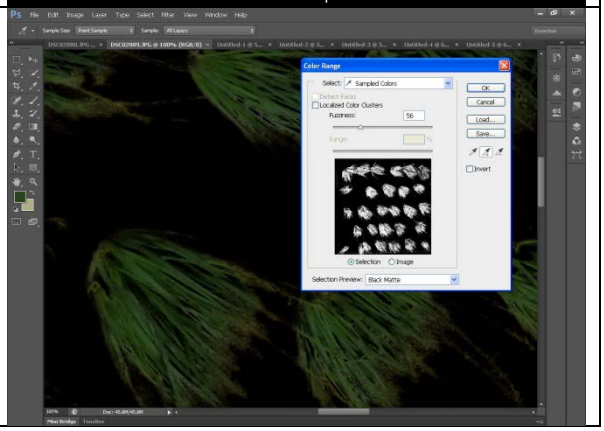

Figure B-1. Annotated procedures to calculate green roof coverage ratios in Adobe Photoshop. Photos courtesy of author.

5. To add additional tones to the selection: i. Continue to click the shaded regions of the plant ii. Move the Fuzziness slider to the right to increase selection o Do this slowly and stop to add different tones of the plant	
6. To make sure desired regions are fully selected, do the following, and click OK. i. Increase Fuzziness till unwanted regions of the image are visible (such as soil artifacts) ii. Then, move slider to position where unwanted regions are not visible any longer. Now only the plants are selected	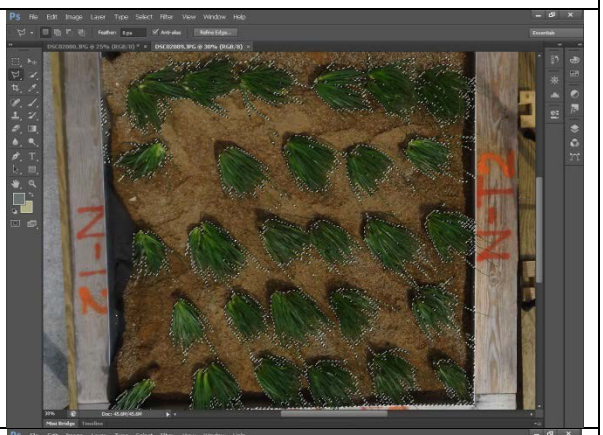
7. Use this method to find the pixels that represent the plants. • Review image closely to make sure only plants are selected. If part of the plants are not selected use the Quick Selection Tool or the Magic Wand Tool (hold down shift). When using Magic Wand you may change the tolerance to make your selection more precise.	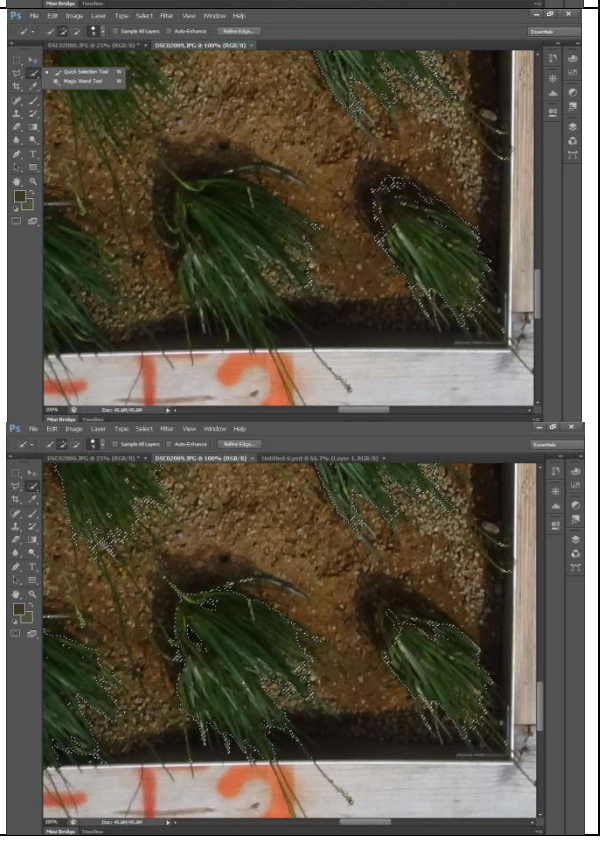

Figure B-1. Continued

8. Find number of pixels in selected region using the Histogram: • If Histogram window is not open in the Edit workspace or the Panel Bin, choose Window > Histogram. o At top right corner of window select the Panel menu and click Expanded View and then click Show Statistics • If the Cache Data Warning icon is displayed at the top right hand corner of the graph (appears as a triangle centered around an exclamation mark), hit the Uncached Refresh button (appears as a circle composed of two arrows) o The number of pixels will be displayed at the bottom left hand corner of the window	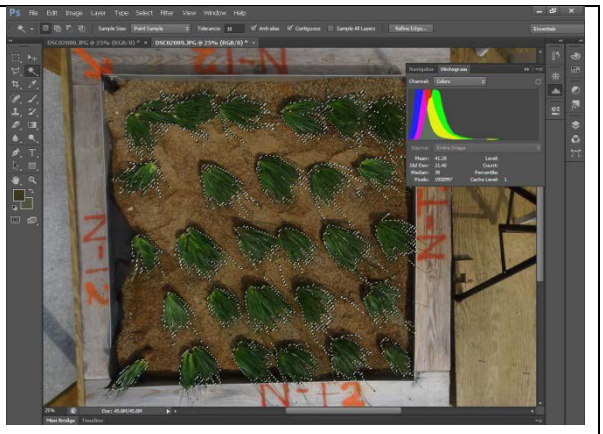
9. Record the number of pixels found for the plant selections.	
10. This step will determine how many total pixels are in the total green roof area. • Select total area (including soil and plants) using the Polygonal Lasso tool, and find number of pixels for this region using Step 7. Record this value.	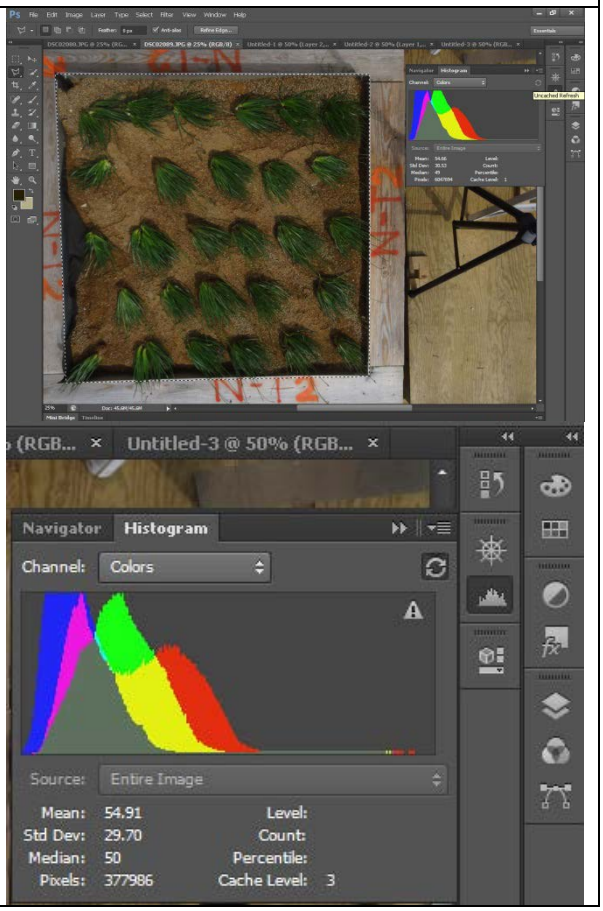

Figure B-1. Continued

11. Determine Coverage Ratio: • Divide the number of pixels of the plants by the number of pixels of the total area. Record values. Repeat for each image.	
Deviations from Specified Procedure (above):	
For the images which fell into the category of plant coverage being greater than 80%, the ratio between pixels of soil to pixels of the total area was calculated, and subtracted from 1. 1. Follow Step 1 through Step 8 specified above. 2. Right click the selection, and choose Select Inverse. 3. Record the number of pixels. This strategy was used for the images: • N-S1 before, N-S1 after • N-S2 before, N-S2 after • S-S1 before, S-S1 middle • S-S2 before, S-S2 after • S-T1 before, S-T1 middle • T5 before • T11 before, T11 after	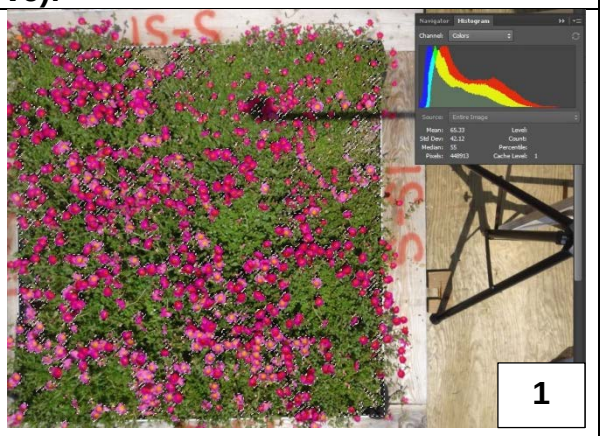 

Figure B-1. Continued

Table B-1. Raw results for Photoshop-calculated coverage ratios.

System	Test ID	Time of Photo[1]	Image ID	Object Selection Pixels	Total Area Pixels	Average Coverage Ratio
BIP	N-S1	B	DSC01941	183689	5853723	96.86%
BIP	N-S1	A	DSC01989	667092	6124859	89.11%
BIP	N-T1	B	DSC01896	4565438	6144118	74.31%
BIP	N-T1	A	DSC01988	2524132	5787662	43.61%
BIP	S-M1	B	CIMG0941	1898902	3490038	54.41%
BIP	S-M1	A	DSC01854	2709834	5357062	50.58%
BIP	N-S2	B	DSC02081	228196	5933363	96.15%
BIP	N-S2	A	DSC02094	1168360	6177572	81.09%
BIP	N-T2	B	DSC02080	2991604	5875015	50.92%
BIP	N-T2	A	DSC02089	1958997	6047694	32.39%
BIP	S-S1	B	DSC02108	118457	5842262	97.97%
BIP	S-S1	A	DSC02114	4568063	5790994	78.88%
BIP	S-S2	B	DSC02098	476105	5780360	91.76%
BIP	S-S2	A	DSC02113	4418014	5657573	78.09%
BIP	S-T1	B	DSC02205	284554	4744354	94.00%
BIP	S-T1	M	DSC02235	3466169	5060846	68.49%
BIP	S-T1	A	DSC02240	3405366	6044578	56.34%
BIP	S-T2	B	DSC02195	2270660	4789102	47.41%
BIP	S-T2	M	DSC02219	1991492	5654564	35.22%
BIP	S-T2	A	DSC02232	1690402	4884804	34.61%
Module	T2	B	DSC02171	3385029	5247845	64.50%
Module	T2	A	DSC02175	3721769	6077588	61.24%
Module	T3	B	DSC02186	3767290	6313795	59.67%
Module	T3	A	N/A	N/A	N/A	N/A
Module	T5	B	DSC02259	823092	6628408	87.58%
Module	T5	A	DSC02286	4826555	6859868	70.36%
Module	T6	B	DSC02248	5090430	7057356	72.13%
Module	T6	A	DSC02256	4805614	7120136	67.49%
Module	T7	B	DSC02299	4257074	7195080	59.17%
Module	T7	M	DSC02310	4142145	8372103	49.48%
Module	T7	A	DSC02314	4494604	8538654	52.64%
Module	T8	B	DSC02247	4908483	7540467	65.10%
Module	T8	A	N/A	N/A	N/A	N/A
Module	T10	B	DSC02317	972073	1262209	77.01%
Module	T10	M	DSC02352	1170808	1671926	70.03%
Module	T10	A	DSC02411	1065286	1698380	62.72%
Module	T11	B	DSC02427	225729	1735635	86.99%
Module	T11	A	DSC02463	319782	1679003	80.95%

[1] B = before, A = after, M = middle of wind testing

APPENDIX C
LABORATORY-MEASURED MOISTURE CONTENTS FOR PHASE 2 WIND AND UPROOT TESTING

Soils oven dried at 105 C for 24hrs
% moisture calculated on a mass/mass basis
Overall weight of soil sample provided in Column 2
Soil subsample wet weight in Column 4
Soil subsample dry weight in Column 5
Soil % moisture content in Column 8

Table C-1. Laboratory-calculated moisture contents for test batch 1.

Sample ID	Bulk Bag + Sample, g	Weigh Boat, g	Wet Soil + weigh boat, g	Dry Soil + Weigh boat, g	Wet Soil, g	Dry Soil, g	% moisture m/m
S-T1-1	221.0	1.01	17.67	14.23	16.66	13.22	20.6%
S-T1-3	141.2	1.01	15.97	12.53	14.96	11.52	23.0%
S-T1-5	242.0	1.01	23.79	17.83	22.78	16.82	26.2%
S-T1-7	195.4	0.96	18.92	14.79	17.96	13.83	23.0%
S-T1-9	232.0	1.01	23.62	17.60	22.61	16.59	26.6%
S-T2-1	212.6	1.02	25.41	20.07	24.39	19.05	21.9%
S-T2-3	243.1	1.01	21.06	16.14	20.05	15.13	24.5%
S-T2-5	231.3	1.02	22.58	17.04	21.56	16.02	25.7%
S-T2-7	272.4	1.01	22.79	16.89	21.78	15.88	27.1%
S-T2-9	190.7	1.00	19.77	14.19	18.77	13.19	29.7%
S-S1-1	201.8	1.00	20.37	15.62	19.37	14.62	24.5%
S-S1-3	275.7	1.02	27.28	18.93	26.26	17.91	31.8%
S-S1-5	218.5	0.98	21.58	14.99	20.60	14.01	32.0%
S-S1-7	250.9	1.00	24.61	17.86	23.61	16.86	28.6%
S-S1-9	286.6	1.02	21.70	15.19	20.68	14.17	31.5%
S-S2-1	220.4	1.00	19.88	14.91	18.88	13.91	26.3%
S-S2-3	267.3	1.00	20.87	15.11	19.87	14.11	29.0%
S-S2-5	286.9	1.03	25.38	18.01	24.35	16.98	30.3%
S-S2-7	234.1	1.00	22.00	16.11	21.00	15.11	28.0%
S-S2-9	251.8	0.98	23.52	16.54	22.54	15.56	31.0%
S-M1-1	227.7	1.01	19.10	14.40	18.09	13.39	26.0%
S-M1-3	218.5	0.96	26.09	18.47	25.13	17.51	30.3%
S-M1-5	199.2	0.99	24.69	17.45	23.70	16.46	30.5%
S-M1-7	168.5	1.02	24.32	18.27	23.30	17.25	26.0%
S-M1-9	106.8	1.07	19.94	14.60	18.87	13.53	28.3%
T2-1	163.4	1.05	22.93	18.39	21.88	17.34	20.7%
T2-2	128.2	1.03	17.13	14.37	16.10	13.34	17.1%

Table C-1. Continued

Sample ID	Bulk Bag + Sample, g	Weigh Boat, g	Wet Soil + weigh boat, g	Dry Soil + Weigh boat, g	Wet Soil, g	Dry Soil, g	% moisture m/m
T2-3	124.5	1.01	20.25	16.05	19.24	15.04	21.8%
T2-4	134.6	0.97	18.69	14.61	17.72	13.64	23.0%
T2-5	124.2	1.00	20.76	15.92	19.76	14.92	24.5%
T2-6	137.8	1.02	22.70	17.60	21.68	16.58	23.5%
T2-7	163.1	1.01	20.62	16.34	19.61	15.33	21.8%
T2-8	153.8	1.05	19.54	15.70	18.49	14.65	20.8%
T2-9	116.4	1.00	18.74	15.46	17.74	14.46	18.5%
T5-1	119.9	1.01	22.69	20.31	21.68	19.30	11.0%
T5-2	167.4	1.02	23.61	18.87	22.59	17.85	21.0%
T5-3	196.8	0.99	20.88	16.60	19.89	15.61	21.5%
T5-4	144.6	0.99	24.73	20.92	23.74	19.93	16.0%
T5-5	206.7	1.00	22.82	17.04	21.82	16.04	26.5%
T5-6	185.5	0.98	22.28	17.10	21.30	16.12	24.3%
T5-7	114.6	0.98	17.74	15.93	16.76	14.95	10.8%
T5-8	142.2	1.01	24.62	21.01	23.61	20.00	15.3%
T5-9	231.1	0.98	24.00	19.31	23.02	18.33	20.4%
T6-1	134.8	1.01	17.50	14.68	16.49	13.67	17.1%
T6-2	211.8	0.99	21.77	16.45	20.78	15.46	25.6%
T6-3	174.5	0.99	21.48	17.24	20.49	16.25	20.7%
T6-4	126.2	1.01	21.55	17.42	20.54	16.41	20.1%
T6-5	176.0	1.01	19.63	15.13	18.62	14.12	24.2%
T6-6	261.4	1.00	22.48	17.70	21.48	16.70	22.3%
T6-7	124.2	1.00	22.44	16.86	21.44	15.86	26.0%
T6-8	194.2	0.99	22.16	17.25	21.17	16.26	23.2%
T6-9	220.6	1.01	22.63	17.98	21.62	16.97	21.5%
T7-1	118.1	0.99	18.85	14.64	17.86	13.65	23.6%
T7-2	87.6	0.99	21.06	16.41	20.07	15.42	23.2%
T7-3	177.6	1.02	20.60	15.18	19.58	14.16	27.7%
T7-4	208.3	1.01	22.89	17.24	21.88	16.23	25.8%
T7-5	196.0	1.01	23.03	16.43	22.02	15.42	30.0%
T7-6	211.3	1.02	22.45	16.16	21.43	15.14	29.4%
T7-7	164.3	1.03	28.74	20.13	27.71	19.10	31.1%
T7-8	119.5	1.02	21.55	16.19	20.53	15.17	26.1%
T7-9	187.8	1.00	24.91	19.58	23.91	18.58	22.3%
D-4"-5/T2-2	123.9	1.00	20.06	17.60	19.06	16.60	12.9%
D-4"-2/T2-3	124.4	0.95	20.17	17.08	19.22	16.13	16.1%
D-4"-3/T2-5	107.3	1.03	19.17	16.33	18.14	15.30	15.7%

Table C-1. Continued

Sample ID	Bulk Bag + Sample, g	Weigh Boat, g	Wet Soil + weigh boat, g	Dry Soil + Weigh boat, g	Wet Soil, g	Dry Soil, g	% moisture m/m
D-4-5/T2-8	127.0	1.00	19.70	15.36	18.70	14.36	23.2%
D-4-1/APE LAN T2-9	164.7	1.01	20.58	17.49	19.57	16.48	15.8%
W-4-1/T1-1 Wet	180.9	0.98	26.96	17.52	25.98	16.54	36.3%
N-T1-1	225.2	1.03	21.34	16.50	20.31	15.47	23.8%
N-T1-3	192.8	1.00	25.24	19.31	24.24	18.31	24.5%
N-T1-5	174.8	0.98	22.89	16.63	21.91	15.65	28.6%
N-T1-7	215.9	1.01	20.44	15.64	19.43	14.63	24.7%
N-T1-9	164.3	0.97	19.47	14.70	18.50	13.73	25.8%
N-T2-1	325.0	0.97	20.35	16.18	19.38	15.21	21.5%
N-T2-3	256.2	0.99	23.64	17.29	22.65	16.30	28.0%
N-T2-5	247.5	0.96	23.82	17.94	22.86	16.98	25.7%
N-T2-7	185.6	1.02	23.99	18.05	22.97	17.03	25.9%
N-T2-9	232.6	1.00	24.65	18.32	23.65	17.32	26.8%
N-S1-1	199.1	0.99	25.37	20.21	24.38	19.22	21.2%
N-S1-3	175.5	1.00	21.46	16.54	20.46	15.54	24.0%
N-S1-5	213.3	1.01	24.09	17.69	23.08	16.68	27.7%
N-S1-7	142.2	1.00	22.71	18.37	21.71	17.37	20.0%
N-S1-9	264.5	1.01	19.40	14.69	18.39	13.68	25.6%
N-S2-1	133.5	1.00	25.77	22.05	24.77	21.05	15.0%
N-S2-3	238.2	0.98	23.82	18.16	22.84	17.18	24.8%
N-S2-5	266.4	0.97	18.07	13.94	17.10	12.97	24.2%
N-S2-7	201.6	1.01	20.25	16.46	19.24	15.45	19.7%
N-S2-9	255.2	0.98	20.09	15.86	19.11	14.88	22.1%

Table C-2. Laboratory-calculated moisture contents for test batch 2.

Sample ID	Bulk Bag + Sample, g	Weigh Boat, g	Wet Soil + weigh boat, g	Dry Soil + Weigh boat, g	Wet Soil, g	Dry Soil, g	% moisture m/m
D-4"-1-T9-8	186.7	0.99	36.57	24.82	35.58	23.83	33.0%
D-4"-2-T9-6	181.8	0.98	28.74	18.39	27.76	17.41	37.3%
D-4"-3-T9-5	157.5	0.97	35.15	23.40	34.18	22.43	34.4%
D-4"-04-6 month-T9-1	173.7	1.02	24.32	15.83	23.30	14.81	36.4%
D-4-05-6 month-T9-2	168.2	0.98	25.10	16.54	24.12	15.56	35.5%
D-4-06-6 month-T9-4	170.7	1.01	26.49	18.72	25.48	17.71	30.5%
D-8-01/T4-7	265.2	0.97	26.65	19.75	25.68	18.78	26.9%
D-8-02/T4-5	251.4	0.98	25.62	19.06	24.64	18.08	26.6%
D-8-03/T4-3	253.2	1.00	24.46	18.41	23.46	17.41	25.8%
D-8-5?/T5-4	202.9	1.03	22.31	19.87	21.28	18.84	11.5%
W-4-2/T1-6	162.6	1.00	28.82	20.57	27.82	19.57	29.7%
W-4-3/T1-5	198.8	0.98	30.69	20.59	29.71	19.61	34.0%
W-4-04/T3-7	164.1	1.02	25.72	18.58	24.70	17.56	28.9%
W-4-05/T3-4	194.1	1.02	28.84	18.12	27.82	17.10	38.5%
W-4-07-6 month/T7-9	258.2	0.98	34.88	24.34	33.90	23.36	31.1%
W-4-08-6 month/T7-3	179.5	1.03	25.04	18.32	24.01	17.29	28.0%
W-4-08-6 month/T7-6	298.5	0.98	25.30	17.53	24.32	16.55	31.9%
W-8-6/T4-4	297.5	1.05	31.64	21.85	30.59	20.80	32.0%
W-8-7/T5-6	253.7	1.03	27.85	19.44	26.82	18.41	31.4%
W-8-08/T4-8	309.7	1.02	23.27	16.45	22.25	15.43	30.7%
W-8"-09-6 month/T11-8	254.9	1.00	27.23	18.72	26.23	17.72	32.4%
W-8"-10-6 month/T11-1	221.8	0.99	34.61	23.44	33.62	22.45	33.2%
W-8"-11-6 month/T11-3	310.7	0.98	30.91	21.03	29.93	20.05	33.0%
W-8"-12-6 month/T10-1	351.8	1.00	34.51	25.19	33.51	24.19	27.8%
W-8"-13-6 month/T10-2	370.2	1.02	26.12	17.83	25.10	16.81	33.0%
W-8"-14-6 month/T10-3	327.7	0.99	29.62	20.11	28.63	19.12	33.2%
M2-6/25/2012-5:56 PM	806.6	1.01	34.53	24.00	33.52	22.99	31.4%
T10-1	184.5	0.97	30.63	25.46	29.66	24.49	17.4%
T10-2	220.7	1.03	25.82	22.22	24.79	21.19	14.5%
T10-3	172.3	1.03	24.99	19.13	23.96	18.10	24.5%
T10-4	185.8	1.00	26.70	22.60	25.70	21.60	16.0%
T10-5	231.7	1.00	26.34	20.91	25.34	19.91	21.4%
T10-6	174.6	1.01	22.54	17.80	21.53	16.79	22.0%
T10-7	101.5	0.99	28.45	23.12	27.46	22.13	19.4%
T10-8	212.3	0.99	28.44	23.57	27.45	22.58	17.7%
T10-9	172.5	1.07	26.25	21.38	25.18	20.31	19.3%

Table C-2. Continued

Sample ID	Bulk Bag + Sample, g	Weigh Boat, g	Wet Soil + weigh boat, g	Dry Soil + Weigh boat, g	Wet Soil, g	Dry Soil, g	% moisture m/m
T11-1	165.3	0.98	26.77	19.83	25.79	18.85	26.9%
T11-2	266.3	1.03	28.61	21.24	27.58	20.21	26.7%
T11-3	281.5	1.00	24.73	17.88	23.73	16.88	28.9%
T11-4	242.2	0.98	25.16	18.84	24.18	17.86	26.1%
T11-5	221.1	1.00	22.30	16.12	21.30	15.12	29.0%
T11-6	281.3	0.98	25.76	18.89	24.78	17.91	27.7%
T11-7	179.9	0.98	30.58	26.01	29.60	25.03	15.4%
T11-8	100.6	0.97	28.80	23.84	27.83	22.87	17.8%
T11-9	261.0	0.99	23.22	18.63	22.23	17.64	20.6%

Table C-3. Laboratory-calculated moisture contents for test batch 3.

Sample ID	Bulk Bag + Sample, g	Weigh Boat, g	Wet Soil + weigh boat, g	Dry Soil + Weigh boat, g	Wet Soil, g	Dry Soil, g	% moisture m/m
D-8"-01, T12-8, 6/27/12	379.5	1.01	24.49	17.39	23.48	16.38	30.2%
D-8"-02, T12-1, 6/27/12	339.7	1.02	23.65	16.99	22.63	15.97	29.4%
D-8"-03, T12-5, 6/27/12	333.9	1.00	26.12	18.78	25.12	17.78	29.2%
D-8"-04, 6 month, T11-6, APT, 6/27/12	381.9	0.97	26.61	20.81	25.64	19.84	22.6%
D-8"-05, 6 month, T11-7, APT, 6/27/12	350.1	1.01	25.26	18.53	24.25	17.52	27.8%
D-8"-06, 6 month, T10-6, GAL, 6/27/12	300.9	1.03	24.90	17.79	23.87	16.76	29.8%
D-8"-07, 6 month, T10-5, 6/27/12	294.0	1.03	23.71	17.22	22.68	16.19	28.6%
D-8"-08, 6 month, T10-9, 6/27/12	379.7	1.01	26.69	19.23	25.68	18.22	29.0%
D-8"-01, 6 month, T12-?, 6/28/12	314.8	1.01	24.25	18.15	23.24	17.14	26.2%
D-8"-02, 6 month, T12-7, 6/28/12	358.3	1.00	24.72	18.35	23.72	17.35	26.9%
D-8"-03, 6 month, T12-6, 6/28/12	323.9	0.99	23.58	17.67	22.59	16.68	26.2%

APPENDIX D
SUMMARY OF MOISTURE CONTENTS AND RAINFALL DATA COLLECTED FOR PHASE 2 WIND TESTING

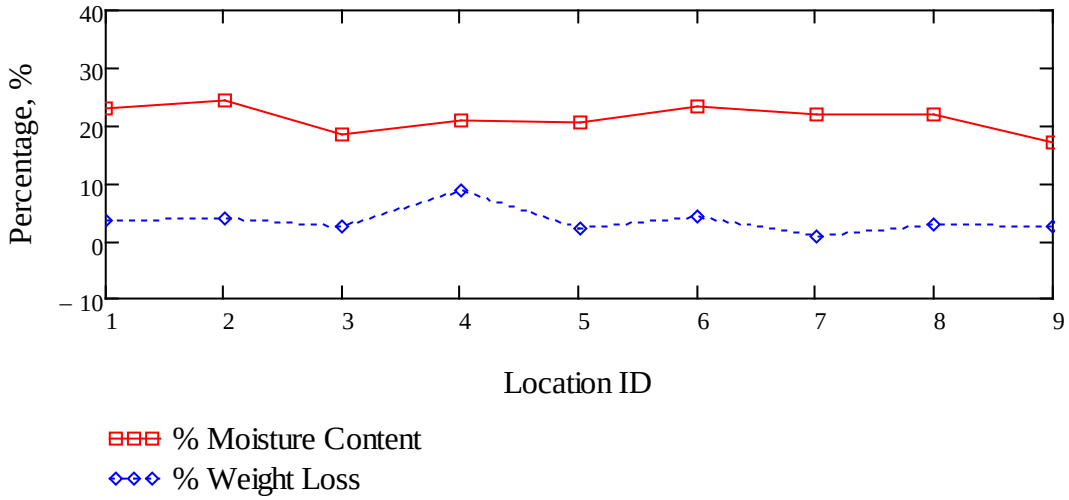

Figure D-1. Moisture content plotted against percentage weight losses (%) for modular tray test trial T2 (10 minute test duration)

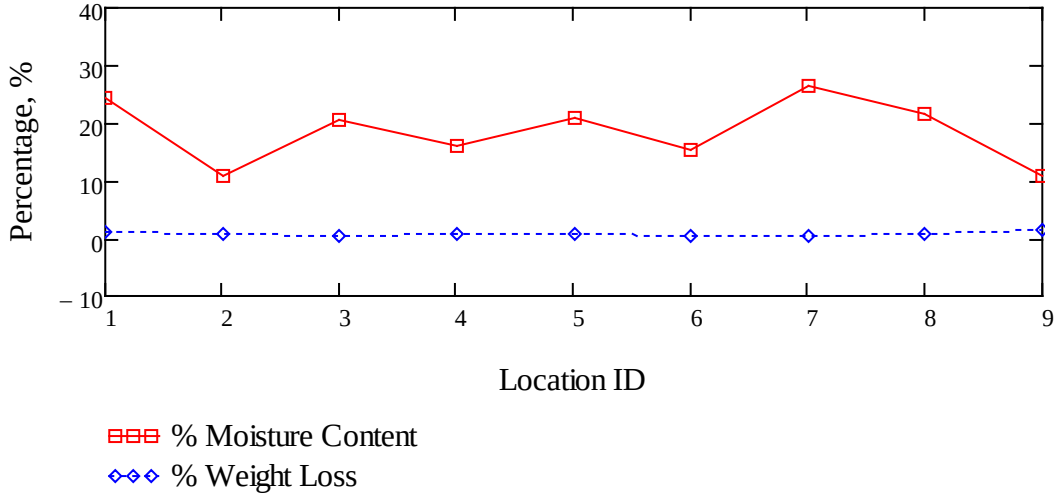

Figure D-2. Moisture content plotted against percentage weight losses (%) for modular tray test trial T5 (10 minute test duration)

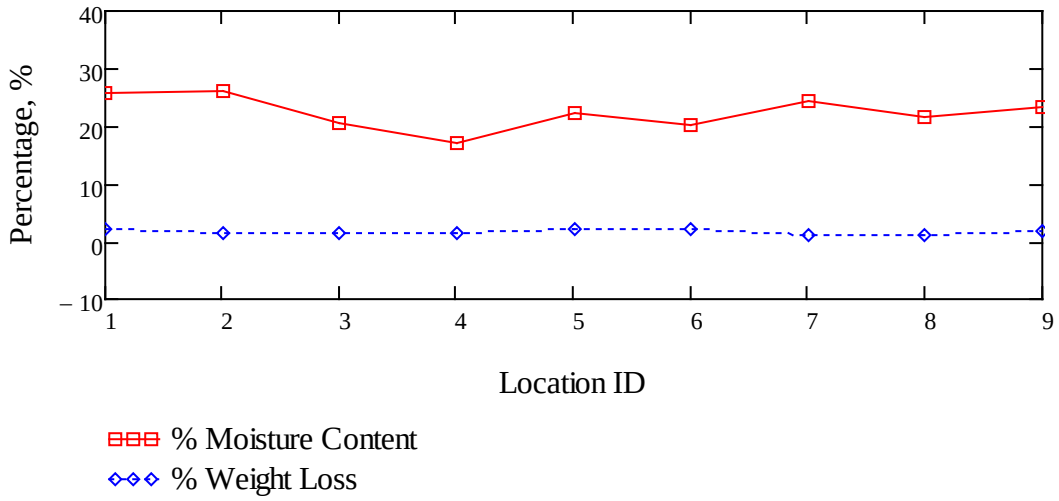

Figure D-3. Moisture content plotted against percentage weight losses (%) for modular tray test trial T6 (10 minute test duration)

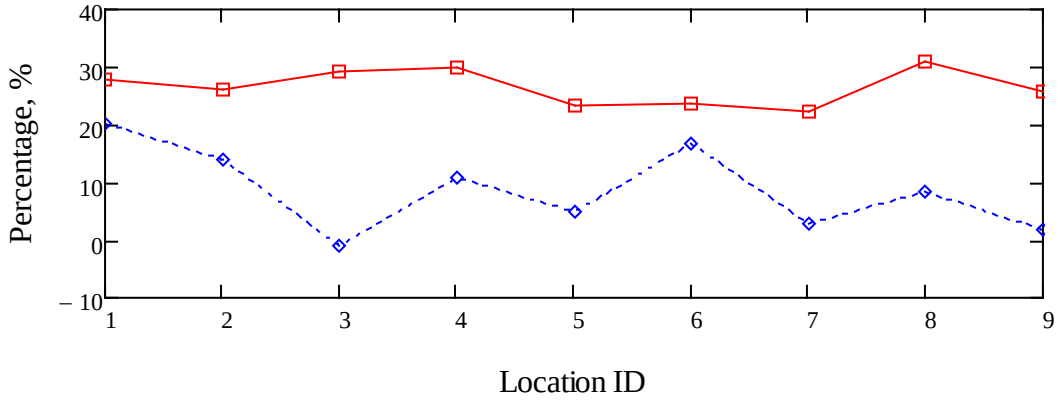

Figure D-4. Moisture content plotted against percentage weight losses (%) for modular tray test trial T7 (20 minute test duration)

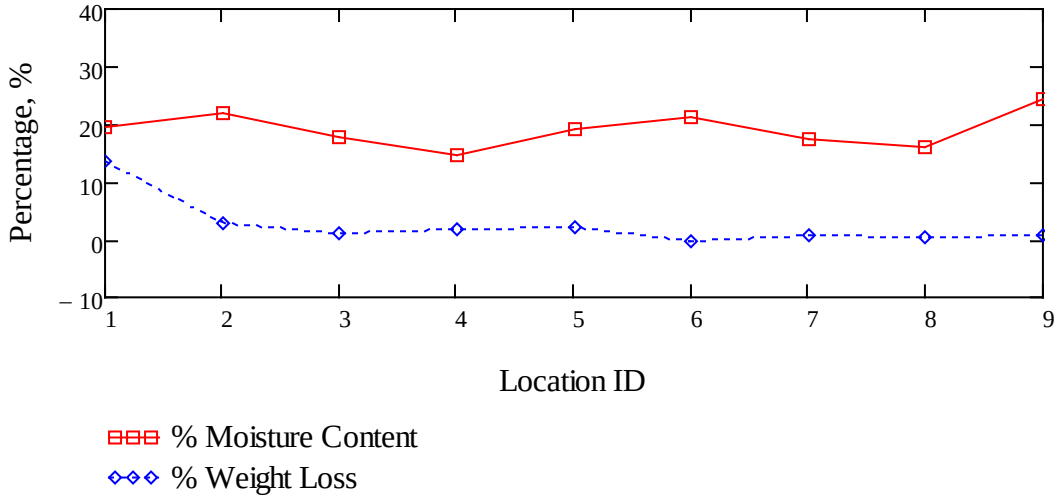

Figure D-5. Moisture content plotted against percentage weight losses (%) for modular tray test trial T10 (20 minute test duration)

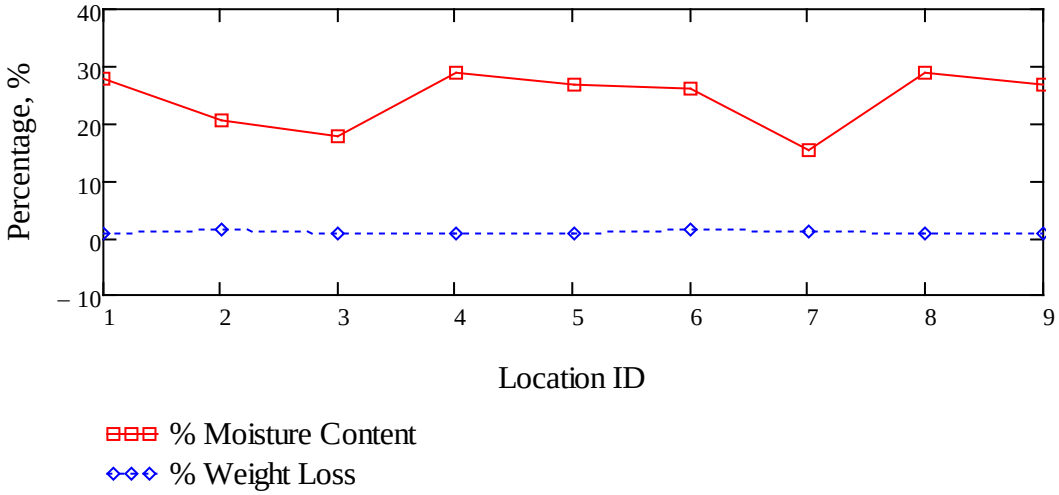

Figure D-6. Moisture content plotted against percentage weight losses (%) for modular tray test trial T11 (10 minute test duration)

Table D-1. Summary of averaged moisture contents for built-in-place assemblies in Phase 2.

Tray ID	L (in.)	C (in.)	R (in.)	208 L Depletion Time	Sample Collection Time	Time Elapsed (min)	Sample ID	Sample % MC[1]	Averaged % MC[1]
S-S1	27.9	38.1	21.6	4:56 PM	5:33 PM	37	S-S1-1	24.52%	29.68%
							S-S1-3	31.80%	
							S-S1-5	31.99%	
							S-S1-7	28.59%	
							S-S1-9	31.48%	
S-S2	35.6	38.1	25.4	3:50 PM	4:36 PM	46	S-S2-1	26.32%	28.92%
							S-S2-3	28.99%	
							S-S2-5	30.27%	
							S-S2-7	28.05%	
							S-S2-9	30.97%	
S-T1	15.2	68.6	21.6	2:15 PM	4:32 PM	137	S-T1-1	20.65%	23.89%
							S-T1-3	22.99%	
							S-T1-5	26.16%	
							S-T1-7	23.00%	
							S-T1-9	26.63%	
S-T2	24.1	30.5	6.4	10:40 AM	1:28 PM	168	S-T2-1	21.89%	25.79%
							S-T2-3	24.54%	
							S-T2-5	25.70%	
							S-T2-7	27.09%	
							S-T2-9	29.73%	
N-S1	-	-	-	6:29 PM	7:01 PM	32	N-S1-1	21.16%	23.71%
							N-S1-3	24.05%	
							N-S1-5	27.73%	
							N-S1-7	19.99%	
							N-S1-9	25.61%	
N-S2	-	-	-	10:36 AM	11:40 AM	64	N-S2-1	15.02%	21.16%
							N-S2-3	24.78%	
							N-S2-5	24.15%	
							N-S2-7	19.70%	
							N-S2-9	22.14%	
N-T1	-	-	-	5:30 PM	6:10 PM	40	N-T1-1	23.83%	25.47%
							N-T1-3	24.46%	
							N-T1-5	28.57%	
							N-T1-7	24.70%	
							N-T1-9	25.78%	
N-T2	-	-	-	9:49 AM	10:36 AM	47	N-T2-1	21.52%	25.58%
							N-T2-3	28.04%	
							N-T2-5	25.72%	
							N-T2-7	25.86%	
							N-T2-9	26.77%	

[1]MC = Moisture content

Table D-2. Daily rainfall records on wind test dates (source: wunderground.com for Gainesville, FL, Zip code: 32609)

Date:	06/12	06/13	06/14	06/17	06/18	06/19	06/20	06/21	06/22
Rainfall (mm)	0.51	6.86	51.56	0.00	0.00	0.00	100.58	0.25	8.89
Time(s) of Rainfall Event(s)	3:51PM to 4:53PM	9:53PM to 10:53PM	12:53AM to 1:53AM; 3:37PM to 7:53PM	-	-	-	7:53AM to 8:53AM	2:53PM to 3:53PM	4:06AM to 4:53AM; 3:46PM to 6:53PM
Test Trials Conducted	N-S1 N-T1	N-S2 N-T2 S-S1 S-S2	-	-	T2 T3	S-T1 S-T2	T5 T6 T8	T7	T10 T11

APPENDIX E
PHASE 2 WIND TESTING OBSERVATION LOGS

Table E-1. Observation logs for built-in-place assembly green roof test trials in Phase 2.

Test ID	Plant Height	1st Five Minute Segment	2nd Five Minute Segment	3rd Five Minute Segment	4th Five Minute Segment
N-S1	Short	No signs of damage from ground. Plants are seen to displace in shape of wind flow.	No losses observed.	-	-
N-S2	Short	Plants stay relatively still. Windward corner is exposed as plant displaced in direction of wind flow.	No losses observed.	-	-
N-T1	Tall	Small, windborne debris is observed in the form of leaves and flowers. Root lodging is observed as predominant failure mode.	Plant loss is observed approximately 2 minutes into 2nd segment.	-	-
N-T2	Tall	No noted plant structure loss. All plants bend in direction of wind flow. Root lodging on all plants.	No losses observed. Root lodging is magnified.	-	-
S-S1	Short	No losses observed. Plant displacement in direction of wind flow.	Plant loss observed at approximately 3 minutes into 2nd segment	-	-
S-S2	Short	Plants noted to stay relatively still. No losses observed. Plant displacement in direction of wind flow.	No losses observed.	-	-
S-T1	Tall	Plants were observed to bend, but not break off. Root lodging was noted as prominent failure mode.	No losses observed.	No losses observed.	No losses observed.
S-T2	Tall	Three (3) plants were seen to be dislodged immediately. Leaves were observed as windborne debris. Plant loss was identified as originating from leading corner of BIP tray.	No losses observed.	Leaves are seen to be dry and damaged from impact of wind forces. Plants located at the leading edge are noted to be bare of leaves.	No observed losses. Root lodging is prominent along the left windward edge where the highest level of scour is observed.

Table E-2. Observation logs for modular tray green roof test trials in Phase 2.

Test ID	Plant Height (Media Depth)	1st Five Minute Segment	2nd Five Minute Segment	3rd Five Minute Segment	4th Five Minute Segment
T2	Mixed (100 mm)	Some plant loss observed.	No losses observed.	-	-
T3	Mixed (100 mm)	Loss of some leaves observed before failure.	-	-	-
T5	Mixed (200 mm)	Some plant debris loss observed. A lot of leaves were absent on leeward corner module.	Small plant debris loss, but no full plants. Leeward corner module has wilted leaves at end of testing	-	-
T6	Mixed (200 mm)	Taller plants bend over aluminum edge restraint. Dianthus exposed substrate.	Salvia and Lantana regained structural integrity by 2nd segment.	-	-
T7	Tall (100 mm)	Gaillardia bent over apparent. Leading corner plants are bare of leaves.	Plants remain bent over.	None	None
T8	Short (100 mm)	None before failure.	-	-	-
T10	Tall (200 mm)	Plants all bend downwards. Full plant loss was observed four (4) minutes into the 1st segment. Stem lodging is observed (broken stems).	No losses observed.	No losses observed.	No losses observed.
T11	Short (200 mm)	Small plant seen as windborne debris. No plant stresses observed from ground.	No losses observed.	-	-

APPENDIX F
PLANT UPROOT TESTING FORCE VS. DISPLACEMENT DATA

Table F-1. Comparative summary of uproot tests conducted on 200 mm deep modules.

Plot ID	Plant Species	Age (mo.)	Moisture Content	Phase 2 Wind Tested?	Weight Change After Wind Test (%)	Module Location	Peak Load (N)	Max Disp. (mm)
AP	Aptenia	6	29.4%	No	-	-	60.2	130.8
			22.6%	Yes	-0.6%	1	25.6	72.4
			27.8%	Yes	-1.0%	7	99.2	129.5
			32.4%[a]	Yes	-0.6%	3	81.3	101.9
			33.2%[a]	Yes	-0.7%	9	48.8	77.7
			33.0%[a]	Yes	-0.8%	8	28.1	45.2
AP	Aptenia	13	26.9%	No	-	-	209.4	101.6
			26.6%	No	-	-	55.3	63.2
			11.5%	Yes	-0.7%	4	70.7	104.9
			32.0%[a]	No	-	-	109.1	84.3
			31.4%[a]	Yes	-1.1%	1	283.9	95.0
			30.7%[a]	No	-	-	81.8	64.8
DE	Delosperma	6	30.2%	No	-	-	63.2	82.0
			29.4%	No	-	-	60.9	49.5
			29.2%	No	-	-	76.9	44.7
DI	Dianthus	13	26.9%	No	-	-	220.5	105.2
			25.8%	No	-	-	21.4	48.8
			11.5%	Yes	-0.7%	4	76.7	148.8
			32.0%[a]	No	-	-	27.1	37.6
			31.4%[a]	Yes	-1.1%	1	26.8	121.2
			30.7%[a]	No	-	-	81.7	150.1
GA	Gaillardia	6	29.8%	Yes	-2.7%	2	24.2	29.2
			28.6%	Yes	+0.2%	6	81.8	67.8
			29.0%	Yes	-2.3%	5	68.5	64.8
			27.8%[a]	Yes	-0.7%	7	64.4	78.0
			33.0%[a]	Yes	-1.7%	4	39.7	43.7
			33.2%[a]	Yes	-0.9%	9	112.9	110.7
			26.2%	No	-	-	100.0	149.9
			26.9%	No	-	-	57.3	83.6
			26.2%	No	-	-	354.3	150.9
LA	Lantana	13	26.6%	No	-	-	263.9	150.1
			25.8%	No	-	-	119.4	151.9
			11.5%	Yes	-0.7%	4	104.7	150.9
			32.0%[a]	No	-	-	110.3	150.4
			31.4%[a]	Yes	-1.1%	1	126.9	149.9
			30.7%[a]	No	-	4	65.7	61.2

[a] Artificially saturated

Table F-2. Comparative summary of uproot tests conducted on 100 mm deep modules.

Plot/ Stat ID	Plant Species	Age (mo.)	Moisture Content	Phase 2 Wind Tested?	Weight Change After Wind Test (%)	Module Location	Peak Load (N)	Max Disp. (mm)
AP	Aptenia	13	15.7%	Yes	-4.0%	2	64.9	84.1
			15.8%	Yes	-2.5%	7	81.2	102.6
			23.2%	Yes	-8.6%	4	101.1	149.9
			34.0%[a]	No	-	-	102.8	71.9
			28.9%[a]	Yes[b]	-	8	97.3	63.2
			38.5%[a]	Yes[b]	-	7	145.8	149.4
DE	Delosperma	6	33.0%	No	-	-	29.0	82.6
			37.3%	No	-	-	10.0	147.1
			34.4%	No	-	-	32.3	84.1
DI	Dianthus	13	16.1%	Yes	-2.8%	8	85.4	128.5
			15.7%	Yes	-4.0%	2	89.1	151.1
			15.8%	Yes	-2.5%	7	94.7	150.4
			36.3%[a]	No	-	-	74.0	54.9
			34.0%[a]	No	-	-	132.2	150.4
			29.7%[a]	No	-	-	132.3	150.4
GA	Gaillardia	6	36.4%	No	-	-	38.9	84.3
			35.5%	No	-	-	44.5	149.4
			30.5%	No	-	-	40.1	147.8
			31.9%[a]	Yes	+0.8%	3	51.9	150.1
			28.0%[a]	Yes	-20.3%	1	49.8	149.6
			31.1%[a]	Yes	-2.7%	7	39.1	149.6
LA	Lantana	13	12.9%	Yes	-2.6%	9	114.3	152.7
			15.7%	Yes	-4.0%	2	102.5	150.9
			15.8%	Yes	-2.5%	3	95.0	130.0
			36.3%[a]	No	-	-	114.4	150.4
			34.0%[a]	No	-	-	143.5	150.4
			29.7%[a]	No	-	-	81.0	150.4

[a] Artificially saturated

[b] Module from test trial T3 which remained on roof following blow-off failure

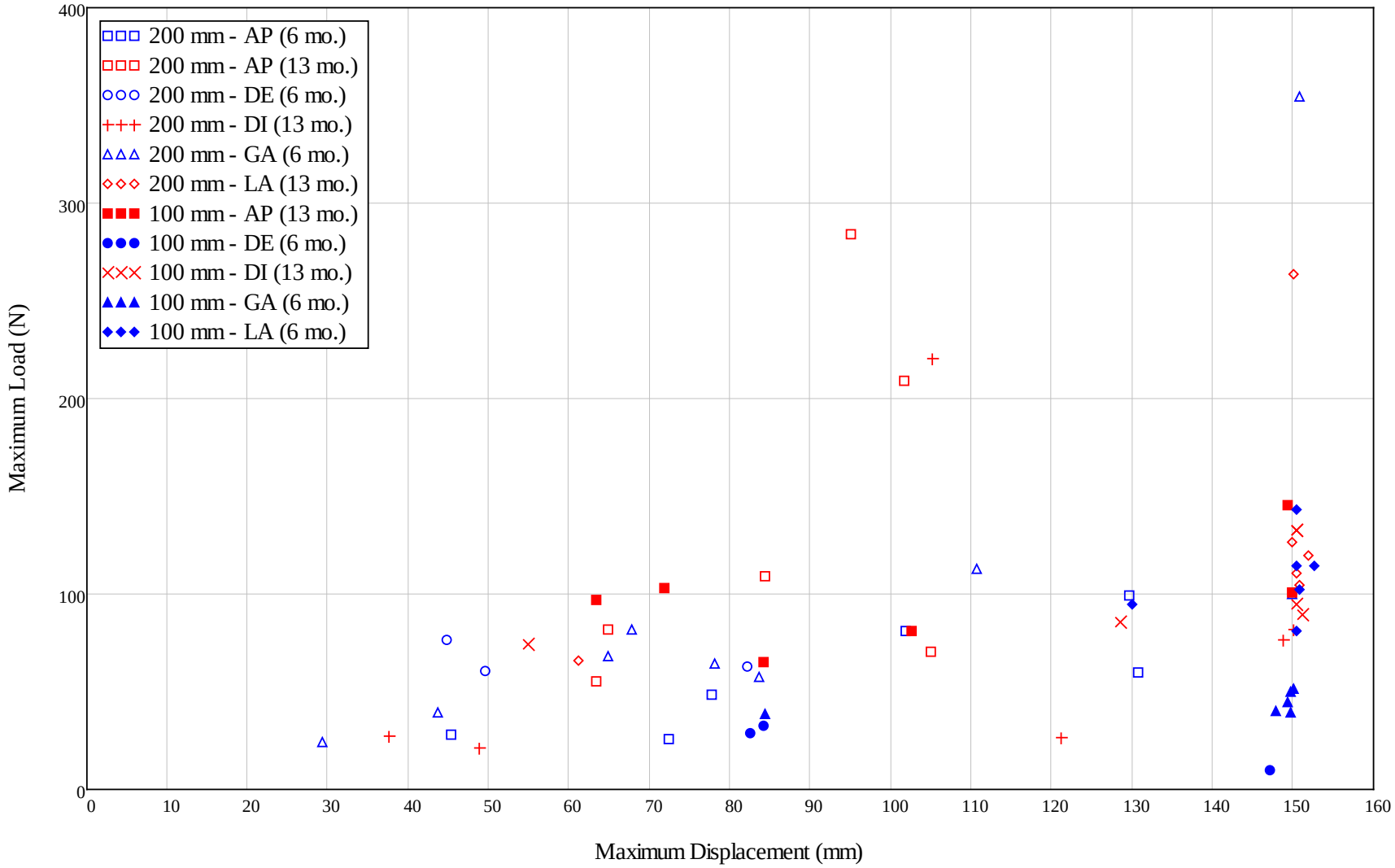

Figure F-1. Summary maximum load vs. displacement plot for the uproot tests (refer to Tables F-1 or F-2 for abbreviation definitions).

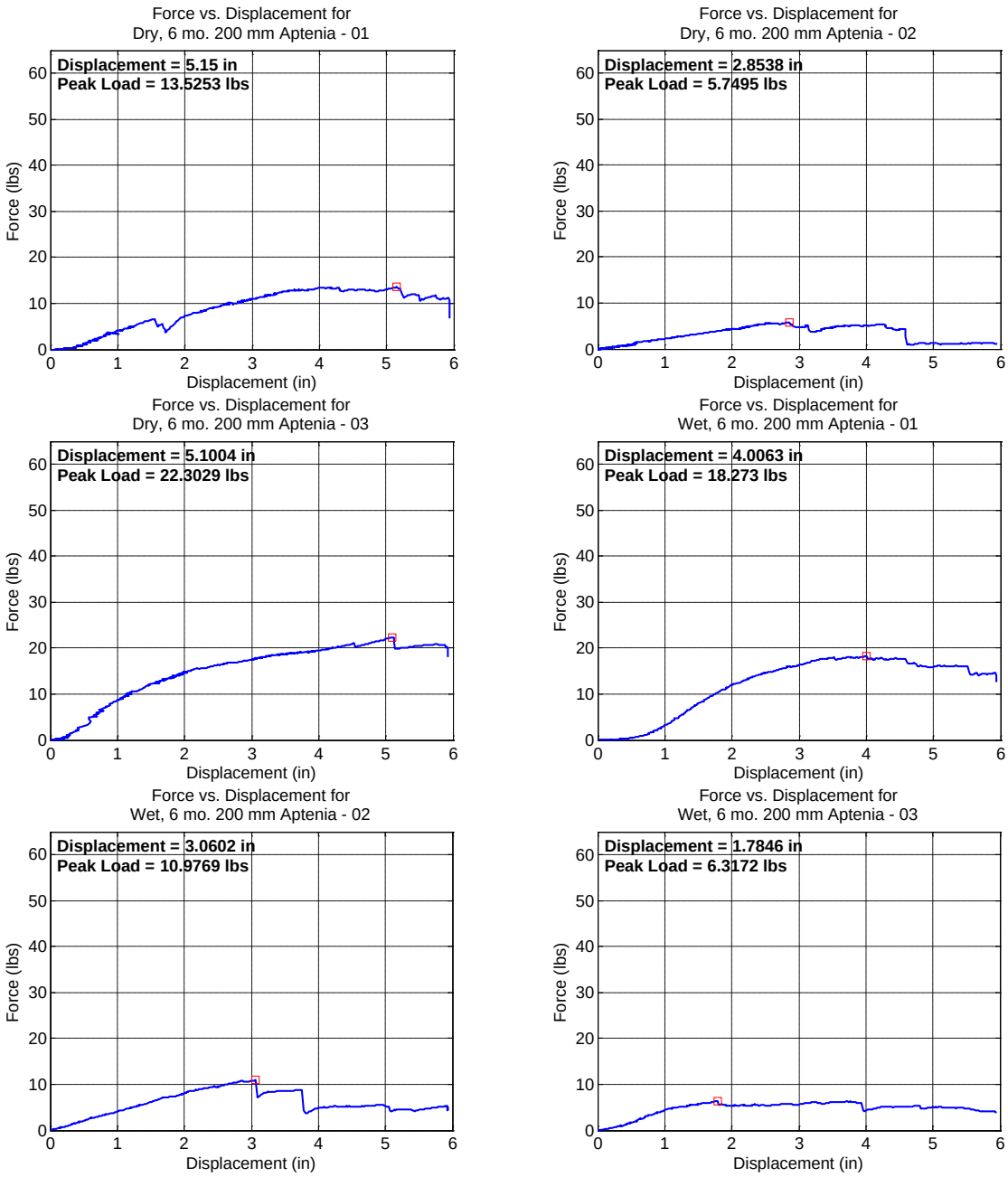

Figure F-2. Force vs. displacement plots for Aptenia plant species in 200 mm deep modules grown for 6 months.

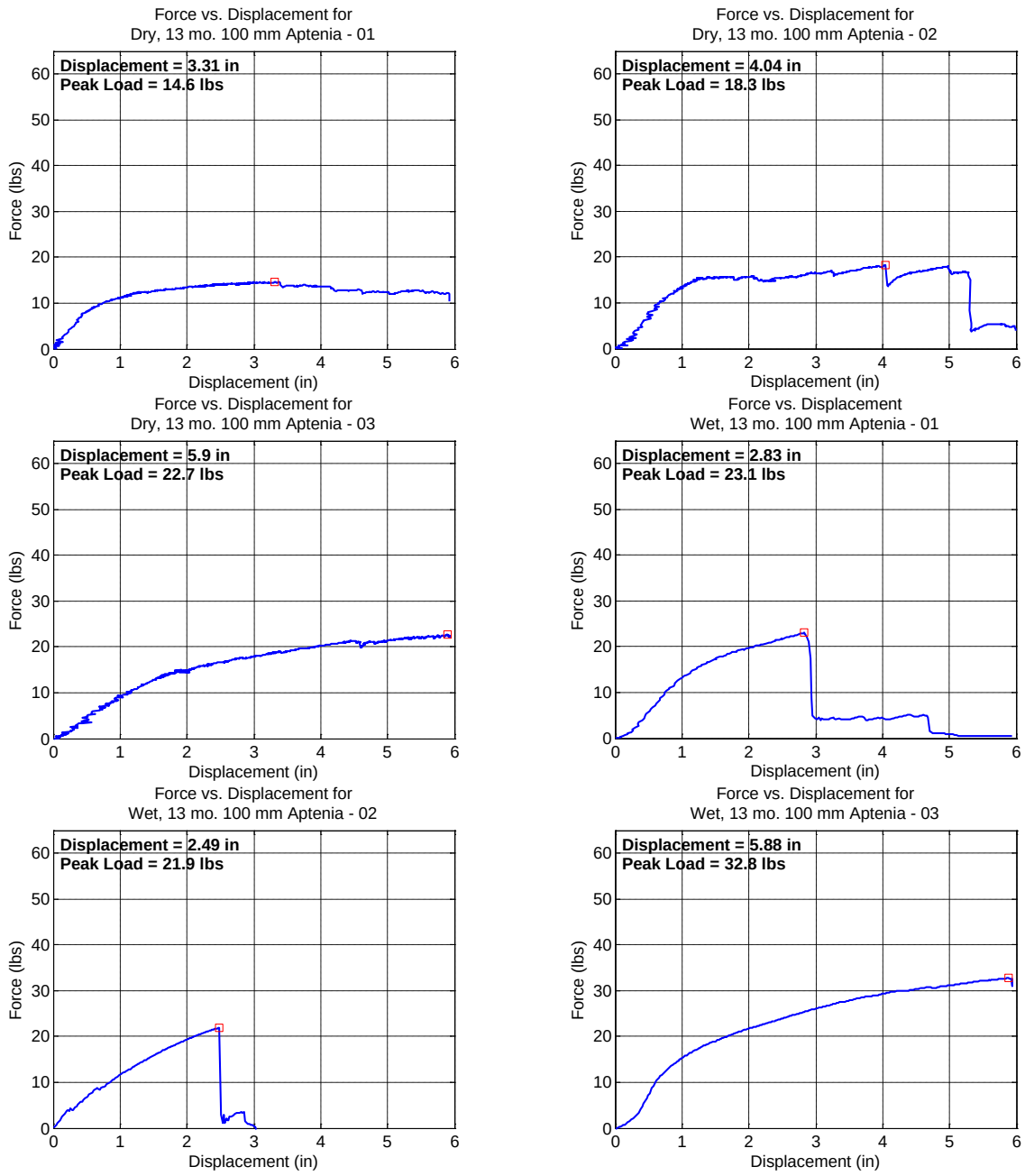

Figure F-3. Force vs. displacement plots for Aptenia plant species in 100 mm deep modules grown for 13 months.

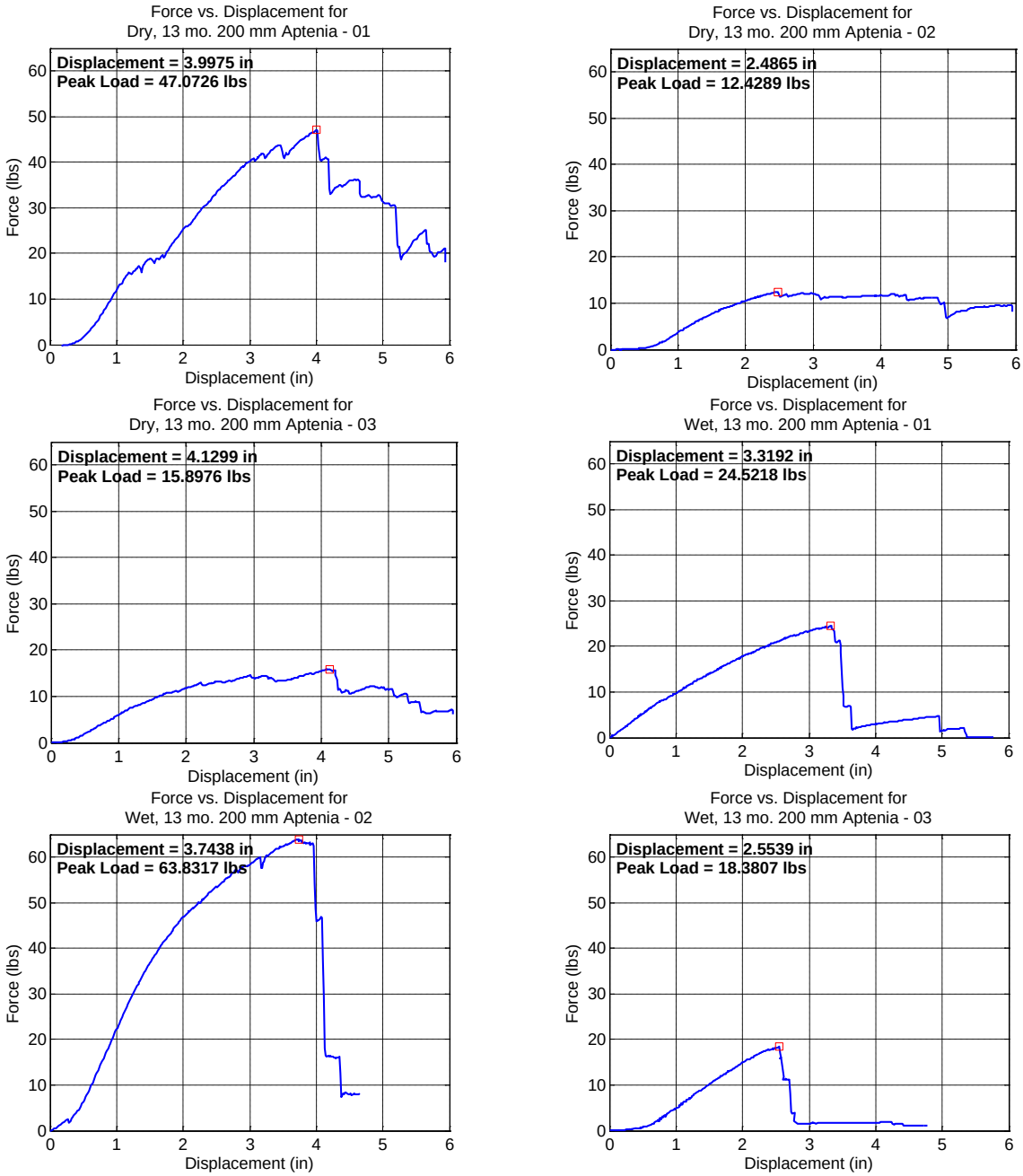

Figure F-4. Force vs. displacement plots for Aptenia plant species in 200 mm deep modules grown for 13 months.

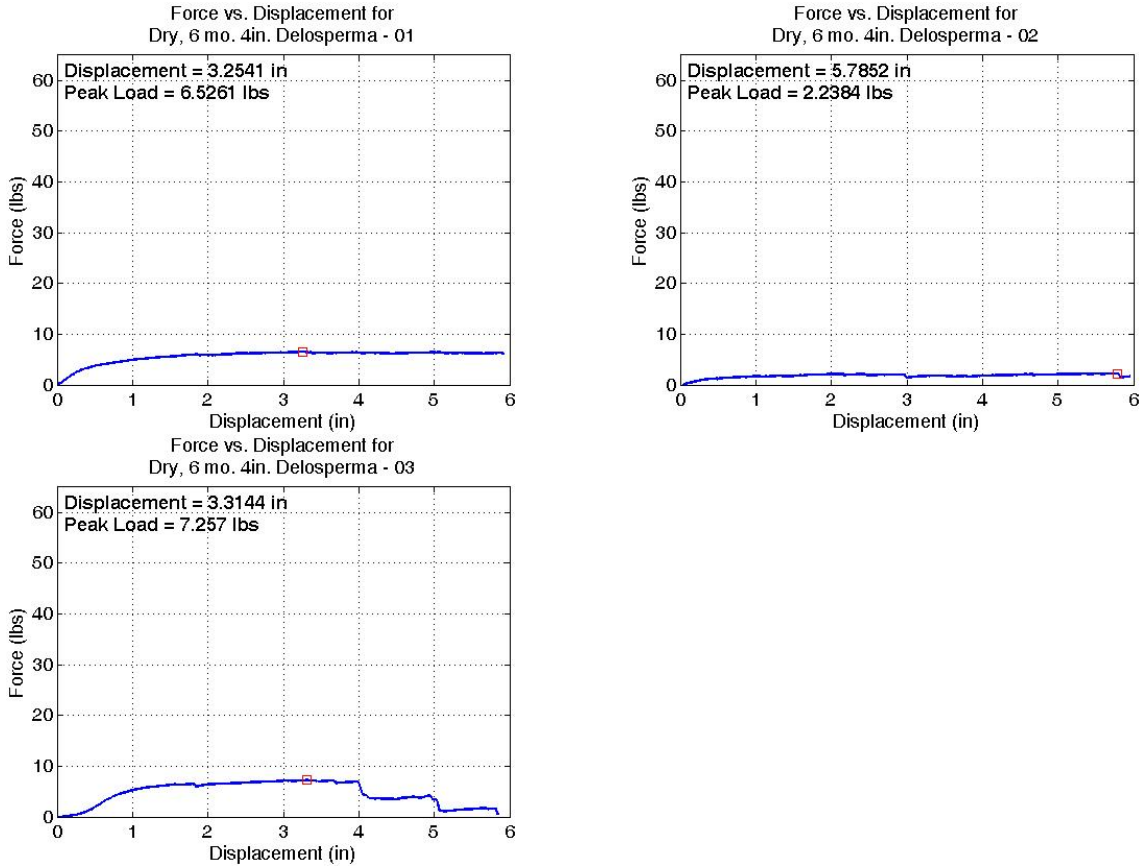

Figure F-5. Force vs. displacement plots for Delosperma plant species in 100 mm deep modules grown for 6 months.

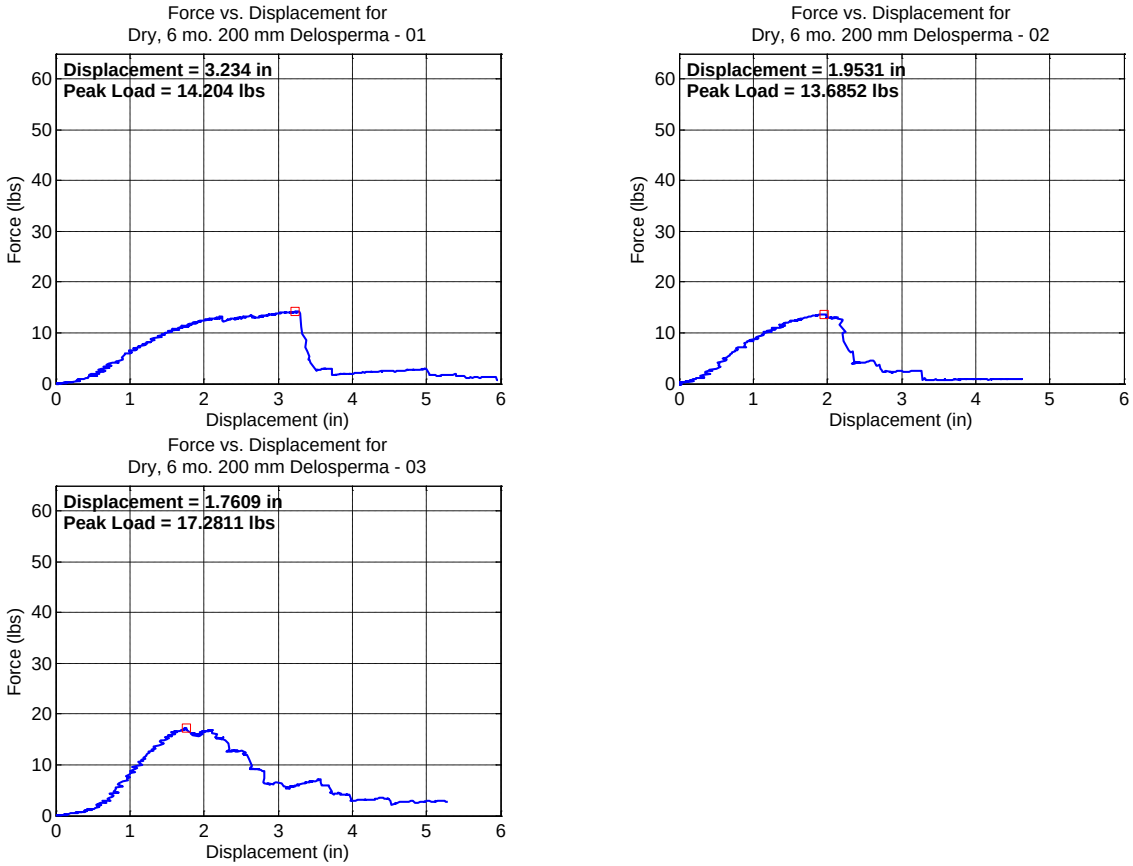

Figure F-6. Force vs. displacement plots for Delosperma plant species in 200 mm deep modules grown for 6 months.

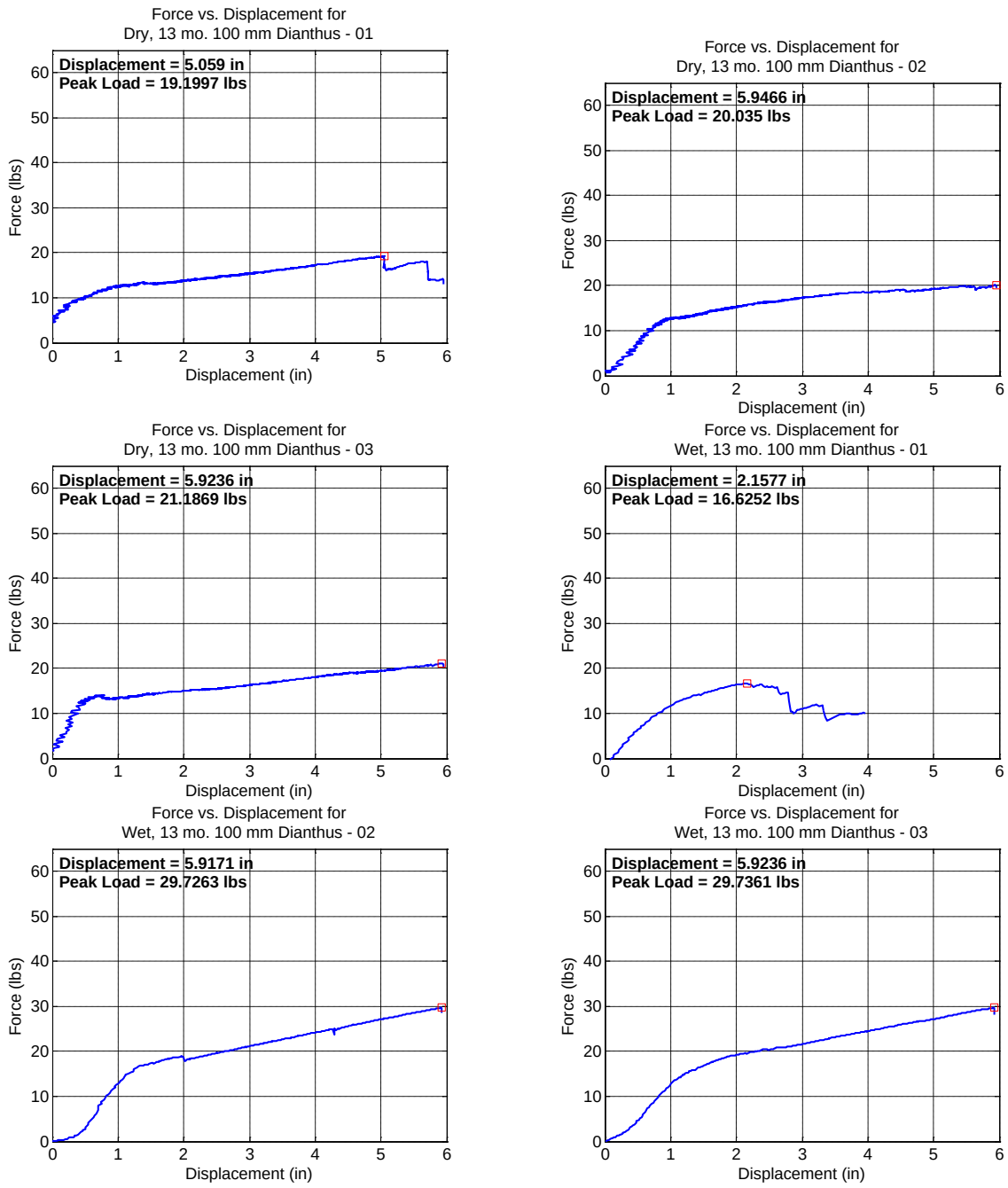

Figure F-7. Force vs. displacement plots for Dianthus plant species in 100 mm deep modules grown for 13 months.

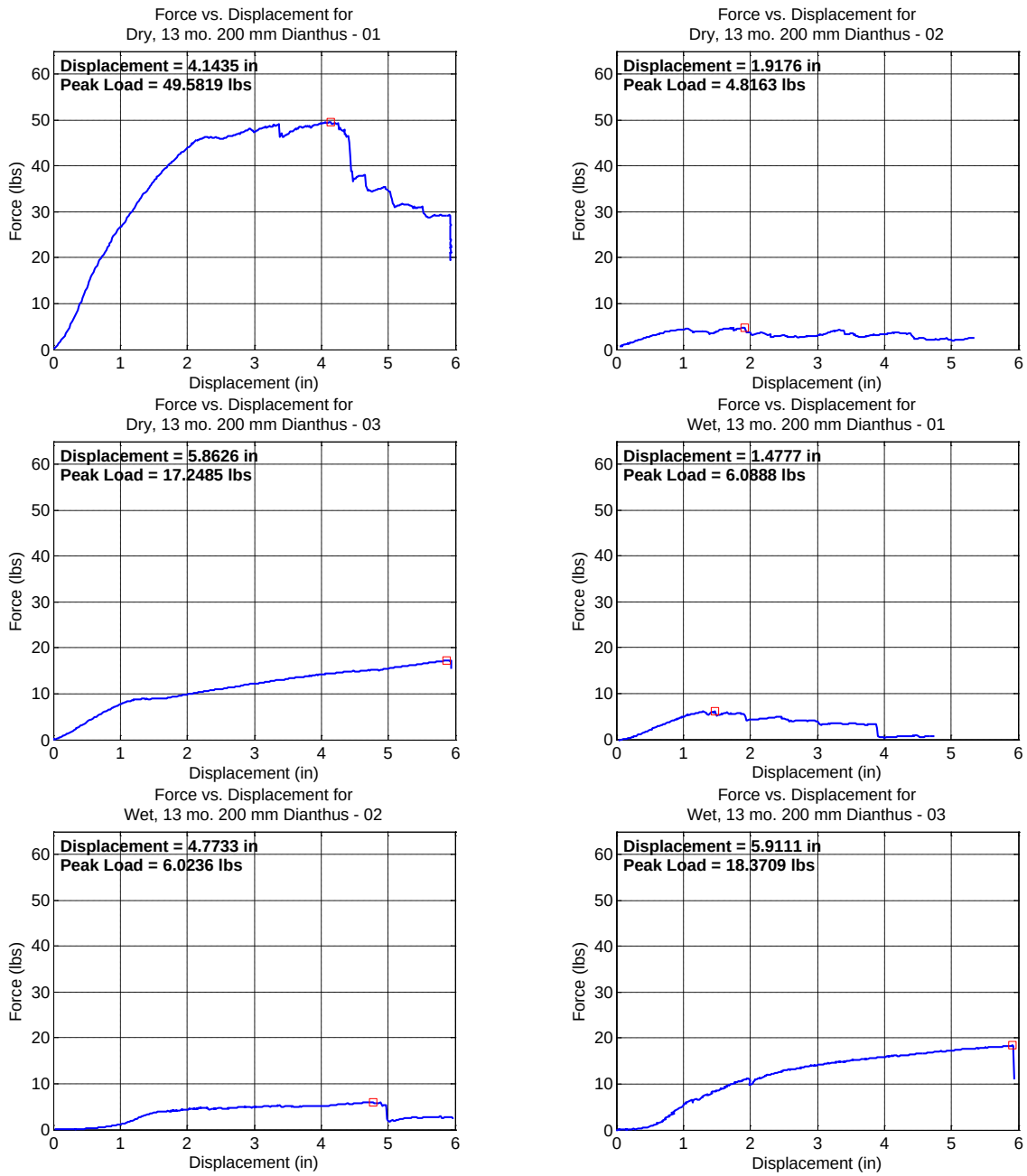

Figure F-8. Force vs. displacement plots for Dianthus plant species in 200 mm deep modules grown for 13 months.

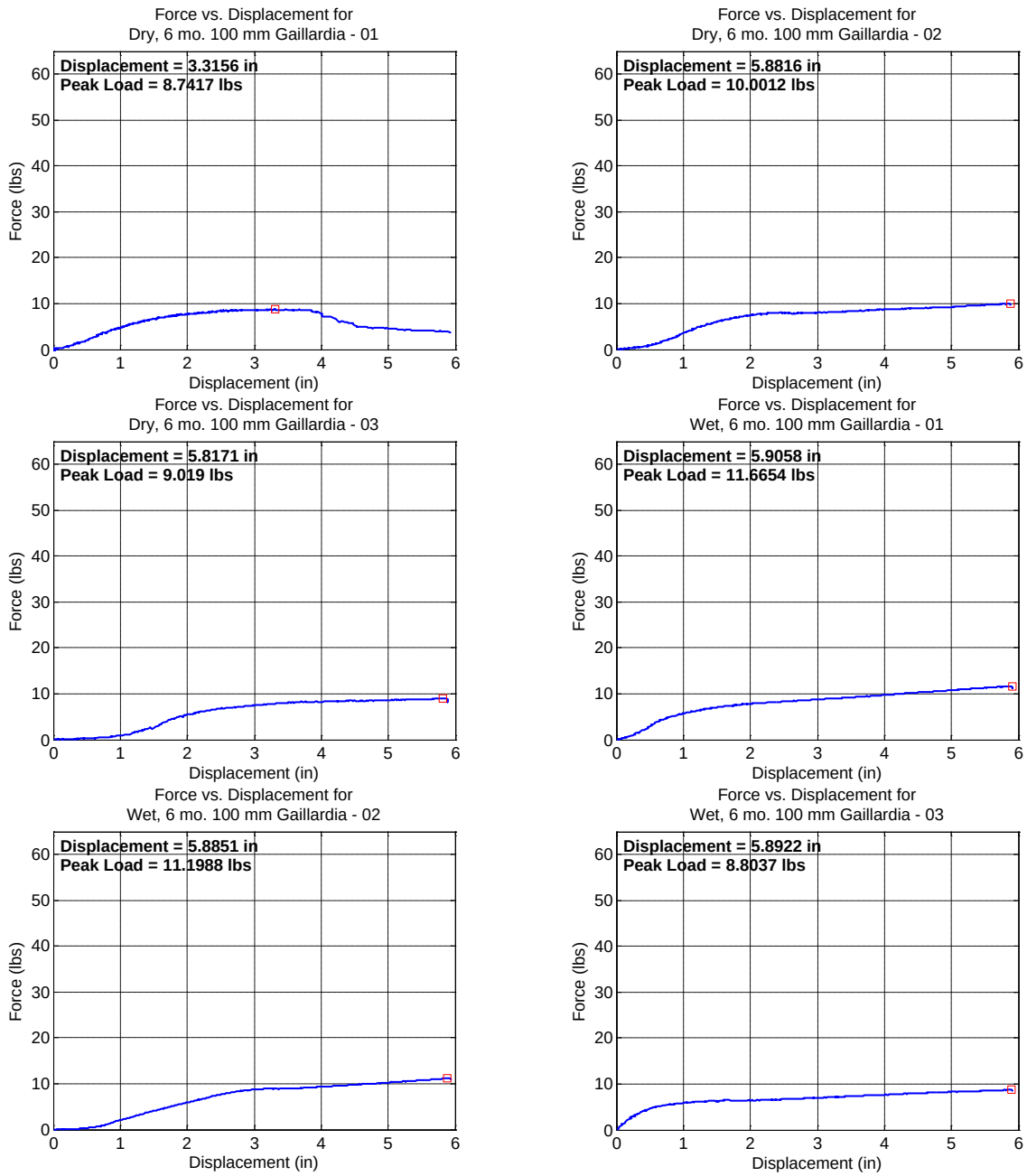

Figure F-9. Force vs. displacement plots for Gaillardia plant species in 100 mm deep modules grown for 6 months.

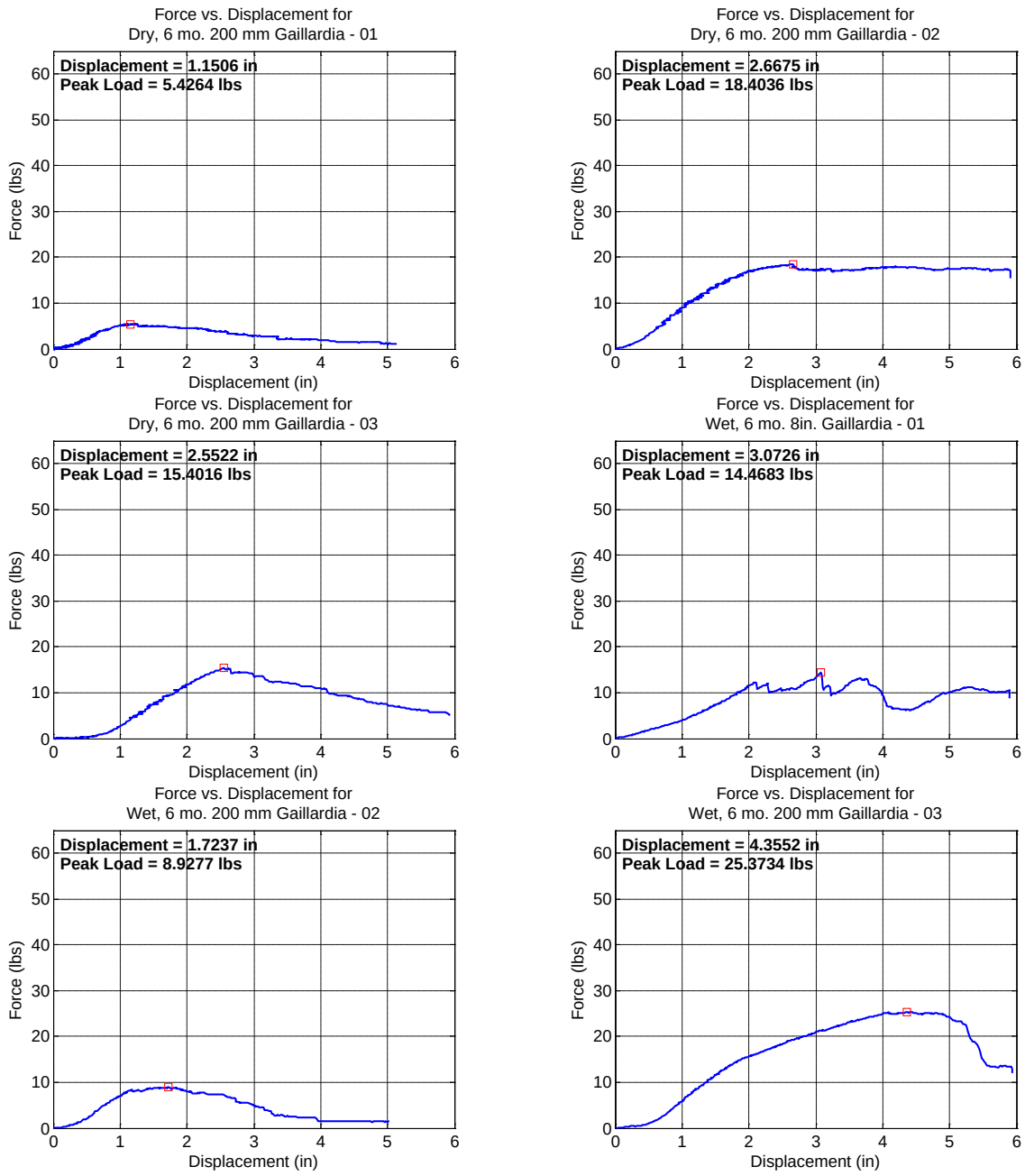

Figure F-10. Force vs. displacement plots for Gaillardia plant species in 200 mm deep modules grown for 6 months.

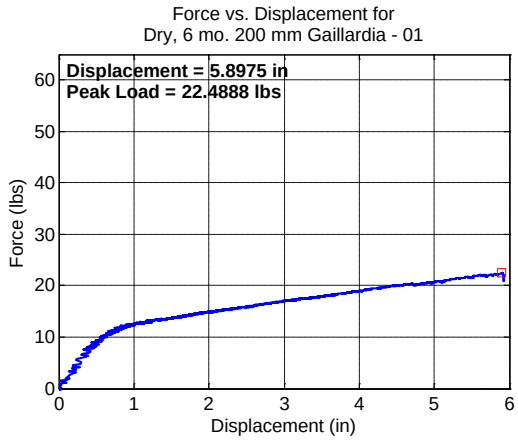

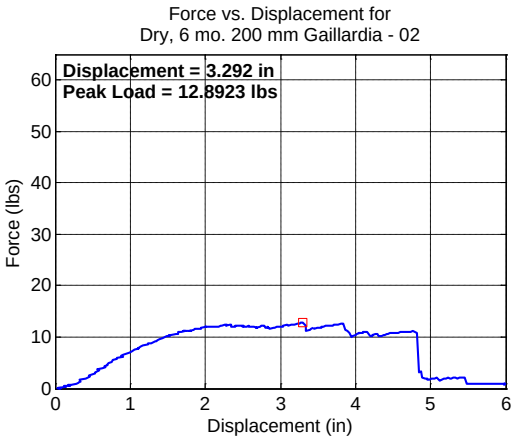

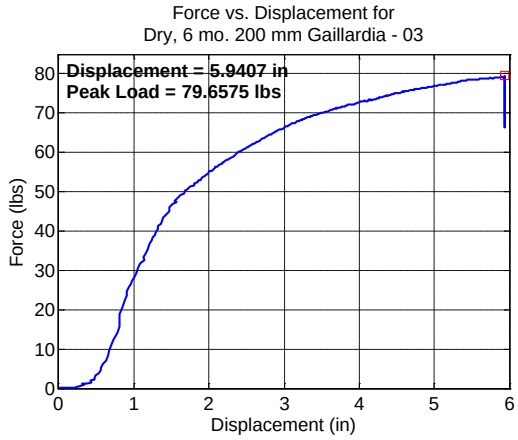

Figure F-10. Continued

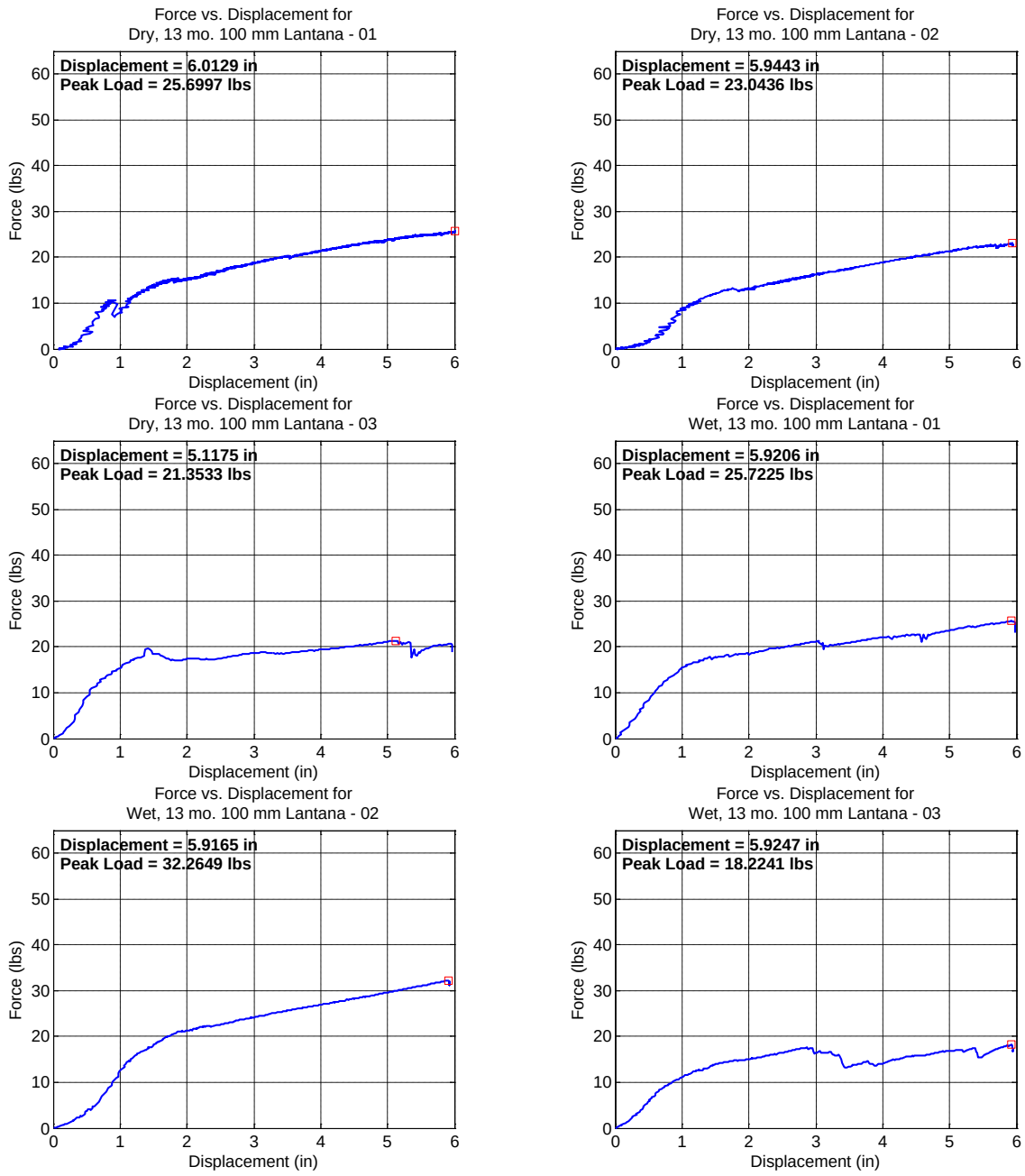

Figure F-11. Force vs. displacement plots for Lantana plant species in 100 mm deep modules grown for 13 months.

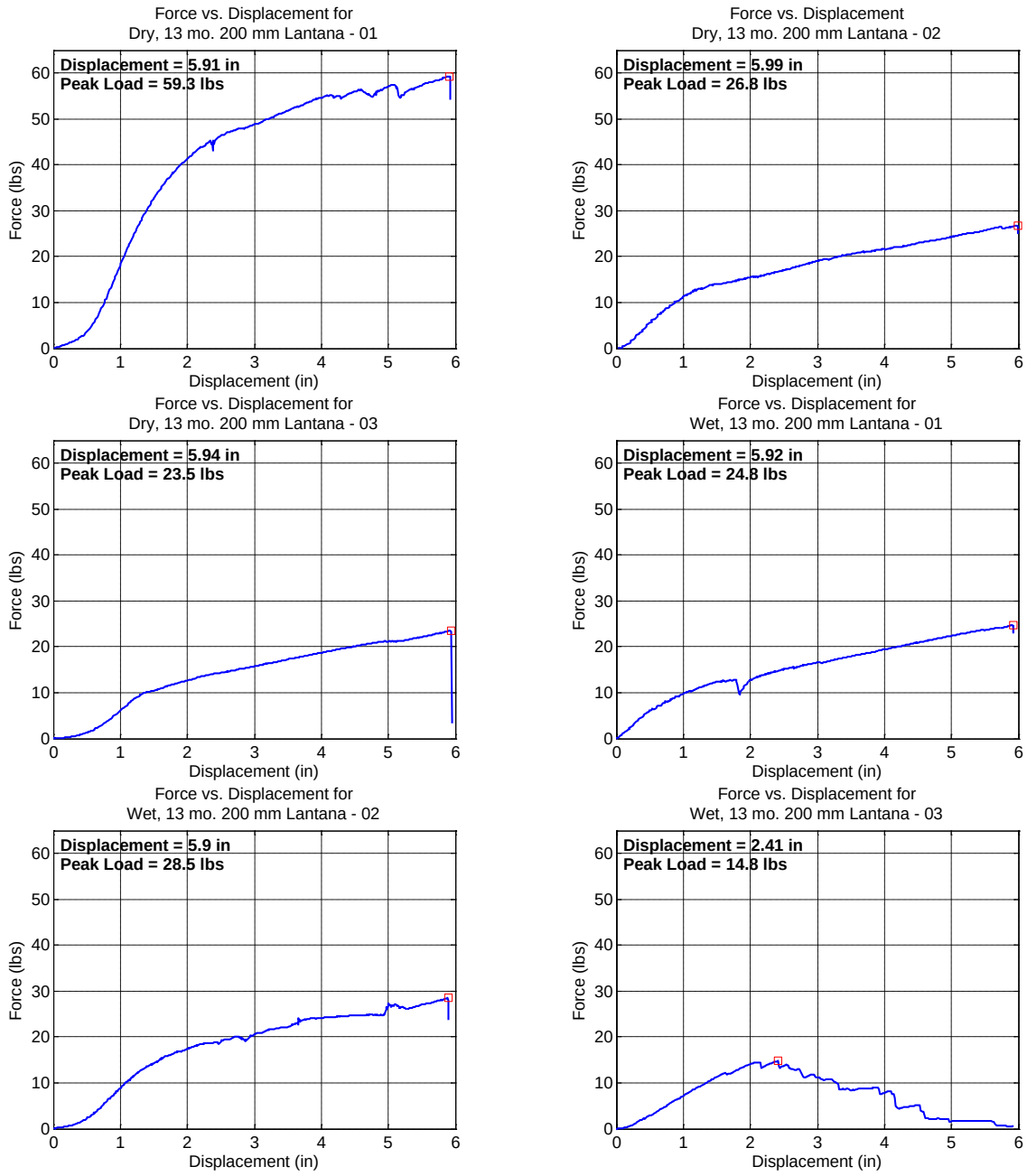

Figure F-12. Force vs. displacement plots for Lantana plant species in 200 mm deep modules grown for 13 months.

LIST OF REFERENCES

Aly, A. M., Bitsuamlak, G. T., & Chowdhury, A. G. (2012). Full-scale aerodynamic testing of a loose concrete roof paver system. *Engineering Structures, 44*(0), 260-270. Retrieved from http://www.sciencedirect.com/science/article/pii/S0141029612002441

ANSI/SPRI. (2008). RP-4 2008 Wind Design Standard For Ballasted Single-ply Roofing Systems. (pp. 33). Waltham, MA: SPRI.

ANSI/SPRI. (2010). RP-14 2010 Wind Design Standard for Vegetative Roofing Systems. (pp. 36). Waltham, MA: SPRI.

Applied Technology Council (2013). *Wind Speed by Location*. Retrieved April 24, 2013, from http://www.atcouncil.org/windspeed/index.php

ASCE. (2010). *Minimum Design Loads for Buildings and Other Structures: ASCE Standard 7-10*. Virginia: American Society of Civil Engineers.

ASTM. (2001). ASTM E1592-01 - Standard test method for structural performance of sheet metal roof and siding systems by uniform static air pressure difference. Philadelphia: ASTM.

Bailey, P. H. J., Currey, J. D., & Fitter, A. H. (2002). The role of root system architecture and root hairs in promoting anchorage against uprooting forces in Allium cepa and root mutants of Arabidopsis thaliana. *Journal of Experimental Botany, 53*(367), 333-340.

Baskaran, A., & Stathopoulos, T. (1988). Roof corner wind loads and parapet configurations. *Journal of Wind Engineering and Industrial Aerodynamics, 29 pt 2*(1-3), 79-88.

Berry, P. M., Sterling, M., & Mooney, S. J. (2006). Development of a Model of Lodging for Barley. *Journal of Agronomy and Crop Science, 192*(2), 151-158.

Bienkiewicz, B., & Meroney, R. N. (1988). Wind Effects on Roof Ballast Pavers. *Journal of Structural Engineering, 114*(6), 1250-1267.

Bienkiewicz, B., & Sun, Y. (1992). Local wind loading on the roof of a low-rise building. *Journal of Wind Engineering and Industrial Aerodynamics, 45*(1), 11-24.

Bienkiewicz, B., & Sun, Y. (1992). Wind-tunnel study of wind loading on loose-laid roofing systems. *Journal of Wind Engineering and Industrial Aerodynamics, 43*(pt 3), 1817-1828.

Bienkiewicz, B., & Sun, Y. (1997). Wind loading and resistance of loose-laid roof paver systems. *Journal of Wind Engineering and Industrial Aerodynamics, 72*(1-3), 401-410.

Bing Maps (2013). *Bonita Bay Green Roof at the Shadow Wood Preserve Country Club's Storage Shed* [bird's eye map]. Retrieved from http://binged.it/17N9vUv

Blessing, C., Chowdhury, A. G., Lin, J., & Huang, P. (2009). Full-scale validation of vortex suppression techniques for mitigation of roof uplift. *Engineering Structures, 31*(12), 2936-2946.

Bofah, K. K., Gerhardt, H. J., & Kramer, C. (1996). Calculations of pressure equilibration underneath loose-laid, flow permeable roof insulation boards. *Journal of Wind Engineering and Industrial Aerodynamics, 59*(1), 23-37.

Breuning, J. (2008). *Fire and Wind on Extensive Green Roofs.* Paper presented at the 6th Annual Greening Rooftops for Sustainable Communities Conference, Baltimore, Maryland.

Burri, K., Gromke, C., Lehning, M., & Graf, F. (2011). Aeolian sediment transport over vegetation canopies: A wind tunnel study with live plants. *Aeolian Research, 3*(2), 205-213.

Clark, M., Acomb, G., & Lang, S. (2008). *Fact Sheet: Green Roofs/Eco-roofs*. Gainesville, FL: University of Florida. Retrieved October 24, 2013, from http://buildgreen.ufl.edu/Fact_sheet_Green_Roofs_Eco_roofs.pdf

Colbond. (2008a). Case History No. 0407: Medical Building is Solid Gold with a Roof That is Producing a Lot of Green. pp. 2. Retrieved from http://www.colbond-usa.com/technical-docs/building-roofing/category/90-case-studies.html?download=234:texas-medical-gr-roof

Colbond. (2008b). Zero Damage Texas Green Roof. pp. 2. Retrieved from http://www.colbond-usa.com/technical-docs/building-roofing/category/90-case-studies.html?download=235:zero-damage-texas-gr-roof

Cook, N. J., Keevil, A. P., & Stobart, R. K. (1988). Brerwulf-the big bad wolf: I'll huff and I'll puff and I'll blow your house down! *Journal of Wind Engineering and Industrial Aerodynamics, 29*(1), 99-107.

Duan, J. G., Barkdoll, B., & French, R. (2006). Lodging velocity for an emergent aquatic plant in open channels. *Journal of Hydraulic Engineering, 132*(10), 1015-1020.

FEMA (2005). *Mitigation Assessment Team Report: Hurricane Charley in Florida*, [FEMA 488]. Washington, D.C.: FEMA.

FEMA (2013). *Hurricane Ike in Texas and Louisiana - Building Performance Observations, Recommendations, and Technical Guidance*: Federal Emergency Management Agency.

Fischer, K. T. (2013). *Modular Green Roof Performance in High Wind Conditions: A New Method for Uplift Analysis and Design.* Boston Architectural College.

FLL (2008). Guidelines for the Planning, Construction and Maintenance of Green Roofing - Green Roofing Guideline. pp. 125. Colmantstraße, Bonn: Forschungsgesellschaft Landschaftsentwicklung Landschaftsbau e.V. (FLL).

FM Global (2011). 1-35: Property Loss Prevention Data Sheets Green Roof Systems. (pp. 27).

Gerhardt, H. J., Kramer, C., & Bofah, K. K. (1990). Wind loading on loosely laid pavers and insulation boards for flat roofs. *Journal of Wind Engineering and Industrial Aerodynamics, 36, Part 1*(0), 309-318.

Green Roofs for Healthy Cities. (2012). *Annual Green Roof Industry Survey for 2011*, Chicago, IL.

Greenroofs.com (2012). *Greenroof and Greenwall Project Database*. Retrieved November 4, 2012, from http://www.greenroofs.com/projects/

Hamza, O., Bengough, A. G., Bransby, M. F., Davies, M. C. R., & Hallett, P. D. (2007). Mechanics of root-pullout from soil: A novel image and stress analysis procedure In *Eco- and Ground Bio-Engineering: The Use of Vegetation to Improve Slope Stability*. Stokes, I. Spanos, J. E. Norris & E. Cammeraat (Eds.), (Vol. 103, pp. 213-221): Springer Netherlands. Retrieved from http://link.springer.com/book/10.1007/978-1-4020-5593-5

Irwin, P., Cicci, M., Thompson, G., & Dragoiescu, C. (2012). Wind Tunnel Model Studies of Aerodynamic Lifting of Roof Pavers. In *Advances in Hurricane Engineering* (pp. 496-505): American Society of Civil Engineers.

Jin, X., Fourcaud, T., Li, B., & Guo, Y. (2010). *Towards modeling and analyzing stem lodging for two contrasting rice cultivars.* Paper presented at the 3rd International Symposium on Plant Growth Modeling, Simulation, Visualization and Applications, PMA09, November 9, 2009 - November 13, 2009, Beijing, China.

Karimpour, A., & Kaye, N. B. (2012). The critical velocity for aggregate blow-off from a built-up roof. *Journal of Wind Engineering and Industrial Aerodynamics, 107–108*(0), 83-93.

Karimpour, A., & Kaye, N. B. (2013). Wind tunnel measurement of the parapet height role on roof gravel blow-off rate for two dimensional low rise buildings. *Journal of Wind Engineering and Industrial Aerodynamics, 114*(0), 38-47

Kim, D. S., Cho, G. H., & White, B. R. (2000). A Wind-tunnel Study of Atmospheric Boundary-Layer Flow over Vegetated Surfaces to Suppress PM10 Emission on Owens (dry) Lake. *Boundary-Layer Meteorology, 97*(2), 309-329.

Kind, R. J. (1974a). *Estimation of critical wind speeds for scouring of gravel or crushed stone on rooftops*, [LTR-LA-142]. Ottawa, Canada.

Kind, R. J. (1974b). *Wind tunnel tests on some building models to measure wind speeds at which gravel is blown off rooftops*, [LTR-LA-162]. Ottawa, Canada: National Research Council Canada.

Kind, R. J., & Wardlaw, R. L. (1976). *Design of rooftops against gravel blow-off*, Canada: National Research Council Canada.

Kind, R. J., & Wardlaw, R. L. (1982). Failure mechanisms of loose-laid roof-insulation systems. *Journal of Wind Engineering and Industrial Aerodynamics, 9*(3), 325-341.

Kopp, G. A., Morrison, M. J., Gavanski, E., Henderson, D. J., & Hong, H. P. (2010). “Three Little Pigs” Project: Hurricane Risk Mitigation by Integrated Wind Tunnel and Full-Scale Laboratory Tests. *Natural Hazards Review, 11*(4), 151-161.

Kramer, C., & Gerhardt, H. J. (1999). *Assessment of positional security against wind uplift for a roof planting system that is permeable to wind*, [1/21010/10.99]. Aachen, Germany: WSP Engineering.

Lancaster, N., & Baas, A. (1998). Influence of vegetation cover on sand transport by wind: field studies at Owens Lake, California. *Earth Surface Processes and Landforms, 23*(1), 69-82.

LiveRoof (2012). *Architecture & Engineering*. Retrieved October 21, 2013, from http://www.liveroof.com/?page=ArchitectureEngineering#WindPressure

Livingston, E., Fikoski, K., Miller, C., Lohr, M., & Denison, T. (2009). *A Case Study for the EDGE On-line Tool: Shadow Wood Preserve - Green Roof Evaluation*. Retrieved August 22, 2013, from http://www.johnsongis.com/PDF/GreenRoof/Green%20Roof%20for%20EDGE%202009%20Update.pdf

Masters, F., & Gurley, K. (2008). *Performance of Embedded Gravel Roof Systems in Extreme Wind Loading*, Gainesville, FL: University of Florida. Retrieved: March 18, 2008,

Masters, F. J., Gurley, K. R., & Prevatt, D. O. (2008). Full-scale simulation of turbulent wind-driven rain effects on fenestration and wall systems. In *3rd International Symposium on Wind Effects on Buildings and Urban Environment*. Tokyo, Japan.

Mattacchione, A., & Mattacchione, L. (1999). Uplift on rooftop walkways and cable trays. *Canadian Journal of Civil Engineering, 26*(1), 119-122.

Mcdonald, J. R., Wang, W., & Smith, D. A. (1994). Field Experiments for Wind Loads on Pavers. In *9th International Conference on Wind Engineering*. pp. 488-499). New Delhi, India:(Wiley Eastern Limited, New Delhi).

Mensah, A. F., Datin, P. L., Prevatt, D. O., Gupta, R., & Lindt, J. W. v. d. (2011). Database-assisted design methodology to predict wind-induced structural behavior of a light-framed wood building. *Engineering Structures, 33*(2), 674-684.

Miller, C. (2007). Design Strategies to Address Wind Uplift and Scour in Green Roofs. (pp. 3). Philadelphia, PA: Roofscapes, Inc.

Molleti, S., Ko, S. K. P., & Baskaran, B. A. (2010). Effect of fastener-deck strength on the wind-uplift performance of mechanically attached roofing assemblies. *Practice Periodical on Structural Design and Construction, 15*(1), 27-39.

Pindado, S., & Meseguer, J. (2003). Wind tunnel study on the influence of different parapets on the roof pressure distribution of low-rise buildings. *Journal of Wind Engineering and Industrial Aerodynamics, 91*(9), 1133-1139.

Prevatt, D. O., Acomb, G. A., Masters, F. J., Vo, T. D., & Schild, N. K. (2012). *Comprehensive Wind Uplift Study of Modular and Built-in-Place Green Roof Systems*, [UF01-12]. Gainesville, FL, USA: University of Florida.

Prevatt, D. O., & Dixon, C. R. (2010). What Do We Learn from Wind Uplift Tests of Roof Systems? In *Structures Congress 2010* (pp. 2405-2416): American Society of Civil Engineers.

Prevatt, D. O., Masters, F. J., & Vo, T. D. (2011). *State of Knowledge of Green Roofs in State of Florida*, [UF04-11]. Gainesville, FL, USA: University of Florida.

Prevatt, D. O., Schiff, S. D., Stamm, J. S., & Kulkarni, A. S. (2008). Wind uplift behavior of mechanically attached single-ply roofing systems: The need for correction factors in standardized tests. *Journal of Structural Engineering, 134*(3), 489-498.

PRISM. (2012). *Plant Hardiness Zone Map: Florida* [map]. Washington, D.C.: USDA's Aggricultural Research Service. Retreived from http://planthardiness.ars.usda.gov/PHZMWeb/

Retzlaff, W., Celik, S., & Morgan, S. (2009). *Final Report: Wind Uplift of Green Roof Systems*: Southern Illinois University Edwardsville. Retrieved: March 12, 2009,

Retzlaff, W., Celik, S., Morgan, S., Graham, M., & Luckett, K. (2010). Into the Wind - Wind Tunnel Testing of Green Roof Systems. In *Cities Alive: 8th Annual Green Roof and Wall Conference and Proceedings*. pp. 21). Vancouver, Canada.

Sposaro, M. M., Chimenti, C. A., & Hall, A. J. (2008). Root lodging in sunflower. Variations in anchorage strength across genotypes, soil types, crop population densities and crop developmental stages. *Field Crops Research, 106*(2), 179-186.

Stathopoulos, T., & Baskaran, A. (1988). Turbulent wind loading of roofs with parapet configurations. *Canadian journal of civil engineering, 15*(4), 570-578.

Stathopoulos, T., Baskaran, A., & Goh, P. A. (1990). Full-scale measurements of wind pressures on flat roof corners. *Journal of Wind Engineering and Industrial Aerodynamics, 36, Part 2*(0), 1063-1072.

Sterling, M., Baker, C. J., Berry, P. M., & Wade, A. (2003). An experimental investigation of the lodging of wheat. *Agricultural and Forest Meteorology, 119*(3–4), 149-165.

Underwriters Laboratories. (1996). *Standard UL 580* - Test for uplift resistance of roof assemblies.

Vo, T., Prevatt, D., Acomb, G., & Masters, F. (2013). *A Preliminary Approach to Determining Component and Cladding Wind Loads on Modular Green Roof Systems.* Paper presented at the The 12th Americas Conference on Wind Engineering, Seattle, Washington, USA.

Vo, T. D., Prevatt, D. O., Acomb, G. A., Schild, N. K., & Fischer, K. T. (2012). High speed wind uplift research on green roof assemblies. In *Cities Alive: 10th Annual Green Roof and Wall Conference*. pp. 11). Chicago, Illinois.

Vo, T. D., Prevatt, D. O., Agdas, D., & Acomb, G. A. (2013, February 2013). *Modular Green Roof Systems in Mid-rise Multifamily Residential Units.* Paper presented at the 1st Annual Residential Building Design & Construction Conference, Bethlehem, Pennsylvania.

Walter, B., Gromke, C., Leonard, K., Clifton, A., & Lehning, M. (2011). Measurements of surface shear stress distribution in live plant canopies. In *13th International Conference on Wind Engineering*. pp. 8). Amsterdam, The Netherlands.

Wanielista, M., Minareci, M., Catbas, N., & Hardin, M. (2011). *Green roofs and wind loading*: University of Central Florida.

Webb, J. D. (2009). *Green Roof Performance Including Category 2 Hurricane Impacts.* Paper presented at the 7th Annual Greening Rooftops for Sustainable Communities, Atlanta, GA.

Webb, J. D. (2012). *Water. Wind. Green Roofs. Resilience.* Retrieved August 22, 2013, from http://mydigitalpublication.com/display_article.php?id=1112252

Whiting, G. (2007). Gravel Scour in Corner Region atop a Winn Dixie in Jensen Beach, Florida. In W. D. P. O. 04 (Ed.).

BIOGRAPHICAL SKETCH

Tuan Vo was born on November 1988, in Bethlehem, Pennsylvania. He moved to Orlando, Florida by the age of 2 where his parents continued working as technicians for a local semiconductor plant. When his parents had to move again for work mid-2007, he chose to stay behind and finish his senior year at Harmony High School. He prepared and planned over two years to pursue a major in architecture. After being accepted to the University of Florida, however, he attended the first day of college previews, and was immediately swayed to switch to civil engineering.

In January 2010, striving to graduate with highest honors, he came to Dr. David Prevatt in search of research work. After expressing his interest in sustainability, he began working as an undergraduate research assistant for Dr. Prevatt. He aided in various on-going graduate projects such as chamber pressure testing of residential roof panels, and the construction of full-sized gable roofs to investigate the wind resistance of polyurethane foam. By the Summer of 2010, he was granted a two-year project investigating the wind effects on green roof systems and their feasibility in hurricane-prone regions. This resulted in an undergraduate Honors thesis, where after, he graduated Summa Cum Laude in the Fall of 2011 with a Bachelor of Science in Civil Engineering.

Following his Fall 2011 graduation, he continued both his education and green roof research at the University of Florida as a graduate research assistant. He was one of the last researcher to utilize UF's hurricane simulator for full-scale wind testing before it was recommissioned for the wind tunnel at the Powell Family Structures and Material Laboratory late 2012. From this research, he published three conference papers (refer to list of references), and attended two of the conferences (12th Americas Conference

on Wind Engineering and 10th Annual CitiesAlive Green Roof and Wall Conference). He plans on publishing at least one more paper either before graduation. Following his graduate work, he plans on taking a short amount of time off to travel, before continuing with his career as a structural design engineer.